Université de Montréal

Biodisponibilité et effets transcriptomiques du cérium chez *Chlamydomonas reinhardtii*

Par

Elise Morel

Département de sciences biologiques, Faculté des arts et sciences

Thèse présentée en vue de l'obtention du grade de Philosophiae Doctor (Ph. D.)
en sciences biologiques.

Janvier 2020

© Elise Morel, 2020

Université de Montréal
Département de sciences biologiques, Faculté des arts et sciences

Cette thèse intitulée

Biodisponibilité et effets transcriptomiques du cérium chez *Chlamydomonas reinhardtii*

Présenté par
Elise Morel

A été évaluée par un jury composé des personnes suivantes

Marc Amyot
Président-rapporteur

Kévin Wilkinson
Directeur de recherche

William Zerges
Codirecteur

Maikel Rosabal Rodriguez
Membre du jury

Isabelle Lavoie
Examinateur externe (pour une thèse)

Résumé

Du fait de leurs propriétés spécifiques, les éléments de terres rares (ETRs) sont des métaux devenus indispensables au développement de notre société moderne. Avec leurs utilisations croissantes, des modifications importantes du cycle biogéochimique des ETRs sont attendues alors que peu est encore connu sur leur devenir et leurs effets une fois rejetés dans l'environnement.

Le cérium (Ce) a la particularité d'être utilisé sous forme de sels ou de nanoparticules dans différents produits d'utilisation courante (e.g. additifs de diesel, peintures). En raison de sa réactivité redox particulière, le Ce est naturellement peu soluble dans les eaux de surface et va donc principalement se retrouver dans les sédiments de ces écosystèmes aquatiques. Cependant les propriétés physicochimiques du Ce anthropique peuvent modifier le transport et le comportement de ce dernier. Par exemple, les nanoparticules manufacturées d'oxydes de cérium (Ce NMs) pourvues d'un enrobage peuvent présenter une stabilité colloïdale différente de celles naturellement formées. Les organismes pélagiques des milieux aquatiques, dont les micro-organismes photosynthétiques, d'intérêt dans ce projet, pourraient ainsi être exposés à de nouvelles formes de Ce et à différentes concentrations.

Comme il est difficile d'observer des réponses biologiques significatives pour des concentrations d'exposition représentatives de celles susceptibles d'être retrouvées dans l'environnement (< 1 µM), les impacts potentiels du Ce sur le phytoplancton dans des scénarios d'exposition réalistes sont encore mal élucidés. Des résultats contradictoires ont notamment été observés dans la littérature en ce qui concerne la biodisponibilité des Ce NMs pour les microalgues unicellulaires et la relation entre leurs propriétés de surface (i.e. rapport Ce (III)/Ce (IV), enrobage) et les réponses cellulaires. Des données quantitatives sont ainsi toujours nécessaires pour l'évaluation des risques potentiels du Ce pour l'Environnement.

Dans ce projet, *Chlamydomonas reinhardtii* a été sélectionnée comme organisme modèle pour représenter les microalgues présentent dans les eaux douces. Des sels solubles de Ce, Tm, Y et trois types de petites Ce NMs (<10 nm) avec différents enrobages (i.e. non enrobées, fonctionnalisées par du citrate ou enrobées de poly(acide acrylique) (PAA)) ont été injectés dans des milieux aqueux simplifiés (i.e. sans phosphates) à des concentrations représentatives de celles

attendues dans des environnements anthropisés. La spectrométrie de masse à plasma à couplage inductif en mode simple particule (SP-ICP-MS) a constitué l'une des techniques analytiques de pointe déployées dans ce projet. Elle a permis de quantifier les formes dissoutes et nanoparticulaires du Ce présentent dans les milieux d'exposition des microalgues et de caractériser les petites Ce NMs à des concentrations similaires à celles utilisées pour exposer les microalgues. L'analyse de profilage du transcriptome entier (ARN-Seq) a constitué une autre technique émergente en nano(éco)toxicologie. Elle a permis d'identifier des gènes et voies métaboliques mobilisés chez les populations algales de *C. reinhardtii* pour s'adapter à leurs expositions soit à des Ce NMs soit à des sels d'ETRs pour des concentrations d'exposition de 0,5 µM Ce, Tm ou Y en milieux contrôlés à pH 7.0.

Les microalgues *C. reinhardtii* ont d'abord été exposées au sel de Ce soluble et aux Ce NMs afin d'en comparer la biodisponibilité et les réponses biologiques sous-létales associées. Les résultats ont révélé que les Ce NMs sont biodisponibles pour *C. reinhardtii* mais et produisent un stress modéré auquel ces dernières semblent s'acclimater à court terme à des concentrations pertinentes pour l'environnement. Des effets transcriptomiques distincts entre Ce ionique et Ce NMs ont également été observés. L'hypothèse selon laquelle seuls les produits de dissolution des Ce NMs sont biodisponibles pour *C. reinhardtii* a donc pu être infirmée. En effet, les microalgues exposées aux Ce NMs testées ont spécifiquement modulé l'expression des gènes impliqués dans le système ubiquitine-protéasome et la structure des flagelles. Malgré ces effets communs entres les Ce NMs, leur biodisponibilité est principalement influencée par leurs enrobages, et non par le rapport de Ce(III)/Ce(IV) des atomes de surface des NMs. L'enrobage de citrate a d'ailleurs particulièrement atténué les effets transcriptomiques des Ce NMs sur les microalgues, probablement en raison des effets bénéfiques de la désorption du citrate à leur surface.

Les profils de temps-réponses (0 à 360 min.) et concentrations-réponses (0 à 3 µM) de gènes spécifiques des Ce NMs ou du Ce ionique ont par la suite été analysés pour vérifier leur potentielle utilisation en tant que biomarqueurs d'exposition des micoalgues au Ce ionique. En raison de leur spécificité élevée et de la linéarité relative de l'expression des biomarqueurs en fonction du temps sur une plage de concentrations pertinentes pour l'environnement (0,03 à 3 µM), quatre biomarqueurs (*Cre17.g737300*, *GTR12*, *MMP6* et *HSP22E*) ont été identifiés comme

étant spécifiques au Ce ionique pour *C. reinhardtii*. Une variabilité beaucoup plus grande des niveaux d'ARNm a été observée lorsque le pH du milieu variait (5,0 à 8,0). Ce résultat reflète probablement la complexité de la spéciation du Ce résultant de la formation d'espèces métastables même dans des milieux aqueux simples.

Les effets transcriptomiques de sels de Ce, Tm, Y solubles appliqués individuellement ou sous forme de mixture équimolaire ont été caractérisés par ARN-Seq chez *C. reinhardtii* afin de comparer la biodisponibilité du Ce à celle des autres ETRs pour les microalgues, sachant le comportement atypique du Ce en solution. Les microalgues exposées au Ce ont spécifiquement modulé l'expression de gènes impliqués dans le métabolisme du glutamate et au repliement des protéines. Cependant des interactions compétitives ont été identifiées entre les ETRs lorsqu'appliqués en tant que mixture. Ces résultats suggèrent que l'approche des agences gouvernementales pour dériver des données de toxicité à partir d'un seul métal simple serait largement conservatrice pour les métaux de terres rares.

Par ce projet, l'analyse des réponses transcriptomiques par ARN-Seq chez *C. reinhardtii* a permis de caractériser la biodisponibilité du Ce et d'identifier des biomarqueurs transcriptomiques d'exposition chez les microalgues dans différents contextes ; en présence de Ce NMs ou d'autres ETRs. L'intégration de tels biomarqueurs pour le développement d'un bio-essai *in situ* nécessite cependant de plus amples investigations.

Mots-clés : Éléments de terres rares, cérium, nanoparticules manufacturées, phytoplancton, *Chlamydomonas reinhardtii*, ARN-Seq, transcriptome, biodisponibilité, biomarqueurs d'exposition.

Abstract

Due to their specific properties, rare earth elements (REEs) are metals that have become essential to the development of our modern society. With their increasing uses, significant modifications to the biogeochemical cycle of REEs are expected while little is known about their fate and their effects once released into the environment.

Cerium (Ce) has the particularity of being used in the form of salts or nanoparticles in various commonly used products (e.g. diesel additives, paints). Due to its particular redox reactivity, Ce is naturally poorly soluble in surface water and will therefore mainly be found in the sediments of these aquatic ecosystems. However, the physicochemical properties of the anthropogenic Ce can modify its transport and behavior. For example, engineered cerium oxide nanoparticles (Ce ENPs) are generally coated and thus may exhibit different colloidal stability from those naturally formed. Pelagic organisms in aquatic environments, including photosynthetic microorganisms, of interest in this project, could thus be exposed to new forms of Ce and at different concentrations.

As it is difficult to observe significant biological responses for environmentally relevant exposure concentrations (<1 µM Ce), the potential impacts of Ce on phytoplankton in realistic exposure scenarios are still poorly understood. Contradictory results have notably been reported with regard to the bioavailability of Ce ENPs for unicellular microalgae and the relationship between their surface properties (i.e. Ce(III)/Ce(IV) ratio, coating) and cellular responses. Quantitative data are thus always necessary for the evaluation of the potential risks of Ce for the Environment.

In this project, *Chlamydomonas reinhardtii* was selected as a model organism to represent microalgae in freshwater. Soluble salts of Ce, Tm, Y and three types of small Ce ENPs (<10 nm) with different coatings (i.e. uncoated, functionalized with citrate or coated with poly (acrylic acid) (PAA)) were injected into simplified aqueous media (i.e. without phosphates) at concentrations representative of those expected in contaminated environments. One of the advanced analytical techniques deployed in this project was inductively coupled plasma mass spectrometry in single particle mode (SP-ICP-MS). It has made it possible to quantify the dissolved and nanoparticulate forms of Ce present in microalgae exposure media and to

characterize small Ce NMs at concentrations similar to those used to expose microalgae. Another emerging nano(eco)toxicology analysis used in this project is the whole transcriptome sequencing (RNA-Seq). RNA-Seq has permitted to identify genes and metabolic pathways that were regulated by *C. reinhardtii* cells when exposed to either Ce ENPs or to salts of REEs for exposure concentrations of 0.5 µM Ce, Tm or Y in controlled environments at pH 7.0.

C. reinhardtii cells were first exposed to soluble Ce salt and Ce ENPs in order to compare relative bioavailabilities of these anthropogenic Ce forms and their associated sub-lethal biological responses. The results revealed that Ce ENPs are bioavailable to *C. reinhardtii* but produce a manageable toward microalgae cells who seem to acclimatize for short-term exposures at environmentally relevant concentrations. Separate transcriptomic effects of Ce ionic and Ce ENPs have also been observed. The hypothesis that only the dissolution products of Ce ENPs are bioavailable for *C. reinhardtii* could therefore be rejected. Indeed, the microalgae exposed to the tested ENPs specifically modulated the expression of the genes involved in the ubiquitin-proteasome system and the structure of flagella. Despite these common effects between Ce ENPs, their bioavailability was mainly influenced by their coatings, and not by the Ce(III)/Ce(IV) ratio of surface atoms of ENPs. The coating of citrate has attenuated the transcriptomic effects of Ce ENPs on microalgae, probably due to the beneficial effects of the desorption of citrate on their surface.

The time-response (0 to 360 min.) and concentration-response (0 to 3 µM) profiles of specific Ce ENPs or ionic Ce genes were then analyzed to verify their potential use as biomarkers of exposure to ionic Ce. Due to their high specificity and the relative linearity of the expression of biomarkers as a function of both time and concentration, over a range of concentrations relevant to the environment (0,03 à 3 µM), four biomarkers (*Cre17.g737300*, *GTR12*, *MMP6* and *HSP22E*) have been identified as being specific to the ionic Ce for *C. reinhardtii*. Much greater variability in mRNA levels was observed when the pH of the medium varied (5.0 to 8.0). This result probably reflects the complexity of the speciation of Ce resulting from the formation of metastable species even in simple aqueous media.

The transcriptomic effects of soluble Ce, Tm, Y salts applied individually or in the form of an equimolar mixture were characterized by RNA-Seq in order to determine the relative bioavailability of Ce compare to the one of other REEs for microalgae, due to Ce atypical

behavior in solution. The microalgae exposed to Ce specifically modulated the expression of genes involved in glutamate metabolism and protein folding. However, competitive interactions have been identified between the REEs when applied as a mixture. These results suggest that the approach of government agencies to derive toxicity data from a single metal would be largely conservative for rare earth metals.

Throughout this project, the analysis of transcriptomic responses by RNA-Seq in *C. reinhardtii* made it possible to characterize the bioavailability of Ce and to identify transcriptomic biomarkers of exposure in microalgae in different contexts; in the presence of ENPs or other REEs. However, the integration of such biomarkers in the development of *in situ* bioassays seems limited.

Keywords: Rare earth elements, cerium, engineered nanoparticles, phytoplankton, *Chlamydomonas reinhardtii*, transcriptome, RNA-Seq, bioavailability, exposure biomarkers.

Table des matières

Liste des tableaux

Chapitre 3

Conclusions

Annexes

Liste des figures

Introduction

Chapitre 1

Chapitre 2

Chapitre 3

Conclusions

Figure 1. – Diagramme de Venn obtenu pour les gènes différentiellement exprimés dans le chapitre 1 (n=3, $Log_2FC > |1|$, $p_{adj} < 0.001$) et dans le chapitre 2 (n=5, $Log_2FC > |3|$, $p_{adj} < 0.001$) suite à une exposition de *C. reinhardtii* à 0,5 µM de Ce ionique pendant deux heures à pH 7.0. 117

Annexes

Liste des sigles et abréviations

Analytical ultracentrifugation (AUC)
Calcium (Ca)
Cérium (Ce)
Differentially expressed genes (DEGs)
Dynamic light scattering (DLS)
Éléments de terres rares (ETRs)
Engineered nanoparticles (ENPs)
Espèce réactive de l'oxygène (ROS)
Flux d'internalisation (J_{int})
Gadolinium (Gd)
Inhibition de croissance (IC)
Instant (t)
Lanthane (La)
Lutétium (Lu)
Manganèse (Mn)
Modèle du ligand biotique (BLM)
Nanoparticules manufacturées d'oxydes de Ce (Ce NMs)
Poly(acrylic acid) (PAA)
Principal component (PC)
Principal component analysis (PCA)
Potentiel d'oxydoréduction (E_h)
Rare earth elements (REEs)
Réaction de polymérisation en chaîne par transcription inverse en temps réelle (RT-*q*PCR)
Récepteurs membranaires (R_S)
Samarium (Sm)
Scandium (Sc)
Séquençage aléatoire du transcriptome entier (ARN-Seq)
Single particle inductively coupled plasma mass spectrometry (SP-ICP-MS)
Terbium (Tb)
Thulium (Tm)

X-ray photoelectron spectroscopy (XPS)
Yttrium (Y)

L’enfer et le paradis ne sont que des états de l’esprit. (S. Rinpoché)

À Mohammad, de chez Seagate, pour sa compassion et son humanité.

Remerciements

Je remercie tout d'abord M. Wilkinson, mon directeur de thèse de m'avoir donné l'opportunité de faire un doctorat dans un laboratoire aussi bien équipé en jouets de chimie analytique. Chef, je me dois aussi de vous remercier pour toutes ces expériences très formatrices et stimulantes que vous m'avez offertes de vivre durant ces six années. Je pense notamment à mon échange à Genève, ma participation à la SETAC en 2017 et à l'ICEENN en 2018, aux tâches d'enseignement, à l'encadrement des Valérie et Jessica. Votre patience durant mes moments peu glorieux a été largement appréciée.

Je remercie également M. Zerges, mon codirecteur de thèse dont l'efficacité et la pertinence sont redoutables. Merci à M. Amyot d'avoir accepté à la fois de siéger sur mon comité thèse et de constituer le président de mon jury ainsi qu'aux autres membres de mon jury de thèse, à savoir M. Rosabal Rodriguez et Mme Lavoie, qui ont pris le temps de me fournir des commentaires rigoureux et pertinents sur le manuscrit.

Une pensée spéciale est offerte à toute l'équipe Nano du CEREGE de Aix-en-Provence, c'est vous qui m'avez donné le gout de me lancer dans cette aventure qu'est le doctorat (peut-être devrais-je vous blâmer de m'avoir fourni une vision idéalisée de la recherche ?). Les membres actifs de l'AECBUM qui m'ont permis de rester connectée au département de Sciences biologiques de l'Université de Montréal. D'ailleurs, je tiens à remercier le département de Sciences biologiques de l'UdeM de m'avoir ouvert l'accès à la réalisation de ce doctorat en tant qu'étudiante étrangère. J'adresse un spécial merci à madame Aubin, qui de loin ou de près aura toujours était d'un soutien et d'une gentillesse incroyable.

Pour le reste, je remercie tous ceux qui comprendront que je n'ai pas le temps de les remercier ! Je pense notamment aux universitaires (permanents, en étude, en stage ou en échange), aux amis; Montréalais (ou non), apnéistes (ou non), et à la familia.

Introduction

Le cérium; un métal, de multiples contaminants émergents

La famille des éléments de terres rares (ETRs), comprenant le cérium (Ce) et les quatorze autres lanthanides ainsi que le scandium (Sc) et l'yttrium (Y), est encore relativement peu connue du grand public. Pourtant les éléments qui la composent sont devenus indispensables à notre société moderne. Du fait de leurs propriétés optiques, catalytiques et magnétiques uniques, les ETRs sont notamment incorporés dans les produits de haute-technologie ou dits « de technologie verte » utilisés quotidiennement.[1] Par exemple, selon Molycorp Inc., leader mondial dans l'incorporation des ETRs dans des produits finaux, le Ce serait présent sous forme de sels ou d'oxydes dans au moins cinq compartiments d'un véhicule hybride (écrans LCD, batterie hybride, convertisseur catalytique, additifs de carburants diesels et vitres).

Le Ce (z=58) possède une configuration électronique [Xe] $4f^2\ 5d^0\ 6s^2$ et appartient aux ETRs légers (lanthane (La) - gadolinium (Gd)), qui sont distingués des ETRs lourds (terbium (Tb) – lutétium (Lu)) par un plus grand rayon atomique.[2] Lorsqu'il est sous forme d'ion libre non hydraté, le Ce^{3+} présente un rayon atomique de 1.14 Å.[3] Comme il présente deux degrés d'oxydation stables dans les systèmes naturels ; Ce(III)/Ce(IV), le Ce est, avec l'europium (Eu), l'une des deux exceptions parmi les lanthanides qui sont principalement retrouvés sous forme de cations trivalents.[4] Du fait de sa forte affinité pour l'oxygène, le Ce est un métal dit lithophile. Il constitue l'ETR le plus abondant dans la croûte terrestre (0,005% en masse, en moyenne), et il y est entre autres plus présent que le cuivre et le plomb.[5] Il reste cependant considéré comme un élément trace et est classé, avec les autres ETRs, parmi les ions métalliques dits 'accepteurs durs' (classe A) c'est à dire de faibles polarisabilité et électronégativité.

Naturellement émis dans les matrices environnementales via l'altération des roches et des sols, le Ce est mobilisé en quantité plus importante par l'Homme que par la Nature via les activités d'exploitations minières et de combustion des combustibles fossiles (56% du Ce mobilisé par l'Homme contre 43% par la Nature).[6] Et la demande en ETRs devrait croitre de façon significative au cours des 25 prochaines années[1] puisque ces derniers sont considérés comme des métaux stratégiques pour le développement d'un secteur énergétique à faible émission de carbone.[7,8] Des nanoparticules manufacturées d'oxydes de Ce (Ce NMs) sont, par exemple, ajoutées aux carburants diesels pour en améliorer la combustion[9] alors que des sels de Ce sont incorporés dans des lampes LEDs[10] et des piles à combustible à oxyde solide.[11]

Les nanoparticules possèdent une de leurs dimensions comprise entre 1 et 100 nm et, de ce fait, une surface spécifique et une réactivité de surface plus importantes que des particules micrométriques de même composition chimique.[12] Dépendamment des conditions de température et de pression partielle d'oxygène, les Ce NMs peuvent se composer dioxydes de Ce purs (CeO_2), formant des structures cristallines cubiques de type Fluorite, ou d'un mélange CeO_2-Ce_2O_3 du même type de structure, mais contenant une quantité variable de cations Ce^{3+}, alors considérés comme des impuretés, et de sites d'oxygènes vacants.[3] C'est entre autres pour leur capacité élevée de stockage de l'oxygène que les Ce NMs sont intéressantes dans l'industrie automobile.

Différentes tailles, charges, chimie de surface de Ce NMs sont ainsi produites par les industriels pour moduler leurs stabilités, leurs réactivités et leurs biocompatibilités.[13,14] Et ces différentes formes du Ce anthropique sont susceptibles d'être rejetées dans l'environnement tout au long de son cycle de vie.[15] En Chine, l'un des plus grands réservoirs d'oxydes de terres rares au monde (avec l'Australie, la Russie et le Canada),[16] le Ce et les autres ETRs sont retrouvés dans des eaux avoisinant des sites miniers à des concentrations jusqu'à 200 fois supérieures à celles retrouvées dans des cours d'eaux non-contaminés.[17] Ou encore, en Angleterre, la combustion des carburants diesels contenant des Ce NMs induit l'augmentation significative de la concentration en Ce dans les particules ultrafines suspendues dans l'air.[18]

Avec un montant estimé de 28 Gg extrait et purifié par an, le cérium (Ce) constitue l'un des éléments de terres rares les plus utilisés dans notre société moderne.[19] Les sources de rejets de Ce anthropique sont multiples et peuvent être à des échelles importantes (ex. additifs des diesels). Elles impliquent une diversité de formes chimiques et physiques (sels de Ce, particules d'oxydes de Ce de propriétés variables). Constituant des problématiques environnementales émergentes, les ETRs et les NMs ont notamment été classifiés comme des substances prioritaires par Environnement et Changement climatique Canada.[20,21] Il s'agit d'évaluer rapidement les risques potentiels pour l'Homme et l'Environnement de ces catégories de substances, qui sont deux catégories étroitement reliées dans le cas du Ce.

Devenir du Ce anthropique dans les eaux de surfaces

Réactivité redox du Ce et anomalies négatives dans les colonnes d'eaux

Dans les eaux de surfaces, le Ce et les ETRs sont peu solubles et vont de ce fait être plus concentrés dans les sédiments et les fractions colloïdales (inorganiques ou organiques) que dans les colonnes d'eaux.[22-24] Les concentrations en ETRs mesurées dans les eaux de surfaces non contaminées sont inférieures à 5 nM,[24,25] et les concentrations en ETRs dissouts inférieures à 0.1 nM.[26] Cependant, des anomalies positives de concentrations totales en La, Gd et/ou samarium (Sm) ont été détectées dans les colonnes d'eaux de certains systèmes anthropisés, au regard des profils de concentrations obtenus pour l'ensemble des ETRs.[22,27] Dans ces systèmes, ce sont des anomalies négatives qui sont rapportées concernant les concentrations totales mesurées en Ce dans les colonnes d'eaux[22,27] et ce malgré le fait qu'il soit le plus utilisé des ETRs.[19] Ces anomalies négatives résultent d'un comportement complexe du Ce en solution, qui découle de sa réactivité redox paradoxale parmi les ETRs.[28]

En effet, le diagramme de Pourbaix de cet élément prédit la précipitation d'oxydes de cérium dans certaines conditions pH-E_h pouvant correspondre à celles des eaux de surfaces, pour les plus basiques et en équilibre avec l'atmosphère.[29,30] D'autres processus essentiels dans la distribution de différentes formes chimiques du Ce dans ces écosystèmes dépendent entre autres de son état d'oxydation. Par exemple, la complexation du Ce avec les phosphates, aboutissant à la formation de complexes peu solubles (K_{sp} des complexes de $Ce(III)PO_4 = 1\times10^{-23}$),[31] est privilégiée pour le Ce(III), qu'il soit sous forme d'ions libres[32] ou d'atomes à la surface de Ce NMs.[33] De plus, certains ligands organiques et inorganiques du milieu receveur peuvent induire des modifications de l'état d'oxydation des atomes de Ce.[22,34] Par exemple, le phénomène de piégeage par oxydation des atomes de Ce(III) à la surface des oxyhydroxydes de manganèse ou de fer est présenté comme un processus redox important favorisant l'élimination du Ce de la colonne d'eau des systèmes étudiés.[35,36] Enfin, les organismes peuvent également influencer le devenir du Ce dans les eaux de surfaces. La bio-réduction des atomes de Ce à la surface de Ce NMs composées initialement de Ce(IV) a par exemple été mise en évidence en laboratoire lors de l'adsorption des Ce NMs à la surface des bactéries gram négatif (*Escherichia coli*)[37] et au sein d'organismes benthiques (*Planorbus corneus*).[38]

Solubilité modifiée du Ce anthropique

Le devenir du Ce en milieux aqueux est donc complexe à appréhender du fait de la capacité des ions Ce à être oxydés ou réduits suivant ses interactions avec les composantes abiotiques et biotiques du milieu réceptacle. Les propriétés physico-chimiques du Ce d'origine anthropique peuvent également modifier le transport et le comportement de ce dernier. Par exemple, les sels de Ce utilisés comme fertilisants dans le domaine de l'agriculture sont des nitrates et des chlorures de Ce qui sont des composés plus solubles que les complexes Ce hydroxyles et phosphates naturellement retrouvés dans les eaux de surfaces.[39] De même, la solubilité des Ce NMs est susceptible d'être différente de celle des oxydes de Ce naturellement formés. La dissolution des Ce NMs peut être notamment (*i*) favorisée par la présence d'impuretés en quantités importantes (ex. Ce NMs émises lors de la combustion des carburants diesel)[40] ou (*ii*) limitée par l'utilisation de surfactants par les industriels[41] (ex. Ce NMs intégrées dans des produits de protection UV). La stabilisation fournie par certains enrobages serait notamment à l'origine du fort pourcentage de Ce NMs (6% en poids de dioxydes de cérium) retrouvé dans les eaux sortant des stations d'épuration qui sont ensuite rejetées dans l'environnement.[41]

Des expériences en mésocosme simulant un écosystème de rivière sur 28 jours ont montré que l'adsorption à la surface de Ce NMs de citrate négativement chargé à pH 7.0 permet des répulsions électrostatiques suffisantes pour limiter leur homo-agrégation et leur sédimentation.[38] Ainsi, l'instabilité chimique des Ce NMs ajoute un degré de complexité supplémentaire à prendre en compte dans le cadre de l'évaluation de l'exposition des organismes aux différentes formes du Ce. Les organismes pélagiques composant les écosystèmes aquatiques pourraient par exemple voir leur niveau d'exposition aux différentes formes de Ce anthropique augmenter du faits de leurs utilisations croissantes. Il s'agit de savoir quelle sera la fraction de ce dernier qui induira des effets biologiques chez les organismes, aussi appelée fraction biodisponible du Ce.

Biodisponibilité du Ce anthropique pour le phytoplancton

Modèles de biodisponibilité et de spéciation

Selon de nombreux exemples compilés par Campbell et *al.*, (1995), la biodisponibilité de métaux traces pour les microorganismes dépend majoritairement de l'activité de leurs ions libres en solution.[42] Ce rôle clé de l'ion libre d'un métal sur les effets biologiques qui lui sont associés, a conduit au développement de modèles basés sur les équilibres thermodynamiques entre un métal et les ligands abiotiques et biotiques du milieu ; les modèles de l'activité de l'ion libre (FIAM)[42] ou du ligand biotique (BLM).[43] Le BLM assume notamment que les effets biologiques observés chez un organisme exposé à un métal présent à l'état de traces sont directement proportionnels au flux d'internalisation (J_{int}) de ce dernier qui résulte des interactions entre les récepteurs membranaires (R_S) (ex. transporteurs ioniques de faible sélectivité) et l'ion libre du métal (M^{Z+}) présent en solution (**Figure 1**).[44]

Les faibles concentrations de Ce attendues (entre 0.03 et 1.5 nM_{Ce} dans les eaux naturelles non contaminées)[25] et la présence de ligands en excès rendent difficile l'utilisation des techniques analytiques mesurant la spéciation du Ce *in situ.*[45] Il n'existe donc pas à ma connaissance d'étude de terrain où les quantités d'ions libres de Ce auraient été mesurées *in situ*. Elles peuvent cependant être déduites de modélisations appliquées sur les concentrations totales mesurées dans différentes fractions des milieux naturels.

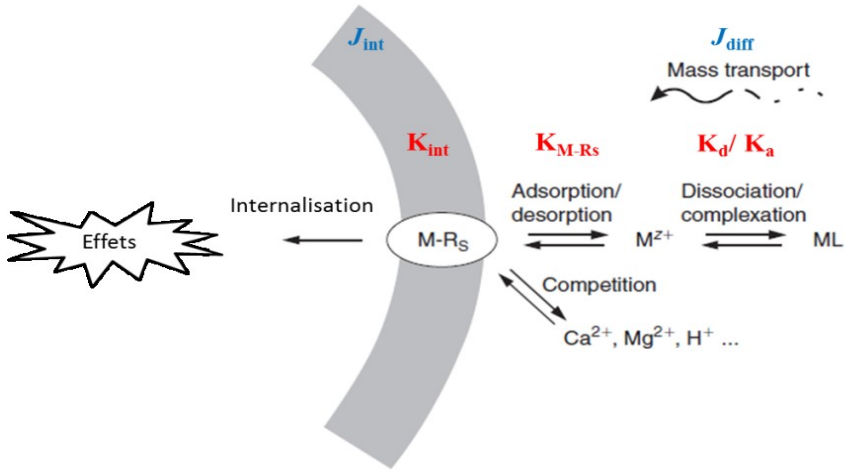

Figure 1. – Résumé du modèle du ligand biotique décrivant l'adsorption avec une constance d'affinité $K_{M\text{-}Rs}$ de cations métalliques libres (M^{Z+}) sur les récepteurs cellulaires (R_S) en présence

d'autres espèces cationiques compétitrices, suivie de leur internalisation avec un flux (J_{int}) après la diffusion (J_{diff}) des complexes hydrophiles contenant le métal d'intérêt (ML) et leurs dissociations (K_d) à proximité de la surface cellulaire.[44]

En effet, des programmes tels que Visual MINTEQ[46] ou WHAM[47] permettent de prédire les concentrations en ions libres en solution à partir des concentrations totales en métal d'intérêt et des paramètres physico-chimiques clefs du milieu (ex. pH, E_h, force ionique, concentrations en ligands organiques, inorganiques, en colloïdes et ions compétiteurs). Ils intègrent les constantes d'équilibres mesurées pour les réactions d'oxydoréduction, de complexation-dissolution, de sorption-désorption observées en milieux contrôlés. Selon ces modèles, les ions libres de Ce^{4+} ne sont pas stables dans les eaux naturelles [29] et les ions libres de Ce^{3+} n'y sont que peu présents. En effet, le Ce est majoritairement complexé à des composés inorganiques (ex. hydroxyles, phosphates, carbonates) et/ou organiques (ex. acides humiques) ou adsorbé sur des oxyhydroxydes de Mn ou de Fe.[28] La biodisponibilité du Ce pour le phytoplancton est donc supposée minime du fait de sa faible solubilité qui limite sa diffusion à proximité des R_S.[48] Cependant, probablement du fait de la diversité de leurs propriétés chimiques intrinsèques, de tels programmes ne permettent pas d'intégrer la présence de Ce NMs. La dissolution de ces dernières qui est favorisée lorsque des petites particules se retrouvent faiblement concentrées dans des eaux de pH plus acides,[31,49] pourrait pourtant devenir une source non négligeable de Ce ionique dans la colonne d'eau.

Bien qu'il soit intégré dans le cadre réglementaire de l'agence de protection de l'environnement des États-Unis,[44] l'applicabilité du BLM pour caractériser la biodisponibilité de métaux traces en milieux naturels reste à confirmer dans le cas des métaux trivalents[50,56] et tétravalents tels que les ETRs. Les concentrations en ions libres de Ce^{3+} sont donc rarement des données mesurées *in situ*, elles peuvent être incertaines lorsque modélisées dans des milieux naturels complexes et leur représentativité de la fraction biodisponible du Ce pour le phytoplancton reste à confirmer dans le cas des ETRs et des Ce NMs. Il est donc nécessaire de produire des données expérimentales ayant trait à la fois à la spéciation et au comportement du Ce d'origine anthropique en solution/suspension et à la biodisponibilité de ce dernier pour les organismes en milieux contrôlés.

Internalisation et biodisponibilité

Suivant le BLM, la fraction biodisponible du Ce pour un organisme donné peut être caractérisée en mesurant les quantités de Ce internalisé par l'organisme d'intérêt. Dans ce projet, c'est l'algue verte unicellulaire, *Chlamydomonas reinhardtii,* qui a constitué l'organisme d'intérêt. Représentative des organismes phytoplanctoniques retrouvés dans des eaux douces de surface, elle fait partie de la classe des *Chlorophyceae* et de l'ordre des Volvocales. Elle vit dans de nombreux environnements (eaux douces et sols) à travers le monde. Sa relative adaptabilité et son temps de génération rapide fait de *C. reinhardtii* un important organisme modèle pour les recherches en biologie et en écotoxicologie.[51] Des années de recherches ont établi des outils génétiques et moléculaires pour la manipulation de *C. reinhardtii,*[52] et son génome est séquencé et annoté.[53] De plus, elle a déjà été utilisée dans les expériences de caractérisation de la biodisponibilité des ETRs[30, 54-57] et des Ce NMs.[58-60]

Par exemple, une forte diminution de l'internalisation du Ce par *C. reinhardtii* a été observée en présence d'acides fulviques.[30] Cette dernière concorde avec la diminution de la concentration de l'ion libre (Ce^{3+}) prédite en solution en présence de matière organique naturelle. Cependant, Yang et *al.* et Zhao et *al.* ont observé que la présence de complexes organiques simples (ex. acides maliques ou citriques) n'induit pas chez *C. reinhardtii* une diminution de l'internalisation du thulium (Tm), de l'Eu et/ou du Sm de manière stœchiométrique comme attendue par le BLM.[54, 56] Les auteurs ont conclu que certains complexes d'ETRs peuvent former des complexes ternaires avec les récepteurs biologiques et doivent ainsi être inclus dans les calculs de la fraction biodisponible de ces métaux.

Le BLM néglige les interactions entre la fraction particulaire des métaux et les surfaces biologiques.[42] Dans le cas des Ce NMs, il n'est pas encore clair dans la littérature si les concentrations mesurées en Ce internalisé chez *C. reinhardtii* sont dues à l'internalisation (*i*) des nanoparticules elles-mêmes (4-7 nm, Ce NMs enrobées de PVP, potentiel de surface non rapporté; 0,08 à 10,00 mg L^{-1}, 72h en milieu d'exposition contenant des phosphates)[58] ou (*ii*) à celle des produits issus de leur dissolution (> 140 nm, Ce NMs non enrobées ~0 mV ou moins, 0 à 34 mg L^{-1}, 2h en milieu d'exposition contenant ou non des phosphates).[32] Une limite d'exclusion de taille pour l'internalisation des Ce NMs par les cellules algales serait fixée autour de 5-20 nm.[32, 61,62] Elle serait ainsi de même ordre que la limite suggérée pour le transport apoplasmique

des nanoparticules chez les plantes supérieures.[63] Cependant, l'applicabilité d'une telle limite peut être remise en question pour certains microorganismes, comme ceux du genre *Chlamydomonas*. En effet, les deux flagelles caractéristiques du genre ne sont pas entourés de paroi cellulaire[64] et pourraient donc constituer un lieu privilégié pour la réalisation d'endocytose, potentiellement favorable à l'internalisation de Ce NMs de tailles supérieures à 20 nm. Par exemple, c'est à l'intérieur de petites vésicules que des Ce NMs internalisées chez *C. reinhardtii* ont été observées.[58] Il s'agit de l'unique étude qui a permis de visualiser des Ce NMs chez ses organismes. Deux autres mécanismes d'internalisation des nanoparticules par les microalgues outrepassant la limite d'exclusion de taille proposée (outre l'endocytose) seraient la diffusion passive[3] et la formation temporaire de «pores»[65] ou les mécanismes qui y sont relatifs tel que celui de pénétration par échange d'enveloppe lipidique.[66] Ils dépendent notamment de l'enrobage et de la charge des Ce NMs. Ce sont des propriétés intrinsèques déterminantes pour l'étendue de l'internalisation des Ce NMs, leur localisation sous-cellulaire et leur translocation dans les différents organes des plantes supérieures et pourraient également avoir un rôle clef la biodisponibilité des Ce NMs chez les cellules algales.[67-69] De plus, même si l'internalisation de Ce NMs a été peu observée chez les micro-organismes photosynthétiques,[3] des effets biologiques induits par de simples contacts entre les Ce NMs et les membranes biologiques ont fréquemment été rapportés.[37,70-72]

Il n'existe donc pas encore de consensus concernant les mécanismes d'interaction et d'internalisation des nanoparticules d'oxydes de métaux par les organismes.[3] La fraction biodisponible du Ce pourrait ainsi ne pas se limiter au Ce^{3+} présent en solution ni au Ce internalisé. L'analyse des effets biologiques observés chez les organismes exposés aux formes de Ce anthropique devrait fournir plus d'informations sur leur relative biodisponibilité chez les microalgues.

Effets biologiques du Ce anthropique chez le phytoplancton

Tests standards de toxicité

L'efficacité d'un composé à induire un effet biologique peut être mesurée à plusieurs niveaux; moléculaire, cellulaire, ou alors au niveau de l'organisme (physiologique ou comportemental) et des populations, notamment via des courbes temps-réponses, concentrations-réponses et/ou doses-réponses obtenues en milieux contrôlés. Elles permettent l'obtention d'indices représentatifs de la toxicité du composé tels que la concentration du Ce induisant une inhibition de croissance (IC) chez 50% de cellules algales (IC_{50}). Les IC_{50} chez *Pseudokirchneriella subcapitata* (algue unicellulaire d'eau douce) induites par le Ce ionique et nanoparticulaire sont respectivement de 45 μM_{Ce}[73] et 60 μM_{Ce}[74], toutes deux plus élevées que celle du cadmium de 30 μM_{Cd}.[73] Le Ce ionique est généralement associé à une toxicité plus faible que celle du cadmium ou du plomb[73] et les Ce NMs semblent encore moins toxiques et donc supposément moins biodisponibles.

Cependant dans les milieux d'exposition standards de microalgues définis par l'Organisation de Coopération et de Développement Économique, le Ce peut présenter une spéciation plus complexe que les métaux divalents classiques, aboutissant ainsi à des modifications de sa biodisponibilité qui ne sont pas prises en compte si seules les concentrations en Ce totales sont mesurées. En effet, les microalgues sont exposées durant 72h dans un milieu riche en phosphates (test 201), nécessaire à leur croissance, mais avec lequel le Ce, seul ou à la surface de Ce NMs, entretient une forte affinité.[32] De grandes variations dans les valeurs de concentrations les plus faibles auxquelles des effets significativement différents du control sont détectées avaient été observées suite à une exposition de différents organismes à des Ce NMs dans les systèmes aquatiques.[72] Il est possible que ces variations puissent être attribuées à un manque de caractérisation du comportement des Ce NMs (ex. agrégation, sédimentation, dissolution, adsorption ou complexation d'éléments du milieu) et donc de leur biodisponibilité pour les organismes. Certains auteurs suggèrent notamment que lors d'essais réalisés en laboratoire, d'importants efforts de caractérisation soient menés avant, pendant et après les phases d'expositions des organismes.[75]

Effets biologiques communs entre Ce ionique et Ce NMs

Le dérèglement de la balance antioxydante constitue l'effet toxique du Ce le plus étudié, qu'il soit sous forme ionique ou nanoparticulaire.[2] Les mécanismes moléculaires aboutissant à la génération d'un stress oxydatif sont bien connus. Ils sont commun à de nombreux organismes lorsqu'exposés à différents types de xénobiotiques.[76] Dans le cas du Ce, les cycles redox entre Ce(III) et Ce(IV), qui ont un rôle clef dans la distribution du Ce dans les eaux des surfaces, sont également considérés comme le moteur des effets redox observés chez les organismes exposés au Ce (seuls ou à la surface de Ce NMs).[77,78] Les contaminants de Ce peuvent ainsi induire des effets à la fois pro-oxydants et antioxydants suivant l'état d'oxydation initial des atomes de Ce qu'ils contiennent.[29, 79] La production d'un stress oxydatif chez les organismes varie également suivant les conditions d'exposition (temps et concentrations) et les caractéristiques physiologiques des organismes eux-mêmes.[80,81]

Les ETRs induisent des effets physiologiques positifs à faibles concentrations et des effets toxiques à plus fortes concentrations. Ils sont donc des éléments dits hormétiques.[77] Cet effet semble moins établi dans le cas des Ce NMs. Il a par exemple été observé pour le développement de biofilm bactérien mais pas pour celui du système racinaire de plantes.[82,83] Ce profil concentration-réponse est atypique pour des éléments non essentiels. Il pourrait résulter du mimétisme entre les ETRs et le calcium (Ca). En effet, une telle compétition a été observée dans des tissus animaux exposés aux lanthanides[84] supposément à cause de la similarité observée entre les rayons atomiques des ETRs et celui du Ca^{2+} lorsque déshydraté. Chez *C. reinhardtii*, une diminution du flux d'internalisation du Ce a été observée en présence de Ca^{2+}.[30] Cette dernière témoigne d'une compétition entre ces deux cations pour la liaison aux Rs à la surface de ces microalgues. Toutefois, les cibles intracellulaires communes entre ETRs et calcium n'ont pas encore été identifiées chez les microalgues. Ce manque d'information résulte probablement de la complexité des processus et acteurs nécessaires au maintien de l'homéostasie du calcium qui est impliqué dans des voies métaboliques complexes[85] (ex. signalisation cellulaire).[86,87]

Plus généralement, des effets compétitifs entre les métaux de classe A entre eux (ex. ETRs et Ca ou Mg) et avec certains métaux de classe intermédiaire (ex. ETRs et Fe) sont attendus du fait leur affinité commune pour l'oxygène. Les groupements carboxyliques des protéines pourraient ainsi constituer des ligands privilégiés pour ce type de métaux (ex.

phytochélatines) tout comme les molécules biologiques contenant des phosphates, de l'oxalate et du citrate.[81] Les Ce NMs peuvent, par exemple, hydrolyser les esters de phosphates *in vitro* et pourraient en faire de même *in vivo*.[88] Cependant, suivant les conditions pH-E_h des compartiments cellulaires dans lesquels ils pourront être retrouvés, d'importantes différences de valence entre ces métaux sont attendues; dans les conditions physiologiques, les métaux traces essentiels seraient généralement divalents alors que les cations de Ce pourraient être tri- ou tétravalents.[29] Cette différence devrait limiter les effets compétitifs entre ces métaux pour les cibles intracellulaires ayant une forte spécificité avec leur substrat telles que des protéines ayant généralement un rôle essentiel dans le métabolisme des organismes (ex. chélatases de Mg(II) impliquées dans la biosynthèse de chlorophylles chez *C. reinhardti*i).[89]

Les cibles intracellulaires et effets biologiques du Ce, notamment sous forme de Ce NMs restent encore peu connus. Chez les microalgues, ils pourraient impliquer d'autres voies métaboliques que l'homéostasie redox, celle du calcium ou encore des phosphates d'autant que des concentrations supérieures aux concentrations attendues dans l'environnement sont souvent nécessaires à l'observation de tels effets biologiques. Il est donc nécessaire de produire des données ayant trait aux effets biologiques du Ce d'origine anthropique à des concentrations plus représentatives de celles attendues dans l'environnement.

Approches 'omiques' en (eco)toxicologie

Qu'il soit mesuré au niveau moléculaire, cellulaire et/ou physiologique, tout effet biologique pouvant témoigner de l'exposition présente ou passée d'un organisme à au moins une substance chimique à caractère polluant, peut constituer un biomarqueur d'exposition de l'organisme à cette substance. Un changement témoignant de la présence d'effets délétères aux mêmes échelles chez ce même organisme peut constituer, quant à lui, un biomarqueur d'effets de la substance sur l'organisme. La détection d'un biomarqueur unique et spécifique d'une exposition à un composé toxique n'existe pas, ce sont donc généralement des ensembles de biomarqueurs qui peuvent être validés.[90,91] Au niveau moléculaire, des biomarqueurs peuvent être identifiés à différentes échelles (**Figure 2**) et selon la prémisse commune d'une expression différentielle du génome entre les organismes qui sont entrés en contact avec un xénobiotique et ceux non exposés à ce même xénobiotique. [80]

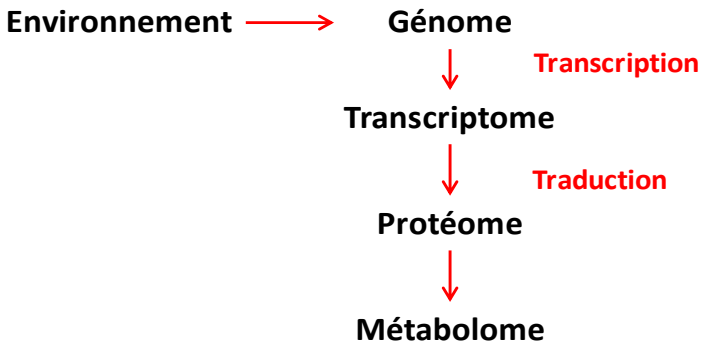

Figure 2. – Échelles principales pour l'identification des biomarqueurs moléculaires d'après Riedmaier et Pfaffl en 2013[90].

À l'échelle du transcriptome (c.-à-d. de l'ensemble des ARN résultant de la transcription du génome et de la dégradation des ARNs), se sont les techniques telles que les puces à ADN ou le séquençage aléatoire du transcriptome entier (ARN-Seq) qui permettent d'identifier l'ensemble des gènes dont le niveau de ARN va être régulé par un organisme à un instant (t) pour s'adapter à son exposition à un xénobiotique (ou à un stimulus). Par la suite, les fonctions connues des gènes différentiellement exprimés peuvent être indicatrices des voies métaboliques et des effets sous-létaux observés à t.[92]

Cette approche commence à être utilisée dans les études (nano)(eco)toxicologiques.[80] Par exemple, des NMs d'oxydes de titane et de zinc induiraient communément avec des quantum dots, une inhibition du protéasome de *C. reinhadrtii*.[92] Les analyses transcriptomiques, notamment couplées à des analyses réalisées à d'autres niveaux biologiques, fournissent ainsi des informations mécanistiques sur les effets biologiques potentiels induits suite aux interactions NMs/organismes.[93] De récentes études réalisées par ARN-Seq témoignent que des variations au niveau de la quantité des ARNm contenus dans des lignées cellulaires (humaines ou de souris) peuvent être spécifiques à des propriétés physico-chimiques de particules composées principalement du même élément. En effet, des patterns d'expression de gènes spécifiques ont été observés pour certaines tailles de particules de Ce (micro ou nano)[94] ou pour certaines propriétés de surfaces de Ce NMs[91]. Grâce à cette approche, Fisichella et *al.*, en 2014 ont pu observer que les Ce NMs non enrobées induisent entre autres une répression de 27 gènes impliqués dans le métabolisme de la respiration cellulaire des cellules humaines (CaCo-2). Alors que des Ce NMs enrobées de citrate de taille similaire n'induisent aucun effet sur cette voix métabolique.[91]

C'est donc pour la rapidité et la spécificité du processus dynamique de régulation des niveaux de ARNm que notre étude vouée à la caractérisation de la biodisponibilité et des effets du Ce chez *C. reinhardtii* a été réalisée à l'échelle transcriptomique. Dans ce projet, nous cherchons à identifier si existe des effets biologiques significativement différents chez les cellules de *C. reinhardtii* exposées à du Ce ionique et des Ce NMs et d'autres ETRs à des concentrations potentiellement retrouvées dans des écosystèmes d'eaux douces de surface anthropisés.

Cadre conceptuel et objectifs généraux de la thèse

Selon des analyses de risques pour les écosystèmes d'eaux douces de surfaces, la concentration maximale permissive en Ce total serait entre 0,007 et 0,2 µM de Ce total. [72,95] Ces valeurs sont légèrement plus élevées que les concentrations mesurées et prédites dans divers eaux douces de surfaces (<0,005 μM_{Ce})[24,25] et largement inférieures aux valeurs de IC_{50} mesurées chez *P. subcapitata* (45 μM_{Ce}[73] et 60 μM_{Ce}[74]). C'est donc pour s'assurer d'obtenir des signaux biologiques et chimiques quantifiables mais restant représentatifs de systèmes de surface faiblement anthropisés que des concentrations de 0,5 μM_{Ce} (**Chapitre 1 et 3**) ou entre 0,03 et 3 μM_{Ce} (**Chapitre 2**) ont été sélectionnées pour l'exposition de *C. reinhardtii* aux sels d'ETRs et Ce NMs.

Comme la caractérisation des NMs dans les matrices environnementales représente un réel défi analytique et cela même dans des milieux aqueux simplifiés,[96] et que la spéciation des ETRs peut être complexe à appréhender,[73] les cellules de *C. reinhardtii* ont été exposées dans des milieux aqueux simplifiés (i.e. sans ligand). Ces milieux ont été préalablement équilibré avec l'atmosphère pendant 24h afin de limiter les variations dans les concentrations lors de l'exposition des organismes (**Annexe, Figure 3**). Des temps courts d'exposition ont été privilégiés (<6h) afin de limiter des modifications des conditions d'exposition par les microalgues elles-mêmes (ex. production d'exsudats), et leur stress lié à l'absence de phosphates dans ces milieux.

Les résultats obtenus dans le cadre de ce projet de recherche ont été compilés dans trois chapitres ayant différents objectifs.

Le modèle du ligand biotique sous-tend que la biodisponibilité du Ce ionique est plus importante que celle des Ce NMs pour *C. reinhardtii* (Hypothèse 1). Le **chapitre 1** vise à vérifier l'applicabilité de ce modèle qui commence à être intégré dans les institutions gouvernementales. Pour ce faire, les effets transcriptomiques d'un sel de Ce soluble ou de Ce NMs ont été caractérisés par ARN-Seq chez des populations exposées (3 réplicas biologiques) ou non (4 réplicas biologiques) à une concentration totale de Ce inférieure à 0,5 µM. Cinq types de Ce NMs avaient été initialement caractérisés pour cette étude (**Annexe, Formes chimiques du Ce**), seules trois petites Ce NMs de tailles inférieures à <10 nm et de formes sphériques ont finalement été sélectionnées. Cette petite taille nominale devait permettre à l'ensemble des NMs de passer à travers la paroi cellulaire complexe de *C. reinhardtii.* Alors que la forme sphérique des NMs est essentielle à l'applicabilité des modèles sur lesquels reposent la plupart des techniques de caractérisation de taille. Comme l'enrobage entourant les NMs d'oxydes de métaux est un facteur déterminant pour leur biodisponibilité chez les microalgues d'eaux douces,[97] les Ce NMs sélectionnées possèdent également des propriétés de surfaces différentes ; non enrobées, fonctionnalisées par du citrate ou enrobées de poly(acide acrylique) (PAA), pour représenter la diversité des Ce NMs produites. Les Ce NMs non enrobées sont notamment incorporées dans des poudres de polissage dans l'industrie du verre,[40] les Ce NMs fonctionnées par du citrate ont été fournies par un industriel qui les intègre dans des peintures alors que celles enrobées de PAA sont actuellement étudiées pour leurs potentielles applications en agriculture.[68]

Comme chaque technique analytique possède ses avantages et ses limitations (**Tableau I**),[98] l'utilisation de plusieurs techniques de caractérisation de la taille des NMs à différents stades expérimentaux a été privilégiée dans ce **chapitre 1**. La microscopie à transmission électronique (TEM) et la spectroscopie photoélectronique X (XPS) ont été initialement utilisées pour mesurer respectivement la distribution de la taille et l'état d'oxydation des atomes de surface des particules (échantillons secs), qui sont des paramètres clefs de la biodisponibilité des Ce NMs.[72] La technique de spectrométrie de masse à plasma à couplage inductif (ICP-MS) en mode simple particule (SP-ICP-MS) a constitué la technique analytique de choix, utilisée dans le **Chapitre 1** pour décrire le comportement du Ce ionique et des Ce NMs dans les milieux d'exposition des microalgues. En effet, cette technique a montré des limites de détections prometteuses pour la caractérisation de l'état d'agrégation des NMs d'oxydes de métaux en suspension.[99] Elle peut notamment permettre de caractériser les distributions de taille d'oxydes de NMs, présentes en

faibles concentrations dans les échantillons environnementaux.[100] De par le principe même de la technique,[101] le SP-ICP-MS permet de mesurer à la fois la concentration d'un métal dans la fraction dissoute et celle présente dans la fraction (nano)particulaire d'un échantillon. Des analyses complémentaires par ultracentrifugation analytique (AUC), diffusion dynamique de la lumière (DLS) et ultrafiltration centrifuge ont également été effectuées pour caractériser la stabilité colloïdale des Ce NMs sur des échantillons plus concentrés non utilisés pour l'exposition des microalgues (excepté les ultrafiltrations centrifuges réalisées dans les milieux d'exposition avant l'introduction des microalgues).

Tableau I : Concentrations en Ce totale, limites de détection et types de diamètres mesurés par les différentes techniques de caractérisation de taille utilisées.

Techniques	Concentration totale (mg L^{-1})	Gamme de taille analysée	Type de diamètre mesuré
TEM	10**	> 0,2 nm	$\mathbf{D_p}$
DLS	50*	0,1 nm – 0,1 mm	$\mathbf{D_H}$
AUC	50*	< 200 nm	$\mathbf{D_H}$
SP-ICP-MS	0,001 – 0,005***	20 nm - 250 nm	$\mathbf{D_p}$
Cytométrie en flux	0,086 -17	> 500 nm	**Taille relative**

* Concentration retenue pour les analyses au DLS et à l'AUC est 50 mg.L^{-1} après une optimisation de l'amplitude de l'autocorrélation recommandée par Baalousha et Lead en 2012[102] pour les mesures au DLS.
** Concentration minimale pour l'observation d'un nombre de Ce NMs > 200.
*** Concentration ajustée pour avoir un nombre de nanoparticules détectées compris entre 200 et 2000.

Seul, le déploiement de techniques analytiques de pointe ne permet pas de contrer l'une des difficultés majeures pour évaluer les effets des NMs d'oxydes de métaux en (éco)toxicologie, à savoir la distinction entre les effets des produits de leur dissolution et les effets des nanoparticules elles-mêmes. Le **chapitre 2** vise à développer un outil biologique pour distinguer les interactions du métal dissout et des Ce NMs chez *C. reinhardtii.* Il suppose que l'intensité de l'altération de l'expression des gènes est proportionnelle au temps d'exposition des algues et à la concentration des différentes formes de Ce dans les milieux d'exposition (Hypothèse 2). Aussi l'utilisation de biomarqueurs transcriptomiques intégrés dans des voies métaboliques d'intérêt devrait présenter l'avantage supplémentaire (comparer à des expériences de bioaccumulation) de

contribuer à notre compréhension des mécanismes impliqués par les cellules pour répondre au Ce ionique (Hypothèse 3). Nous avons donc entrepris dans ce **chapitre 2** de mettre en relation les niveaux d'expression des gènes mesurés avec les réponses observées à l'échelle de l'organisme par cytométrie en flux, en supposant que si des biomarqueurs d'une voie métabolique commune indiquent des effets similaires aux deux échelles d'observation (transcriptomique et cellulaire), nous pouvons valider l'hypothèse 3. La voie métabolique la plus étudiée dans le cadre d'une exposition des organismes à du Ce, toutes formes confondues, étant le dérèglement de la balance oxidative,[2] des biomarqueurs cellulaires aux protocoles bien établies chez *C. reinhardtii* ont ainsi pu être utilisés.[103,104]

Une approche similaire au **chapitre 1** a été déployée dans le **chapitre 3.** Ce dernier vise à caractériser la biodisponibilité relative du Ce ionique par rapport à celle des autres ETRs pour *C. reinhardtii*. Du fait de ses capacités redox particulières, le Ce aurait un effet sur le transcriptome des microalgues différent des autres ETRs (Hypothèse 4). Les effets transcriptomiques de sels de Ce, Tm, Y solubles appliqués individuellement ou sous forme de mixture équimolaire ont été caractérisés par ARN-Seq chez *C. reinhardtii* afin de vérifier si les cibles intracellulaires des ETRs sont réellement distinctes. Ensemble, ils représentent la diversité des éléments de terres rares soit un lanthanide léger (Ce), un lanthanide lourd (Tm) et un élément 'pièce rapportée' aux lanthanides (Y). Les constantes d'affinités de liaisons de différents ETRs pour les récepteurs membranaires de *C. reinhardtii* sont de même ordre,[55] laissant supposer une certaine homogénéité entre ETRs pour les cibles moléculaires extracellulaires de *C. reinhardtii*. Si des cibles cellulaires sont identiques, de possibles interactions compétitives pourraient être identifiées entre les ETRs lorsqu'appliqués en tant que mixture. Ce **chapitre 3** vise à vérifier l'applicabilité du BLM dans le cas de ces métaux trivalents, non pas du point de vue de la bioaccumulation des métaux en tant que telle, mais via l'analyse des effets biologiques que les ETRs devraient produire.

Ma contribution pour l'ensemble des travaux présentés dans **le chapitre 1** consiste en la sélection des nanoparticules manufacturées de cérium d'intérêt et des conditions expérimentales de cette étude, l'optimisation et la réalisation de la majorité des analyses physico-chimiques qui y sont présentées, l'exposition des cellules algales et la préparation de leur ARN totaux, le traitement bio-informatiques des résultats de ARN-Seq et la rédaction de la majorité du

manuscrit. Ibrahim Jreije a effectué les analyses de SP-ICP-MS et le traitement des données obtenues et a rédigé le paragraphe de matériel et méthode relative à cette partie dans le manuscrit. Valerie Tetreault a participé lors d'un stage d'été aux analyses de caractérisation par ultrafiltration, DLS, AUC et ICP-MS de certains échantillons. Charles Hauser, William Zerges et Kévin J. Wilkinson ont constitué les personnes ressources dans la réalisation des analyses, l'interprétation des résultats et ont apporté des commentaires lors de la rédaction du manuscrit. Ma contribution pour l'ensemble des travaux présentés dans **le chapitre 2** consiste en la sélection des conditions et des gènes biomarqueurs testés, j'ai assuré l'exposition des cellules algales, les analyses en cyrtométrie en flux et la préparation de leur ARN totaux, l'optimisation des essais de RT-qPCR et la réalisation de ces derniers ainsi que le traitement de l'ensemble des données obtenues. J'ai rédigé l'entièreté du manuscrit. Jessica Dozois a participé lors d'un stage d'été aux expériences de RT-qPCR ainsi qu'à l'exposition des microalgues. Vera I. Slaveykova et Kévin J. Wilkinson ont constitué les personnes ressources dans la réalisation des analyses, l'interprétation des résultats et ont apporté des commentaires lors de la rédaction du manuscrit. Ma contribution pour l'ensemble des travaux présentés dans **le chapitre 3** consiste en la **s**élection conjointe avec monsieur Wilkinson des conditions expérimentales de cette étude, l'optimisation des conditions d'exposition des cellules algales, l'exposition et de la préparation de des ARN totaux, la réalisation d'une partie du traitement bio-informatiques des résultats de RNA-Seq et des analyses physico-chimiques et la supervision du reste de ces analyses. J'ai rédigé l'entièreté du manuscrit. Cui Lei m'a aidé dans l'optimisation des conditions d'exposition, il a assuré la modélisation de la spéciation des métaux et a effectué une partie du traitement bio-informatique des données de RNA-Seq sous ma supervision. Kévin J. Wilkinson a constitué la personne ressource dans la réalisation de ces analyses. William Zerges et Kévin J. Wilkinson ont apporté leurs commentaires lors de la rédaction du manuscrit.

Chapitre 1 – Bioavailability and cellular processes of Ce nanoparticles with different surface coatings as revealed by RNA-Seq in *Chlamydomonas reinhardtii*

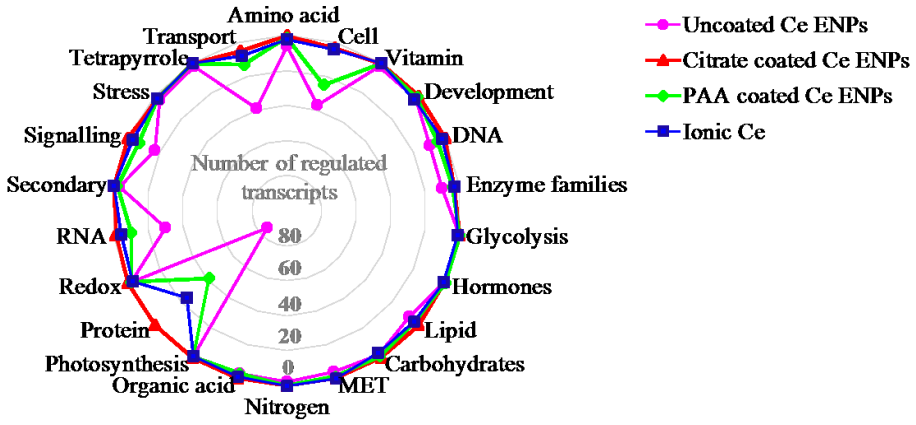

Elise Morel[a], Ibrahim Jreije[a], Valerie Tetreault[a], Charles Hauser[b], William Zerges[c], Kevin J. Wilkinson[a,Ψ]

[a]Biophysical Environmental Chemistry Group, University of Montreal, P.O. Box 6128, Succ. Centre-Ville, H3C 3J7, Montreal, QC, Canada

[b]Biological Sciences, St. Edward's University, 3001 S Congress Ave, 78704, Austin, TX, USA

[c]Dept. of Biology, Concordia University, 7141 Sherbrooke W., H4B 1R6, Montreal, QC, Canada

[Ψ]corresponding author

Modified after its submission to NanoImpact in December 2019

Abstract

In order to better understand the risks of engineered nanoparticles (ENPs), it is necessary to determine their fate and biological effects under realistic exposure scenarios (e.g. low ENP concentrations). For cerium oxide ENPs (Ce ENPs), contradictory results have been observed in the literature with respect to both their bioavailability to aquatic micro-organisms and the relationship between ENP surface properties and cellular responses. In this paper, a unicellular freshwater microalga, *Chlamydomonas reinhardtii*, was exposed for 2 h to one of three small Ce ENPs (i.e. nominal size <20 nm) with different coating properties (i.e. uncoated, citrate or poly-acrylic acid coated) or to a soluble Ce salt at 70 μg L^{-1} Ce. Relative bioavailabilities were deduced from whole transcriptome profiling analysis and results have been interpreted with respect to a multimethod characterization of the Ce ENPs. Although polyacrylic acid coated Ce ENPs were chemically distinct from the other Ce ENPs, they elicited similar patterns of differential gene expression as the uncoated Ce ENPs. In contrast, stabilization of the ENPs by citrate appeared to reduce their bioavailability, as fewer differentially expressed transcripts (10s of genes) were detected as compared to the polyacrylic acid coated or uncoated ENPs. Transcriptome profiling identified metabolic pathways that could be involved in response to the ENP exposures. For the low exposure concentrations examined here, toxicity appeared to be minimal, while few biomarkers of cellular stress were regulated by Ce ENPs.

Introduction

Of the rare earth elements, cerium (Ce) is one of the most used- some 28 kt were extracted and purified in 2007.[19] Its optical and catalytic properties make it an important element in numerous applications, including high technology and green technology industries.[8,13] For example, Ce is incorporated as salts into solid oxide fuel cells[11] or, as engineered nanoparticles (ENPs), into diesel additives.[105] While these technologies enhance energy efficiency, they also can lead to widespread environmental contamination of Ce.[40,106] Novel applications of Ce ENPs in biomedicine,[107] agriculture[108] and water depollution[109] are also expected to increase environmental concentrations.

No clear consensus has yet been established on the relative bioavailabilities of ionic vs. ENP forms of Ce. Several authors have postulated that the effects of dissolved Ce to phytoplankton could be neglected with respect to the ENPs.[110,58,111] Others have shown Ce ENPs to exhibit a lower acute toxicity than ionic Ce.[72,81] In another paper, the photosynthetic yield of *C. reinhardtii* was shown to be decreased, due to dissolved Ce that co-occurred in suspensions of (uncoated) Ce ENPs.[32] The bioavailability of Ce ENPs also appear to be influenced by their agglomeration and valence state,[72] which result from a combination of the intrinsic properties of the ENPs (e.g. size, shape, coatings) and the environmental conditions (e.g. redox potential, pH, ligand concentrations). For example, the stabilization of Ce ENPs by citrate[112] has been shown to lower their bioavailability to bacteria in the activated sludge of a waste water treatment plant in comparison to uncoated Ce ENPs.[113] In addition to their role as a dispersant,[110,114] ENP coatings can act as a protective barrier, preventing direct contact of the core particle with the biological membrane[58] or they can increase ENP biocompatibility.[14] The aqueous-ENP interface is thus one critical factor influencing the bioavailability of Ce ENPs, resulting from the Ce(III)/Ce(IV) ratio,[115,79] the surface charge,[116,62] the specific surface area[111] and the nature of the surface coating.[117]

In many toxicity studies focusing on microalgae, the conditions used were not relevant to those thought to exist in natural waters. For example, toxic effects are often reported for exposures to mg L^{-1} of Ce ENPs, whereas, generally only ng L^{-1} concentrations are thought to be found in natural waters.[118] Median effective concentrations (72 h EC50s) for the growth inhibition of microalgae have ranged from 0.024 mg L^{-1} to 29.6 mg L^{-1}: polyacrylate coated Ce

ENPs (4-10 nm, 0.024 mg L^{-1}),[110] citrate stabilized Ce ENPs (10 nm, 5.6 mg L^{-1})[114] and uncoated Ce ENPs (10 nm and <25 nm, 2.4–29.6 mg L^{-1};[119] 10-20 nm, 10.3 mg L^{-1} [74]); while no adverse effects on growth were measured for polyvidone coated Ce ENPs (4-7 nm, >80 mg L^{-1}).[58] Thus, at environmentally relevant Ce ENP concentrations, more sensitive endpoints are required to distinguish the effects of different particles. For example, recent studies using transcriptome profiling by RNA sequencing (RNA-Seq) have shown patterns of gene expression that correlate with the physicochemical properties of Ce ENPs. Indeed, gene expression has been used to distinguish the effects of particle sizes (micro or nano)[94] or the degree of degradation of a citrate coating.[117] Nonetheless, while Taylor *et al.* observed significant differential gene expression following a 3-d exposure of *C. reinhardtii* to 10 mg L^{-1} of polyvidone coated Ce ENPs, no effects were observed at more environmentally relevant concentrations of 0.144 µg L^{-1}.[58]

Given that there is no consensus on the relative bioavailabilities of the different forms of Ce or on the effects of ENP surface coatings,[120] this study focused on the biological effects of ionic Ce and Ce ENPs with different coatings: uncoated, stabilized by citrate, and coated by poly-acrylic acid, at 70 µg L^{-1} Ce using *C. reinhardtii* as a model organism. We focused on the effects of small Ce ENPs (<20 nm) because they are suspected to be the most bioavailable due to both their high reactivity (i.e. high specific surface area)[70] and sizes that are small enough to pass through pores of the cell wall (i.e. diameters of 5-20 nm).[62,121] Multi-method characterization experiments, including single particle inductively coupled plasma mass spectrometry (SP-ICP-MS), were performed to determine the physicochemical stability of the Ce ENPs. RNA-Seq[80,93] was used: (i) to infer the biological effects from the known functions of the differentially regulated genes and (ii) to compare effects on the microalgal transcriptome among the different Ce ENPs. All of the Ce forms were bioavailable to *Chlamydomonas reinhardtii* with differences between ionic and ENPs highlighted with respect to both the number of differentially expressed genes (DEGs) and the sub-pathways in which these DEGs are known to function.

Materials and methods

Materials

All experiments were performed in polymerware (polypropylene or polycarbonate) or Teflon, which was first soaked in 2% v/v HNO_3 for 24 hours, rinsed 7x with Milli-Q water (total organic carbon < 2×10^{-3} g L^{-1}; resistivity > 18 MΩ cm) and dried under laminar flow conditions (Heraeus). Most reagents were purchased from Fisher Scientific (molecular biology grade), except acetic acid (analytical grade, Fisher Scientific), chloroform (99,8%, Acros organics) and nuclease-free water (QIAGEN). Other chemicals included: K_2HPO_4 and KH_2PO_4 (ACS reagent grade, Fisher Chemical), Tris (Tris-(hydroxymethyl)-aminomethane, BDH USP/EPgrade, VWR), EDTA disodium salt (Bioultra grade, Sigma-Aldrich), Isotone (VWR), HNO_3 (67–70%; BDH Aristar Ultra, VWR), H_2O_2 (30%, BDH Aristar Ultra, VWR), NaOH (Acros Organics), NaMES (2-(N-morpholino)ethanesulfonic sodium salt, Acros Organics), NaHEPES (4-(2-hydroxyethyl)-1-piperazineethanesulfonic sodium salt, Acros Organics).

Preparation and characterization of the nanoparticles

Nanoparticles

$Ce(NO_3)_3$ (**ionic Ce**) was purchased from Inorganic Ventures (1.0 g L^{-1}; ICP-MS standard). **Uncoated Ce ENPs** (nominally 15 - 30 nm) were purchased from Nanostructured & Amorphous Materials as a powder (1406RE). Triammonium **citrate stabilized Ce ENPs** (nominally 10 nm) were obtained from Byk (Nanobyk®-3810). The measured Ce concentration of the stock solution was 187.6 ± 2.7 g L^{-1} Ce ENPs. Sodium **polyacrylic acid coated Ce ENPs** (PAA coated Ce ENPs) (nominally 1-10 nm) were obtained from Sciventions as an aqueous suspension (1.5 g L^{-1} Ce ENPs) and as a powder. Intermediate 1 g L^{-1} suspensions of all ENPs were prepared in polypropylene tubes that were covered with aluminum foil and stored at 4°C. Before use, they were manually shaken and sonicated (sonication bath, 135W, 30 min.) prior to their dilution in the experimental media, where they were equilibrated for 24 h with orbital shaking (100 rpm) at room temperature.

Concentrations

Ce concentrations were determined by adding 400 µL of HNO_3 (67–70%) and 300 µL of H_2O_2 (30%) to 1 mL of sample and then heating the mixture at 80° C for 5 h (DigiPREP, SCP science). Samples were analyzed by inductively coupled plasma mass spectrometry (**ICP-MS**, PerkinElmer; NexION 300X). A Ce calibration curve was run every 20 samples while blanks and quality control standards were run every 10 samples. Indium was used as an internal standard to correct for instrumental drift.

TEM and EDS

ENP size was characterized by transmission electron microscopy (**TEM**) and energy-dispersive x-ray spectroscopy (**EDS**) on a JEOL (model JEM-2100F) microscope. Three drops of a 1.0×10^{-2} g L^{-1} ENP suspension in Milli-Q water were deposited and dried on Cu holey electron microscopy grids (200 mesh; Electron Microscopy Sciences) under laminar flow. Particle diameters were determined using ImageJ ($n\geq50$).[122,123]

SP-ICP-MS

A sector field ICP-MS (Nu Attom, Nu instruments, UK) in single particle mode (**SP-ICP-MS**) was used to quantify the particle size distribution and dissolution of the ENP suspensions at 70.1 µg L^{-1} Ce. Samples were diluted immediately prior to analysis in order to have 1000 – 2000 peaks per measurement time (50 s), which is optimal to avoid concurrent ionization of more than one ENP, while providing statistically significant particle numbers (**Figure S1**). A dwell time of 50 µs, a sample flow rate of 200-250 µL.min^{-1}, a concentric glass nebulizer (internal diameter: 1.5 mm) and a quartz cyclonic spray chamber cooled to 4°C were employed. The isotope ^{140}Ce was monitored and calibration was performed using ionic standards (Inorganic Ventures, CGCE-1) in the range of 0.05 to 2.0 µg L^{-1}. A transport efficiency of 3-5 % was determined from a suspension of 30 nm ultra-uniform gold nanoparticles (Nanocomposix, AUXU30-1M, 20.0×10^{-9} g L^{-1}).[124] It was validated using a suspension of 20 nm silver nanoparticles (NanoXact, ECP1691, 20.0×10^{-9} g L^{-1}) and by frequent analysis of an ionic In standard used to document sensitivity variations. Data were processed using NuQuant software (version 2.2) by imposing a minimum peak width of 200 µs. Peak masses were determined from the ionic calibration and peak diameters were estimated based upon an assumed density and spherical geometry. Average Ce

background was used to calculate the concentration of dissolved metal. All samples were prepared and analyzed in triplicate. More details on single particle ICP-MS and the data processing used by the Nu Quant software can be found elsewhere.[124-126]

Centrifugal ultrafiltration

ENP dissolution in the algal exposure media was also monitored using centrifugal ultrafiltration units (Amicon ultra-4, 3 kDa molar mass cutoff). Four mL samples were centrifuged for 20 min at 3700×g at 20 °C. In order to minimize adsorptive losses to the ultrafiltration membrane, the filtrate was collected after the third centrifugation cycle and analyzed by ICP-MS (**Figure S2**). Mass balances were determined from Ce concentrations: (i) in the filtrate; (ii) in the solution remaining above the filter; and (iii) in an acid (69% v/v HNO_3) extraction of the filter. For blanks, Ce was below detection limits.

Electrophoretic mobility and DLS

Electrophoretic Mobility (**EPM**) and Dynamic Light Scattering (**DLS**) measurements were performed at 20°C in the PEEK flow cell of the Möbiuζ (Wyatt Instruments, 532 nm laser and 168.7° scattering angle). Hydrodynamic diameters and EPM were obtained for 40-50 mg L^{-1} of Ce ENPs in pH buffered exposure media (NaMES: pH 5.0-6.0; NaHEPES: pH 6.5-8.5 containing 10.0 μM of $Ca(NO_3)_2$). A regularization algorithm (7.3.1.15 DynamicSoftware) was used to analyze the DLS autocorrelation function. Diffusion coefficients were converted to hydrodynamic diameters using the Stokes−Einstein equation. The analytical performance of the instrument was systematically verified using a NIST polystyrene standard (Bangs Laboratories, NT02N) with a known diameter of 42 nm that was diluted to 20% (v/v) in Milli-Q water. Experiments were duplicated using freshly prepared samples that were analyzed on separate days. Each individual replicate was divided into two aliquots, which were each analyzed 4x.

Analytical ultracentrifugation

Analytical ultracentrifugation (**AUC**, ProteoLab XLI analytical ultracentrifuge, Beckman XLI)) using interference detection, was performed using 400 μL of the same suspensions that were used for DLS. Sedimentation profiles (900 scans) were generated by ultracentrifuging the samples at 18,144×g for uncoated Ce ENPs, 26,127×g for citrate stabilized Ce ENPs and

72,576×g for PAA coated Ce ENPs. The sedimentation coefficient distribution was determined using SEDFIT (v. 14.1). By assuming a particle density of ρ=7.13 g cm^{-3} for uncoated and citrate stabilized Ce ENPs (https://www.nanoamor.com/msds/msds_CeO_2_1406RE.pdf) and ρ=2.00 g cm^{-3} for the PAA coated Ce ENPs (ρ=1.09 g cm^{-3} for the organic polymer[127] (85 dry wt.%) and ρ=7.13 g cm^{-3} for CeO_2 (15 dry wt.%)), particle size distributions could be determined based on the Stokes−Einstein equation. Further theoretical and methodological considerations are provided in Diaz *et al.*, 2015.[127]

X-ray photoelectron spectroscopy

Ce(III)/Ce(IV) ratios on the surface (~5 nm depth) of the ENPs were analyzed by x-ray photoelectron spectroscopy (**XPS**) on the ENPs powders. XPS spectra were recorded on a VG ESCALAB 3MKII spectrometer using Mg Kα radiation (*hv*= 1253.6 eV). Photoelectrons were detected at 90° with respect to the sample surface. High resolution XPS spectra were obtained for C1s (280-290 eV), O1s (525-535 eV), Ce3d (875-920 eV). Peak fitting (Lorentzian-Gaussian curves) was performed with Avantage software (Thermo Scientific) after a background subtraction (Shirley function). The energies 881.6, 885.1, 899.2 and 903.5 eV were used as component peaks for Ce(III) and 882.6, 888.4, 898.2, 901.1, 906.7 and 916.5 eV as component peaks for Ce(IV).

Culture conditions

C. reinhardtii (Wild type CC-125 (aka 137c) from the *Chlamydomonas* resource center) was inoculated from agar-solidified (1.5% wt/v) Tris-acetate-phosphate (TAP)[128] medium into 75 mL of a 4×diluted TAP medium.[129] This green microalga is ubiquitous to fresh waters and is often used for water quality monitoring and studies examining the toxicology of pollutants in natural waters. The culture was grown at 20°C under conditions of 12 h light/12 h dark (60 mmol s^{-1} m^{-2}), with orbital shaking (100 rpm). Once the culture reached its mid-exponential growth phase (1-5×10^6 cells mL^{-1}; ~3 d), it was used to inoculate 400 mL of 4×diluted TAP. This culture was also grown until a mid-exponential phase (~2 d) and then centrifuged at 2000×g for 3 min to pellet the cells. The cell pellet was resuspended in 10 mM NaHEPES (pH 7.0), containing no metal. This wash procedure was repeated twice in order to prepare a cell concentrate that was

added to the exposure solutions (below). Cell concentrations and cell surface areas were measured using a Multisizer 3 particle counter (50 mm aperture; Beckman Coulter).

Exposure conditions

Approximately 6.5 x 10^4 cells mL^{-1} were exposed for 2 h to 0.5 µM of Ce (70.1 µg L^{-1} Ce and 86.1 µg L^{-1} for Ce ENPs) in 10.0 mM NaHEPES (pH 7.0 containing 10.0 µM $Ca(NO_3)_2$).[130] Control treatments were also conducted in similar exposure medium but without the addition of any Ce forms. This simplified experimental medium was used so that the chemical speciation of Ce could be precisely controlled. For example, Ce precipitates in the presence of phosphate that is routinely found in the growth media. In order to evaluate adsorptive losses and potential contamination, metal concentrations in the media were measured at the start and end of each experiment. Cellular densities were low enough to ensure that Ce concentrations did not decrease over the duration of the exposure of microalgae (**Figure S3**). Following the 2 h exposure, cells were pelleted by centrifugation from 300 mL of the exposure solution (2000×g, 2 min., 4°C). Cell pellets were resuspended in 1 mL nuclease-free water before being transferred into 1.5 mL microtubes where the cells were again pelleted by centrifugation. Cell pellets were frozen on dry ice for 10 minutes and stored at −80 °C.

RNA-Seq analysis

RNA preparation

Cell pellets were thawed and then immediately resuspended in freshly prepared lysis buffer (0.3 M NaCl, 5.0 mM EDTA, 50 mM Tris-HCl (pH 8.0), 2.0% SDS, 3.3 U mL^{-1} proteinase K) where they were incubated at 37 °C for 15 min. Total RNA was isolated by extracting the sample 3x with phenol:chloroform:isoamyl alcohol (25:24:1, pH 6.8) followed by 1x with chloroform:isoamyl alcohol (24:1). At each step, samples were centrifuged (12000xg, 10 min., 4° C) and supernatants were transferred into new tubes. Total RNA was precipitated from the final aqueous phase by isopropanol, then washed with 75% ethanol. After a final centrifugation, the pellet was resuspended in 20-30 µL of nuclease-free water. An aliquot (3 µL) was analyzed by automated electrophoresis for RNA quality (RIN number > 7, 1.8 < ratio

260/280 < 2.1, ratio 260/230>1.8; Bioanalyzer, Agilent) and spectroscopy (OD260) to determine the concentration of RNA (Nanodrop).

cDNA library construction and high-throughput sequencing

mRNA selection, library preparation (NEB/KAPA mRNA stranded library preparation) and Illumina sequencing were carried out at the Genome Quebec facilities (www.gqinnovationcenter.com). Two lanes on a HiSeq (v4) were used for the paired-end sequencing (2 × 125 base pairs) of 16 samples (3 replicates for each Ce treatment: ionic Ce; uncoated Ce ENPs; citrate stabilized Ce ENPs; PAA coated Ce ENPs) and 4 replicates for controls). Replicates (biological) were each from independent cultures.

Sequence analysis, differential expression and functional annotation

For each sample, *ca.* 64 million reads were obtained by Illumina sequencing. Read quality was explored with FastQC[131]. Filtering quality and adapter trimming were conducted with Trim Galore!.[132] Only paired reads obtained after the cleaning step (phred >20, length > 21 bp) were conserved. Reads were aligned to the *C. reinhardtii* genome v5.3 assembly using TopHat2 with standard presets except that intron size was between 30 and 28000 bbp.[133] Approximately 60 million reads were mapped for each sample (around 93% of $(64.2 \pm 2.2)\times10^6$ reads; **Table SI**) with multiple-read alignments accounting for 5.8 ± 0.2% of the total mapped reads in each sample. GeneBody coverage python script (RSeQC) was used to calculate the number of reads for each nucleotide position and to generate a plot illustrating the coverage profile along the gene (**Figure S7**).[134] The number of reads per gene was determined using the Python package HTSeq.[135] Differentially expressed transcripts were identified using DESeq2 for $\log_2$ fold change (Log_2FC) values exceeding |1| and false discovery rates (p_{adj}) < 0.001.[136] Gene annotations were retrieved from MapMan ontology.[137,138] The JGI Comparative Plant Genomics Portal was also used to explore the function of gene sets of interest, such as the "unclassified" gene list obtained from MapMan (**Supplementary Data 7**).[139] The Wilcoxon rank-sum test was used to identify enriched metabolic pathways. The Algal Functional Annotation Tool was used to convert gene and transcript ID, when necessary.[140]

Results and discussion

ENP Characterization

Although the three ENPs were initially thought to be very similar (based upon manufacturer's indications), several important differences (e.g. state of agglomeration, proportion of Ce(III)) were noted. The key results of the ENP characterization are summarized in **Figure 1** with numerous additional details provided in the SI (**Table SI, Figures S4, S5 and S6**).

By combining data from the different techniques, it was possible to conclude that under the conditions of the algal exposures (70.1 μg L^{-1} Ce in NaHEPES at pH 7.0), the Ce ENPs had a mean primary particle size of <10 nm with a negative surface potential (**Figure 1 and Table SI**). Of the three ENP types, the uncoated Ce ENPs were most subject to agglomeration. Nonetheless, SP-ICP-MS results indicated some agglomeration of the citrate stabilized Ce ENPs at low particle concentrations, potentially due to a desorption of the citrate from the particle surface following dilution.[141] Consistent with their propensity for agglomeration, the greatest losses of Ce from the exposure medium were observed for the uncoated and citrate stabilized ENPs, where only about half of the starting Ce was recovered: ionic Ce (60.7 ± 3.9 μg L^{-1} Ce), uncoated Ce ENPs (39.3 ± 10.0 μg L^{-1} Ce), citrate stabilized Ce ENPs (33.2 ± 5.6 μg L^{-1} Ce), and PAA coated Ce ENPs (70.7 ± 2.2 μg L^{-1} Ce) (**Figure S3, Table SII)**. Nonetheless, during the following 2h exposure of microalgae, measured Ce concentrations remained reasonably stable **(Figure S3)**. The PAA coated Ce ENPs did not appear to be 'classical' Ce(IV) ENPs: in contrast to the manufacturer's data, Ce atoms were mainly Ce(III), either complexed by the PAA coating or precipitated as Ce_2O_3. For all exposure media containing Ce ENPs, only negligible dissolved Ce was detected. However, somewhat surprisingly, in the solutions of ionic Ce, up to 20% of the Ce could be classified as incidental nanoparticles.[30]

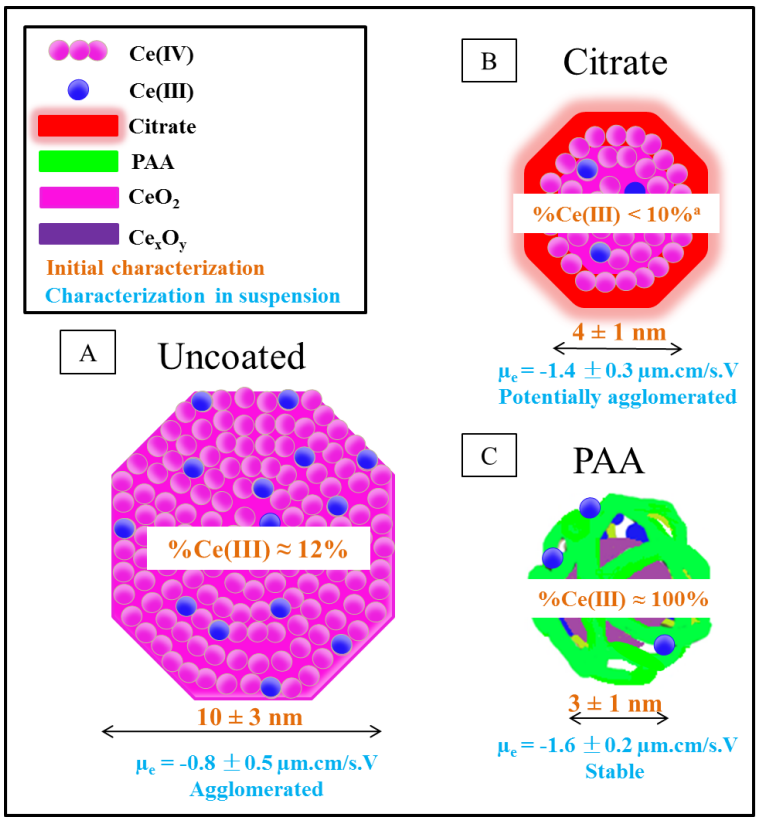

Figure 1. – Summary of results of the Ce ENP characterization. Physical diameters were determined from TEM on the powders or concentrates and in colloidal suspensions using SP-ICP-MS, DLS and AUC; colloidal stability was determined from electrophoretic mobility (μ_e) and ultrafiltration experiments and Ce(III)/Ce(IV) ratios were determined by XPS (**Table SI**). (A) Uncoated Ce ENPs; (B) citrate stabilized Ce ENPs; (C) PAA coated Ce ENPs. Raw TEM and XPS data are provided in the supplemental information (**Figure S4**). XPS data for the citrate stabilized ENPs were taken from Auffan *et al.*[112] Representative SP-ICP-MS size distributions are provided in **Figure S5** and electrophoretic mobilities in **Figure S6**.

Overview of the RNA-Seq data

Of the 19,526 predicted transcripts in *C. reinhardtii,*[142] 16,808 (86%) were detected, indicating that the RNA-Seq data was high quality and unbiased (**Supplementary Data 1**). Eight hundred and forty-eight (848) genes showed at least a 2-fold change with respect to their control values in one or more of the treatments **(Figure 2A, Supplementary Data 2)**. When those DEGs were analyzed by principal component analysis (PCA), data were grouped around the Ce ENPs (associated with PC1, 54% of variance) and ionic Ce (associated with PC2, 23% of variance)

(**Figure S8.B**). Moreover, the uncoated Ce ENPs and the PAA coated Ce ENPs were distinctly grouped from the citrate stabilized Ce ENPs in the variable space of the PCA plot (**Figure S8.B**). Comparisons of the profiles of DEGs elicited by each of the Ce ENPs, i.e. their "transcriptomic signatures", suggest that bioavailability was highest for the uncoated Ce ENPs, intermediate for the PAA coated Ce ENPs, and lowest for the citrate stabilized Ce ENPs. In the sections that follow, we first discuss the results that nano-specific effects were observed (**Section 3.3**) and then secondly, the nature of the differences that were observed among the different Ce ENP surface coatings (**Section 3.4**).

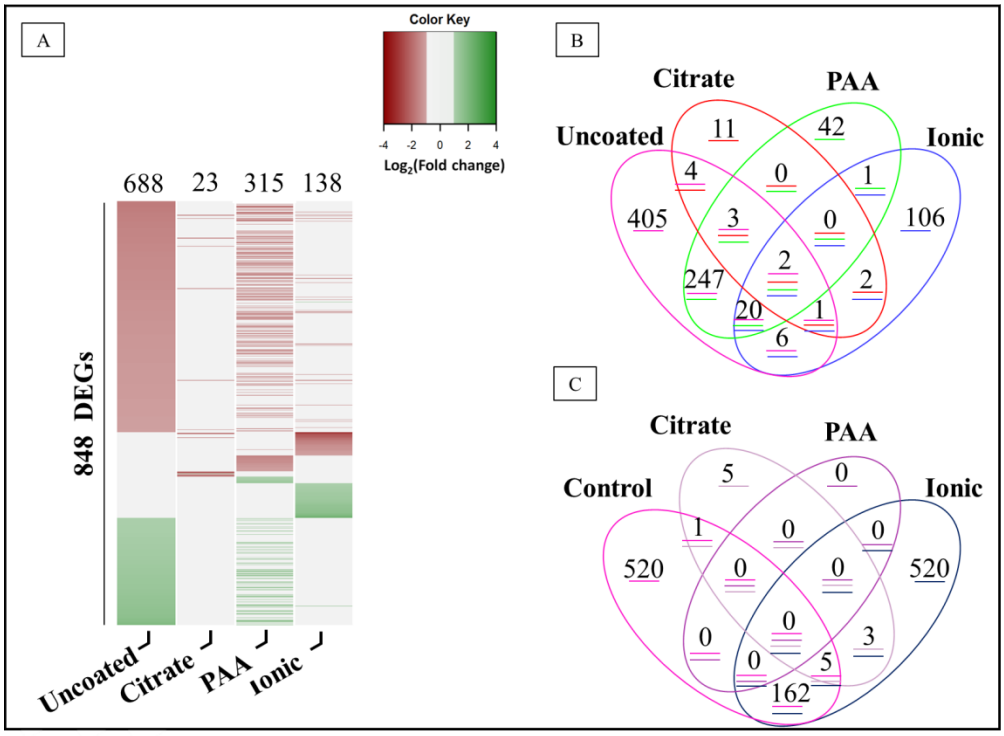

Figure 2. – (A, B) Differentially expressed genes with respect to the control ($Log_2FC > |1|$, $p_{adj} < 0.001$), following a 2 h exposure of *C. reinhardtii* to uncoated Ce ENPs (39.3 ± 10.0 µg L^{-1}), citrate stabilized Ce ENPs (33.2 ± 5.6 µg L^{-1}), PAA coated Ce ENPs (70.7 ± 2.2 µg L^{-1}), and ionic Ce (60.7 ± 3.9 µg L^{-1}). In (A), red represents the genes that were induced by the treatment ($Log_2FC < -1$) while green represents those that were repressed ($Log_2FC > 1$), Grey: $-1 \geq Log_2 FC \leq 1$. In (C), exposures were normalized to the uncoated Ce ENPs, rather than the control treatment ($Log_2FC > |1|$, $p_{adj} < 0.001$).

Transcriptomic signatures reveal nano-specific effects

Bioavailability was first inferred from the number of DEGs and the magnitude of their regulation. Conclusions that were based upon Venn diagrams (**Figure 2.C**) were further substantiated by PCA (**Figure S8.B**). Indeed, 106 genes were differentially expressed in response to ionic Ce but not to the Ce ENPs (**Figure 2.B)**. Among those genes, 52 were differentially expressed with respect to both the control and the ENP ($Log_2FC > |1|$, $p_{adj} < 0.001$) (**Figure S10.A)**. Of the 688 transcripts that were differentially expressed in response to the uncoated Ce ENPs, about one quarter (162 of the 688 DEGs, **Figure 2.C**) were also differentially expressed with respect to the exposure to ionic Ce, *i.e.* most transcripts were specific to the uncoated Ce ENPs.

At the pathway level, our data were consistent with the Ce ENPs having a specific impact on cellular processes. For example, the ENPs altered the expression of genes related to cellular motility (**Table SIII, Figure S9, and Supplementary Data 3**). Of the 26 transcripts linked to cellular flagella biogenesis and functioning and which were regulated by the Ce ENPs, 17 have been identified as being up-regulated during deflagellation in *C. reinhardtii*[143], suggesting that this process plays a key role in the acclimation of microalgae to Ce ENPs. For instance, uncoated and PAA coated Ce ENPs induced the expression of *FAP16*, a gene involved in a pathway that induces detachment of the flagella[144] and both repressed the expression of a gene (*POC7*) related to flagella assembly.[145] Deflagellation could reduce physical exposure to ENPs via two mechanisms. First, as flagella are large structures surrounded by a bare plasma membrane, i.e. without a surrounding cell wall,[146] they may be more accessible to ENPs. Second, in *C. reinhardtii*, endocytosis is localized in a specialized region of the plasma membrane located at the base of the flagella.[147] Deflagellation might thus reduce Ce ENPs access to this region and, thereby, reduce cellular uptake by endocytosis. If observed, deflagellation might suggest that *C. reinhardtii* are exposed to an unfavorable physicochemical environment (e.g. pH shock, heat, alcohol treatment).[146]

Transcript levels of genes involved in the xenobiotic resistance system increased when microalgae where exposed to the Ce ENPs unlike in cells exposed to ionic Ce (**Figure 3, Supplementary Data 4**). Regulation of protein metabolism targets was also different for ionic Ce in comparison to the ENPs **(Supplementary Data 5**). For example, genes with functions in

intracellular protein targeting were enriched for ionic Ce, while protein folding enrichment was found for uncoated Ce ENPs (Wilcoxon test, $p < 0.05$) (**Table SII, Figure 4**). Furthermore, approximately half of the DEGs related to protein metabolism elicited by the uncoated Ce ENPs had annotated functions in post-translational protein modification, a sub-pathway that was not identified to the same extent in cells exposed to ionic Ce (**Table SIII, Figure 4)**. Potential significance of this nano-effect is unclear because post-translational modifications occur in most intracellular processes.

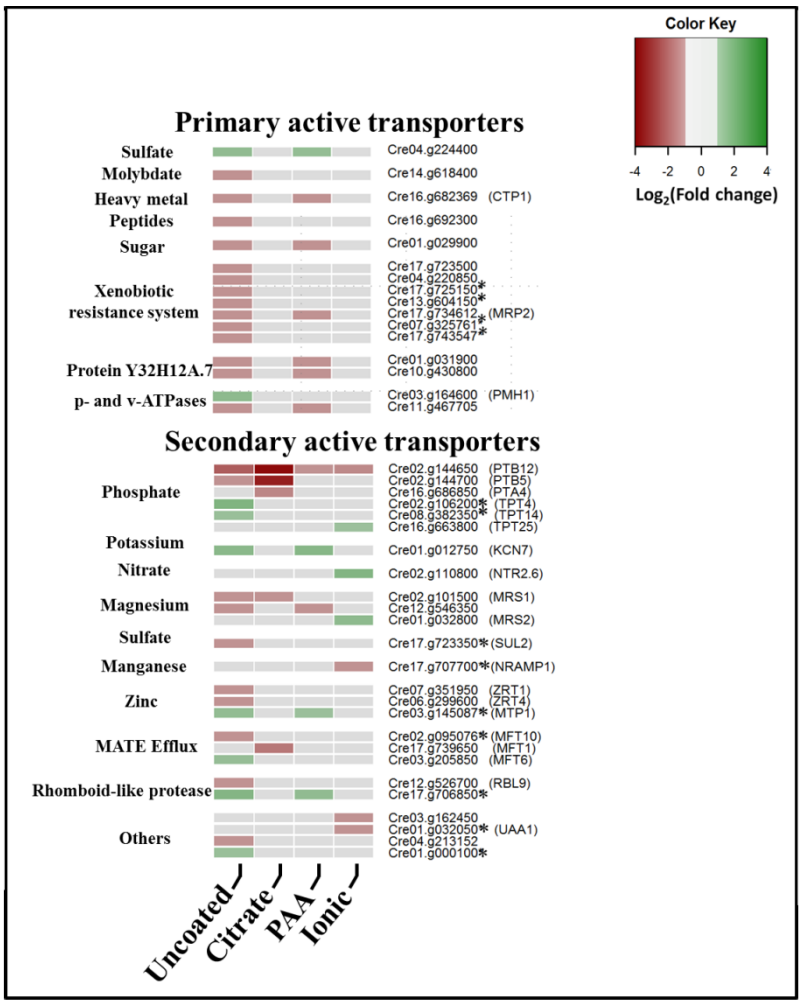

Figure 3. – Heat maps depicting fold changes in transcript levels of transport-related genes regulated by uncoated Ce ENPs (39.33 ± 10.02 µg L^{-1})), citrate stabilized Ce ENPs (33.2 ± 5.6 µg L^{-1}), PAA coated Ce ENPs (70.7 ± 2.2 µg L^{-1}), and ionic Ce (60.7 ± 3.9 µg L^{-1}) with respect to

control ($Log_2FC > |1|$, $p_{adj} < 0.001$) following a 2 h exposure of *C. reinhardtii*. Red represents the genes that were induced by the treatment ($Log_2FC < -1$) while green represents those that were repressed ($Log_2FC > 1$), Grey: $-1 \geq Log_2\ FC \leq 1$. Acronyms are given for genes with annotated functions. Asterisks indicate genes that are differentially expressed between uncoated Ce ENPs and ionic Ce ($Log_2FC > |1|$, $p_{adj} < 0.001$).

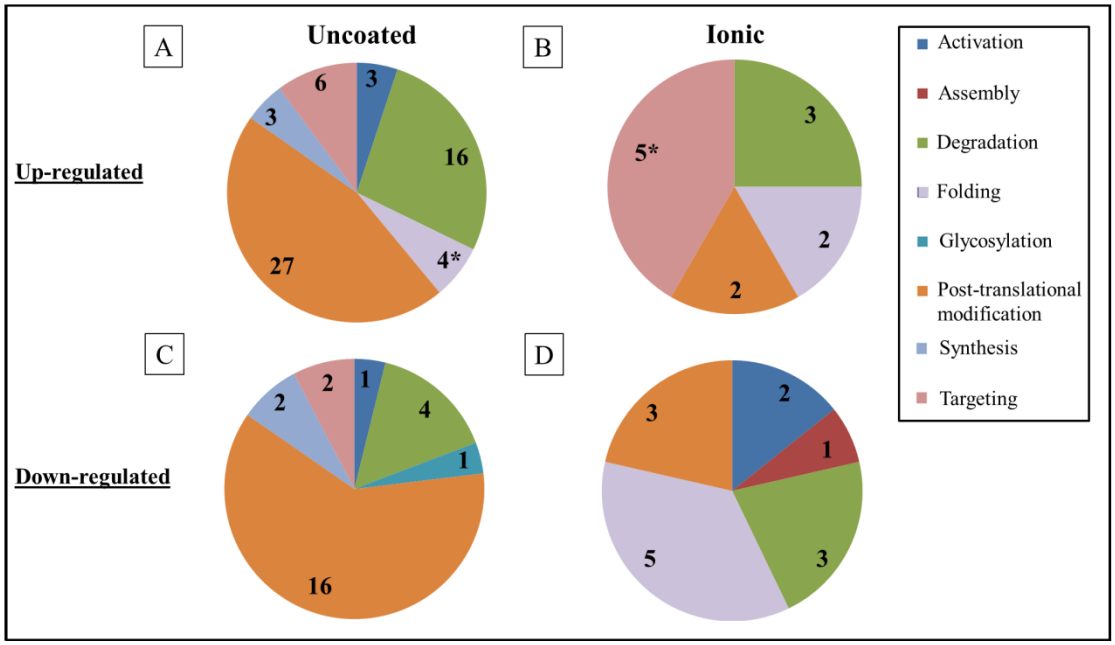

Figure 4. – Up-regulated (A, B) and down-regulated (C, D) gene percentages for different sub-pathways of protein metabolism in *C. reinhardtii* exposed to uncoated Ce ENPs (A, C) and ionic Ce (B, D). The numbers represent the number of DEGs (DeSeq2, $Log_2FC > |1|$, $p_{adj} < 0.001$). Asterisks indicate enriched molecular sub-pathways (Wilcoxon test, $p < 0.05$).

Combination of the above results strongly suggests that bioavailability was different for ionic and particulate forms of Ce. Although the above discussion focused largely on the uncoated Ce ENPs, very similar results were found for the PAA coated ENPs (discussed further below), in agreement with the PCA plot (**Figure S8**). In contrast, exposure to the citrate stabilized Ce ENPs induced several pathways that were common with those induced following exposure to ionic Ce

(e.g. no implication of the xenobiotic resistance system). Differences among the different ENPs are discussed in the following section.

RNA-Seq profiling revealed differences (and similarities) among the effects of surface coatings on Ce bioavailability and cell physiology

As above, differences among the different ENP particle coatings were inferred from DEG numbers, the magnitude and direction of their regulation and pathways in which they are known to function (**Table SIII, Figure S9**). For example, Ce ENPs with a citrate stabilized coating resulted in only 23 DEGs, whereas uncoated and PAA coated Ce ENPs induced 688 and 315 DEGs, respectively (**Figure 2.A, 2.B**). The relatively weak transcriptomic response to the citrate stabilized Ce ENPs was consistent with observations performed on a cultured human cell line (72 h, 21.25 mg L^{-1}) where only 13 DEGs were detected after exposure to a similar citrate stabilized ENPs whereas 1643 DEGs were induced following exposure to small uncoated Ce ENPs (3 nm).[117]

The majority of DEGs elicited by a given Ce ENP were not elicited by any of the other Ce ENPs (**Figure 2.B**). Nonetheless, some overlap of the signatures of two or all three of the Ce ENPs suggest the occurrence of common nano-effects. For example, transcriptomes of microalgae exposed to the uncoated Ce ENPs do not significantly differ from those exposed to PAA coated ENPs ($Log_2FC > |1|$, $p_{adj} < 0.001$) (**Figure 2.C, Figure S10.C**) in spite of important differences in their physicochemical properties (i.e. Ce(III)/Ce(IV) ratio, surface coatings) and their resulting stabilities (i.e. agglomeration state) (**Figure 1**). Moreover, 247 DEGs were common to the uncoated and PAA coated Ce ENPs, however, only 5 DEGs were common to the three Ce ENPs (**Figure 2.B**). Of the 688 DEGs that were identified for the uncoated ENPs ($Log_2FC > |1|$, $p_{adj} < 0.001$), 6 were also differentially expressed in regard to citrate stabilized Ce ENPs ($Log_2FC > |1|$, $p_{adj} < 0.001$) (**Figure 2.C**).

For each of the three Ce ENP types, ontological analysis (MapMan) was carried out to identify biological processes involving multiple DEGs **(Table SIII, Supplementary Data 2**). A major observation was that the uncoated and PAA coated altered expression of genes in protein folding and selective degradation; i.e. proteome homeostasis (i.e. 85 DEGs for uncoated; 41 DEGs for PAA coated; **Table SIII, Figure S9, Supplementary Data 5**). Such effect was not induced by citrate stabilized Ce ENPs. For example, uncoated and PAA coated Ce ENPs altered

the expression of proteins involved in protein folding and selective protein degradation by the ubiquitin-proteasome system (UPS) (i.e. 13 DEGs for uncoated; 5 DEGs for PAA coated) (**Figure S9, Supplementary Data 5**). In *C. reinhardtii,* increases in proteasome activity and protein ubiquitination have previously been reported to occur during various abiotic stresses,[148] e.g. exposure to selenite.[149] Another study found upregulation of transcripts encoding proteasome subunits during exposures to TiO_2 ENPs, ZnO ENPs or quantum dots.[150] As molecular chaperones and the UPS manage non-native proteins, these results might reflect the propensity of these Ce ENPs to cause protein damage, misfolding, or both.

Another clear difference between the effects of the citrate stabilized Ce ENPs and the two other ENPs involved the active trans-membrane transport of small molecules (**Figure 3)**. These include the upregulation of transcripts encoding primary active transporters related to detoxification;[151,152] pleiotropic drug resistance proteins and P-glycoproteins and multidrug resistance associated proteins of the xenobiotic resistance system (**Supplementary Data 4**). Members of these protein families are also up-regulated following exposure to cadmium,[153] mercury[154] or aluminum.[155] Additionally, citrate stabilized Ce ENPs upregulated the expression of a secondary active transporter (*MFT1*) that may be involved with xenobiotic sequestration or efflux (**Figure 3**).[156] In rice, *MFT1* is induced by exposure to Al and is suspected to drive the efflux of Al-citrate.[157]

Phosphate and magnesium transporters were notable in that they were affected by all of the treatments, although phosphate transport enrichment was only found for the uncoated and citrate stabilized Ce ENPs (**Table SIII, Figure 3)**. As the secondary active transporters were up-regulated and each is selective for Mg[158] or phosphate[159] **(Supplementary Data 4)**, their induction likely reflected perturbations of both phosphate and magnesium homeostasis rather than Ce biouptake. For example, a type B high affinity phosphate transporter (*PTB12*) is thought to lead to increased internalization of phosphate,[159] and its strong induction found for all treatments likely reflects the ability of ionic Ce and Ce ENPs to reduce phosphate bioavailability either through direct competition for phosphate or after hydrolysis of phosphate ester bonds.[88] Similarly, two results strongly suggest that these responses do not reflect the induction of Ce *efflux*. First, there was no effect on the expression of the candidate Ce transporters (e.g. non-specific metal transporter such as permeases[160] or Ca^{2+} channels[3]) by ionic Ce or the Ce ENPs,

(**Supplementary Data 4**). Second, for cells exposed to ionic Ce, no regulation of transcription was observed for genes involved in the xenobiotic resistance system, in contrast to results for the ENPs.

Ce and Ce ENPs induce genes for acclimation, but not major cellular damage

None of the Ce forms (ionic or ENPs) appeared to be particularly toxic to *C. reinhardtii* at 70 μg L^{-1} Ce (nominal concentration). For example, no damage biomarkers (e.g. DNA damage or apoptosis signaling) were induced by any of the Ce treatments. Furthermore, the up-regulation of key oxidative stress enzymes involved in the detoxification of reactive oxygen species (e.g. catalase acting in peroxisomes[161]) was not observed (**Supplementary Data 6**). The absence of clear evidence for toxicity is reasonable, considering the sub-lethal exposure concentrations and the short exposure times that were used. Indeed, with the notable exception of a 72h EC50 value for growth inhibition that was 26 μg L^{-1} for PAA coated Ce ENPs[110], much higher (i.e. mg L^{-1}) concentrations of Ce ENPs are generally required to induce toxicity (e.g. lowest-observed-effect concentration (LOEC) of >1 mg L^{-1} for a 72 h exposure of *P. subcapitata*[72]). However, transcript levels of genes related to flagella structure were specifically impacted by Ce ENPs. The uncoated and the PAA coated Ce ENPs also up-regulated mRNA levels of biomarkers of detoxification processes. The molecular responses observed for our exposure conditions (2h, <70 μg L^{-1}), are thus thought to mainly reflect biological responses that allow the microalgae to manage stress.

Relating ENP characterization to bioavailability

The experiment was designed to compare the bioavailabilities of the three ENPs. On paper, the three ENPs had similar sizes, compositions and concentrations. In reality, careful characterization showed that: (i) uncoated Ce ENPs agglomerated significantly; (ii) citrate stabilized Ce ENPs showed limited agglomeration; (iii) some or a majority of the Ce(IV) in the PAA stabilized Ce ENPs was transformed into Ce(III) (either adsorbed Ce^{3+} or Ce_2O_3); (iv) dissolved solutions of ionic Ce actually contained significant quantities of Ce nanoparticles (likely metastable Ce polymers due to hydrolysis). Thus, extensive characterization is necessary in order to properly interpret complex, high throughput exposures examining the biological effects of engineered nanomaterials. While this point may seem obvious to most, some reports

characterize only the stock solutions. Our multi-method characterization showed that different results were obtained for the concentrations and experimental conditions used for the exposures.

ENP bioavailability was not limited to the smallest Ce ENPs (i.e. < 20 nm). In spite of their different sizes, surface charge/coating and Ce(III)/Ce(IV) ratios, uncoated and PAA coated Ce ENPs exhibited few differences with respect to the molecular targets examined at transcriptomic level. One potential explanation is that after microalgae introduction, protein corona or microalgal exudates homogenizes the different ENPs, at least in relation to the microorganism at the level of the biological interface. This also implies that it was the citrate released from the citrate stabilized ENPs that was responsible for the differences observed for that particle. Free citrate in solution could either complex Ce, reducing its bioavailability, or stimulate the microalgae as a fundamental metabolite.

Biological interpretations of the transcriptomic results were limited by the quantity and quality of gene annotation available for *C. reinhardtii* as well as the lack of integrative tools required to interpret the data. For example, important numbers of genes responding to Ce ENPs and/or ionic Ce were either not assigned to a biological pathway (i.e. 244 DEGs) or not associated with a known function (i.e. 266 DEGs) (**Supplementary Data 7**). Thus, it is possible that some key deleterious or beneficial responses might have not been explored completely in the present study. Nonetheless, a promising pool of Ce-responsive genes was identified, which may constitute interesting exposure biomarkers for future experiments and bioassay development (**Supplementary Data 8)**. For example, g15615, a putative ferredoxin was repressed by ionic Ce but induced by uncoated Ce ENPs. Although whole-genome expression analysis provided important information on the potential biological effects of the Ce ENPs, different exposure times, exposure concentrations and biological scales (proteomic and metabolomics) will be required in order to provide more complete information on the impact of the Ce ENPs at the scale of the organism or population. Indeed, important post-transcriptional modifications may occur in *C. reinhardtii* over time scales that have not been taken into account by the short-term approach deployed here.

Conclusions

The results revealed that (i) the Ce ENPs examined in this study are bioavailable; (ii) Ce ENPs had nano-effects that were distinct from the effects of ionic Ce; (iii) coatings could affect the bioavailability and biological effects of Ce ENPs and that (iv) citrate stabilized Ce ENPs appeared to have the fewest effects on the microalgae, likely due to the beneficial effects of citrate desorption from the ENP surface. Our results also suggest that *C. reinhardtii* acclimates to Ce ENPs by remodeling of the UPS, moderate increases in the expression of molecular chaperones and by alterations of the flagella or deflagellation that might reflect a middle stress for short term exposures of *C. reinhardtii* at environmentally relevant concentrations. Several of the DEGs that have been identified here could be used as exposure biomarkers of environmental Ce contamination.

Acknowledgements

Funding for this work was provided by the Natural Sciences and Engineering Research Council of Canada (NSERC Discovery and Strategic projects grants) and the Fonds de Recherche du Québec - Nature et Technologies (FRQNT). Special thanks to Madjid Hadioui for his expert advice on the ICP-MS and SP-ICP-MS analyses.

Supplementary information

Optimization

SP-ICP-MS

With increasing dilution, the signal to noise ratio of the transient Ce signal increased due to a dilution of the dissolved metal in the ENP suspensions. ENP numbers were determined from a range of dilutions but based upon the smallest valid dilution for which corrected particle numbers were invariable (**Figure S1**).

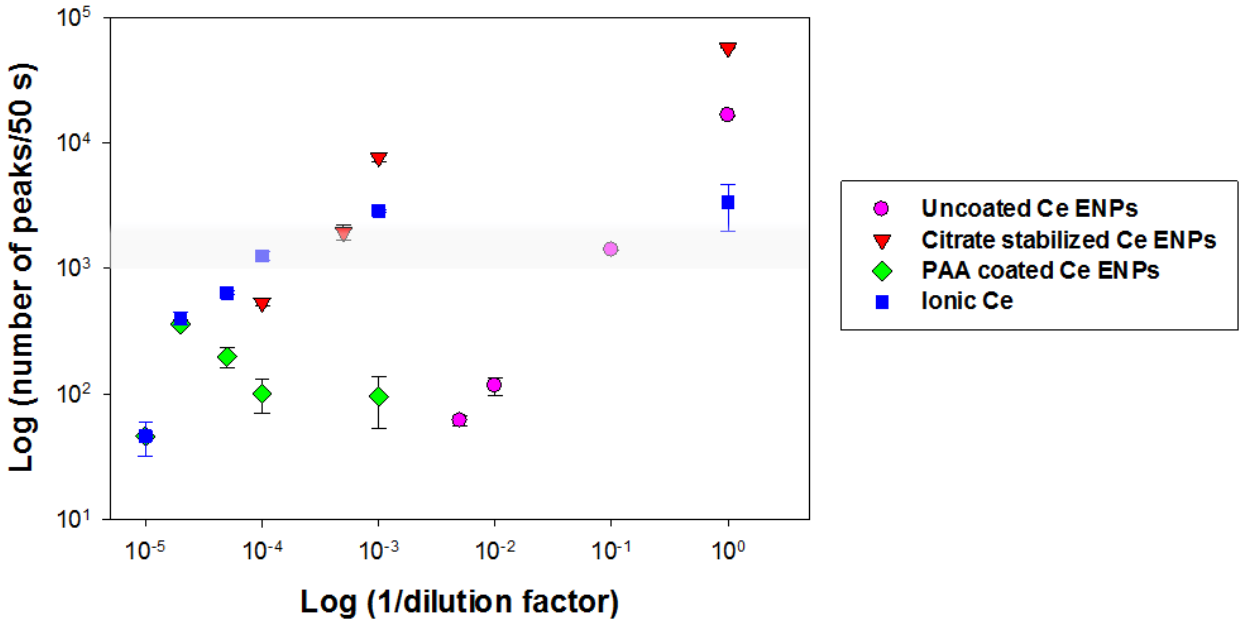

Figure S1. Number of peaks detected by SP-ICP-MS in 50 s as a function of 1/dilution factor for uncoated Ce ENPs (pink circles), citrate stabilized Ce ENPs (red triangles), PAA coated Ce ENPs (green diamonds) and ionic Ce (blue squares). The lightly shaded interval indicates the zone where particle numbers are optimized for detection (i.e. enough peaks to be statistically significant, but not so many that ENPs are detected concurrently (indicated by a decrease in slope)). Based upon the figure, uncoated Ce ENPs were diluted 10x, citrate stabilized Ce ENPs were diluted 2000x, PAA coated Ce ENPs were diluted 20000x and ionic Ce was diluted 10000x prior to SP-ICP-MS measurement. Errors correspond to the standard deviations; n = 2.

Ultrafiltration

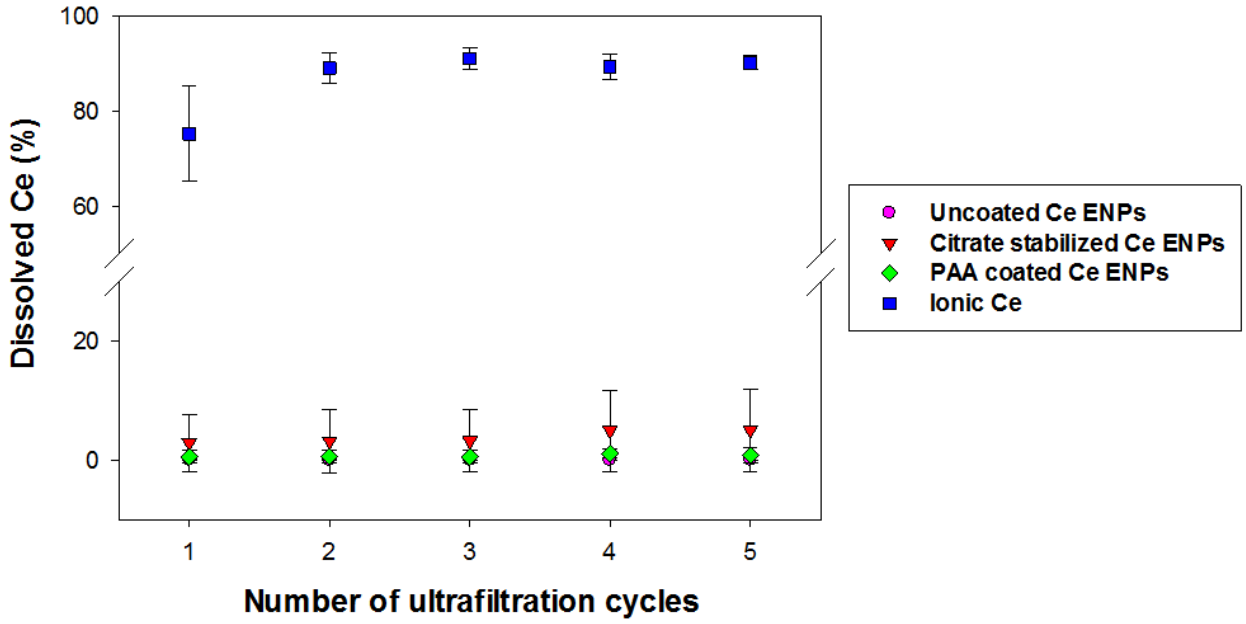

Figure S2. Dissolved Ce detected (%) after 24 h of stabilization in exposure medium (NaHEPES, pH 7.0) containing the uncoated Ce ENPs (pink circles), citrate stabilized Ce ENPs (red triangles), PAA coated Ce ENPs (green diamonds) or ionic Ce at a nominal concentration of 70 µg L^{-1} Ce. Results are provided as a function of the number of centrifugal ultrafiltration cycles realized with the same filter membrane. Errors correspond to the standard deviations; n = 3 to 5.

Exposure concentrations

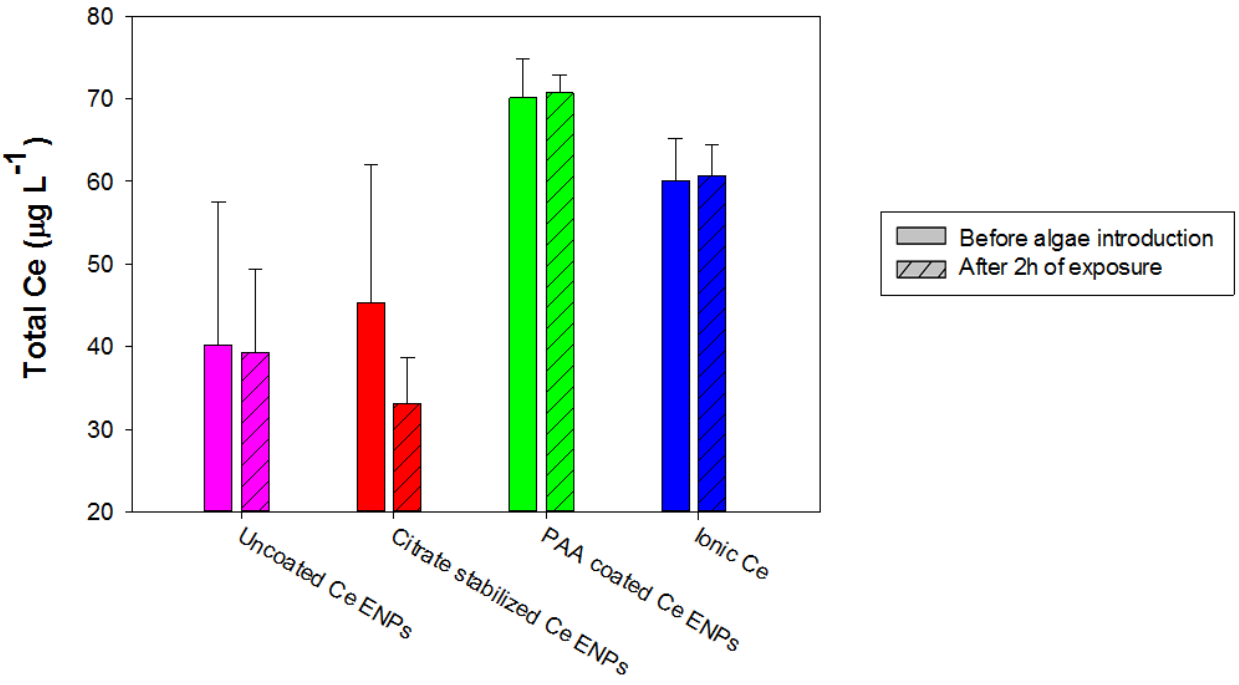

Figure S3. Measured total Ce concentrations after 24 h of stabilization in exposure medium for RNA-Seq experiments (NaHEPES, pH 7.0, nominal Ce concentration = 70 µg L^{-1}) and then after a 2 h exposure of the algae to uncoated Ce ENPs (pink), citrate stabilized Ce ENPs (red), PAA coated Ce ENPs (green) and ionic Ce (blue). Errors correspond to the standard deviations; n = 3.

ENP characterization

Ce ENPs were thoroughly characterized in order to correlate their properties with their biological effects, as assessed by RNAseq below. Sizes were determined by TEM, SP-ICP-MS, DLS and AUC; surface (zeta) potential was evaluated using electrophoretic mobility measurements; dissolution was quantified using centrifugal ultrafiltration and SP-ICP-MS and redox properties were determined using XPS.

Sizes and dissolution

Primary physical diameters (d_p) of Ce ENPs were first analyzed by TEM on the dry material. TEM revealed that Ce ENPs were roughly spherical with a d_p of the primary particles (i.e. excluding agglomerates) of 9.7 ± 2.8 nm for the uncoated Ce ENPs, 4.4 ± 0.9 nm for the citrate stabilized Ce ENPs and 3.0 ± 0.8 nm for the poly-acrylic acid coated Ce ENPs (**Table SI - Figure S4)**. TEM by Auffan *et al.* found a similar size of 3.9±1.8 nm for the citrate stabilized Ce ENPs from the same producer.[112]

Table SI. ENP mean diameters, polydispersity index (PDI), % of mass detected as ENPs and recovery obtained for TEM, AUC, DLS, SP-ICP-MS or analysis by ultrafiltration (3 kDa membrane) for uncoated, citrate stabilized and PAA coated Ce ENPs in NaHEPES at pH 7.0.

$[Ce]_T$ ($\mu g\ L^{-1}$)	Technique	Type of diameter	Mean size distribution (nm)	PDI	% of ENPs detected	Recovery (%)
Ionic Ce						
0.0039 ± 0.0005	SP-ICP-MS	d_p	8.4 ± 0.3	0.16 ± 0.07	35.7 ± 27.7	41.8 ± 2.1
66.6 ± 9.5	Ultrafiltration	-	-	-	21.3 ± 11.3	106.5 ± 2.3
Uncoated (Nanostructured & Amorphous Materials)						
10,380	TEM	d_p	9.7 ± 2.8	-	-	-
50,000 ± 2,000	AUC	d_h	8.0 ± 0.1	0.29 ± 0.04	90.5 ± 3.6	-
50,000 ± 2,000	DLS	d_h	6692 ± 2026	0.51 ± 0.23	100 ± 0.0	-
0.050 ± 0.014	SP-ICPMS	d_p	19.7 ± 1.2	0.95 ± 0.10	98.5 ± 2.1	9.2 ± 0.3
50.5 ± 9.7	Ultrafiltration	-	-	-	99.9 ± 0.0	101.1 ± 3.6
Citrate stabilized (Byk)						
9,780	TEM	d_p	4.4 ± 0.9	-	-	-
42,400 ± 300	AUC	d_h	4.1 ± 0.1	0.02 ± 0.01	96.6 ± 3.0	-
42,400 ± 300	DLS	d_h	6.2 ± 0.3	0.13 ± 0.03	99.6 ± 0.3	-
0.022 ± 0.010	SP-ICP-MS	d_p	22.9 ± 2.4	0.34 ± 0.08	99.0 ± 0.6	57.6 ± 9.5
55 ± 25	Ultrafiltration	-	-	-	99.8 ± 0.2	82.5 ± 0.7
PAA coated (Sciventions)						
9,980	TEM	d_p	3.0 ± 0.8	-	-	-
47,400 ± 500	AUC	d_h	3.1 ± 0.3	0.39 ± 0.05	90.2 ± 2.8	-
47,400 ± 500	DLS	d_h	5.9 ± 2.9	0.64 ± 0.28	99.6 ± 0.4	-
0.0049 ± 0.0014	SP-ICP-MS	d_p	9.9 ± 2.5	0.32 ± 0.29	9.3 ± 2.4	44.6 ± 8.6
70.4 ± 2.9	Ultrafiltration	-	-	-	99.5 ± 0.9	99.7 ± 8.7

Errors correspond to standard deviations obtained for 2 to 4 replicates while PDI gives an indication of the overall particle size distribution. dh: hydrodynamic diameter; dp: physical diameter.

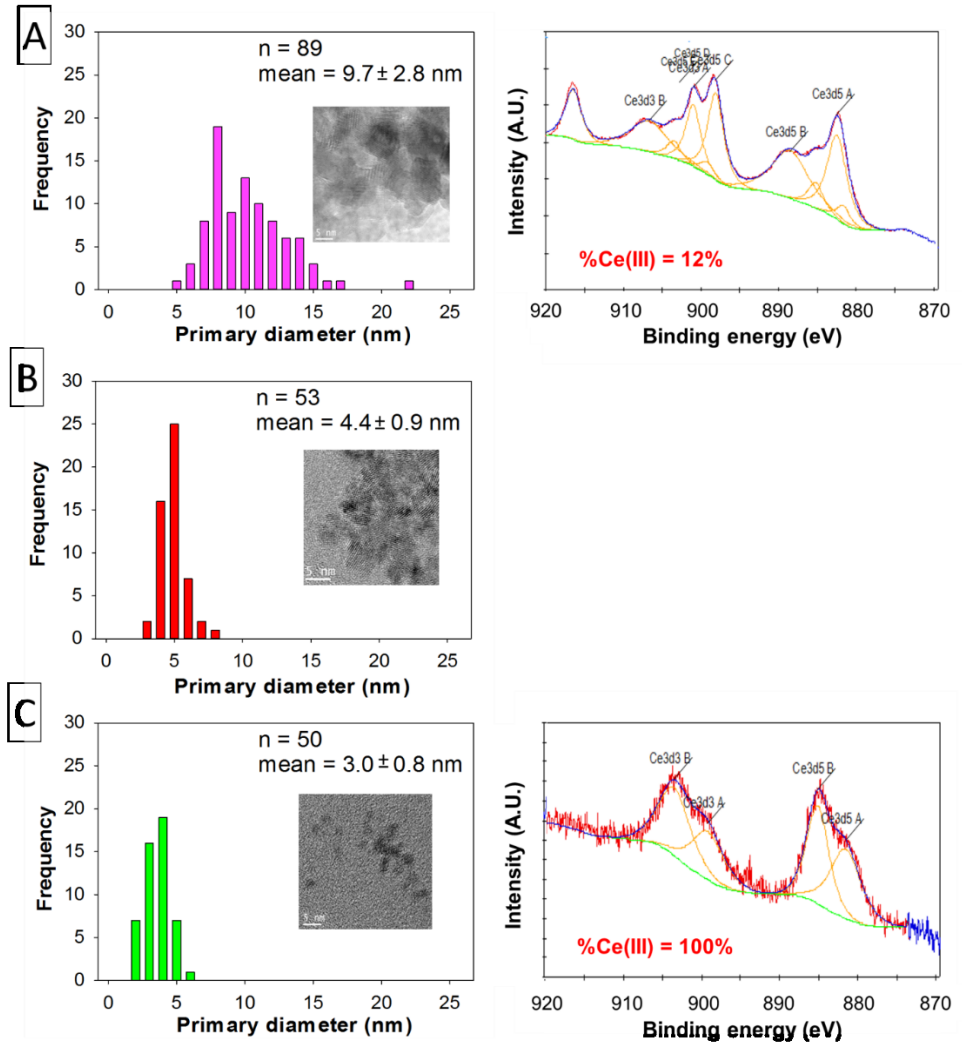

Figure S4. Distributions of physical diameters determined from TEM (TEM micrograph in inset) and Ce(III) composition (XPS spectra of Ce3d on the right) for (A) the uncoated Ce ENPs, (B) the citrate stabilized Ce ENPs and (C) the PAA coated Ce ENPs. For TEM; n: number of analyzed ENP, mean: mean physical diameter obtained ± standard deviation. For XPS spectra; Green curves: background, Fed curves: data, Orange curves: component peaks (881.6, 885.1, 899.2 and 903.5 eV for Ce(III) and 882.6, 888.4, 898.2, 901.1, 906.7 and 916.5 eV for Ce(IV), Blue curve: fitting (sum of component curves). The citrate stabilized Ce ENPs were obtained in a suspension and could not be analyzed, however, its Ce(III) composition was extracted from Auffan *et al.* [112]

The physical diameters and dissolution of the Ce ENPs ***in the exposure medium*** were then assessed by SP-ICP-MS. Samples were diluted (3.9 – 50 ng L^{-1} Ce) immediately preceding analysis in order to avoid coincident events, while maintaining sufficient particle numbers (between 1000 to 2000 ENPs). Uncoated Ce ENPs were partially agglomerated, with a mean d_p of 19.7 nm (**Table SI**). Due to their high polydispersity (PDI = 0.95 ± 0.10), these ENPs were more accurately characterized using their mode diameter (9.0 nm), which was in close agreement with TEM results (**Figure S5**). Agglomeration was also important for the citrate stabilized Ce ENPs, which had a d_p of 22.9 nm and a PDI of 0.34 ± 0.08. However, in this case, the mode d_p (mode d_p = 8.0 nm) was almost 2× higher than the d_p obtained by TEM (i.e. 4.4 ± 0.9 nm). This difference can be explained by the small size of citrate stabilized ENPs which is close to the size detection limit (SDL) of the SP-ICP-MS (3.9 – 5.1 nm). Indeed, below ~5 nm, many ENPs may have been attributed to the dissolved fraction. This explanation could also account for the low proportion of particulate Ce detected in PAA-coated Ce ENPs suspension (9.3 ± 2.4 %). The (false) attribution of the smallest (below SDL) PAA coated and citrate stabilized ENPs to the dissolved fraction is consistent with results obtained by centrifugal ultrafiltration (**Table SI**), where no dissolved Ce was detected in the exposure media. Finally, a surprisingly large fraction of ionic Ce was attributed to the particulate fraction by both SP-ICP-MS (36 ± 28%) and centrifugal ultrafiltration (21 ± 11%) (**Table SI**). The formation of incidental Ce containing nanoparticles from solutions of ionic Ce at neutral pH was consistent with previous work that postulated the formation of metastable oxide or hydroxide precipitates[30], even at these very low Ce concentrations. It is a strong indication that exposure solutions containing ionic Ce do not simply contain Ce^{3+}.

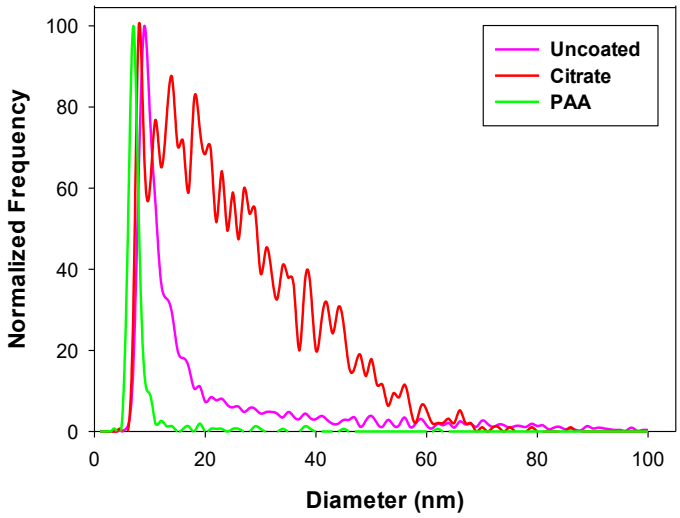

Figure S5. Representative size distributions of uncoated Ce ENPs (pink), citrate stabilized Ce ENPs (red) and PAA coated Ce ENPs (green) as determined by a high- resolution SP-ICP-MS (dwell time 50 µs). Suspensions were prepared in the exposure solutions (10 mM NaHEPES, 10^{-5} M Ca, pH 7.0).

Finally, Ce ENP suspensions were analyzed by DLS and AUC. These measurements are complementary to SP-ICP-MS because they characterize the hydrodynamic diameters (d_h) of suspended particles, although measurements are necessarily performed on more concentrated suspensions (i.e. 40 to 50 mg L^{-1} Ce, NaHEPES at pH 7.0). At these high concentrations, the two coated ENPs were well dispersed with d_h of less than 10 nm **(Table SI)**. For the uncoated Ce ENPs, d_h of 8.0 ± 0.1 nm was determined by AUC, which was in line with the primary size obtained by TEM, whereas micrometer-size agglomerates were detected by DLS (**Table SI**). Given that large agglomerates sediment too quickly to be detected by AUC and since light scattering is biased towards the larger particles (roughly proportional to d_h^6), the results for the uncoated ENPs are consistent with the co-existence of individual particles and larger agglomerates (**Table SI**). Agglomeration was also consistent with electrophoretic mobility measurements that showed that the uncoated Ce ENPs had a less (negative) surface potential than the two coated ENPs (i.e. at pH 7.0, uncoated: -0.8 ± 0.5 µm.cm/s.V; citrate stabilized: -1.4 ± 0.3 µm.cm/s.V; PAA coated: -1.6 ± 0.2 µm.cm/s.V, **Figure S6**).

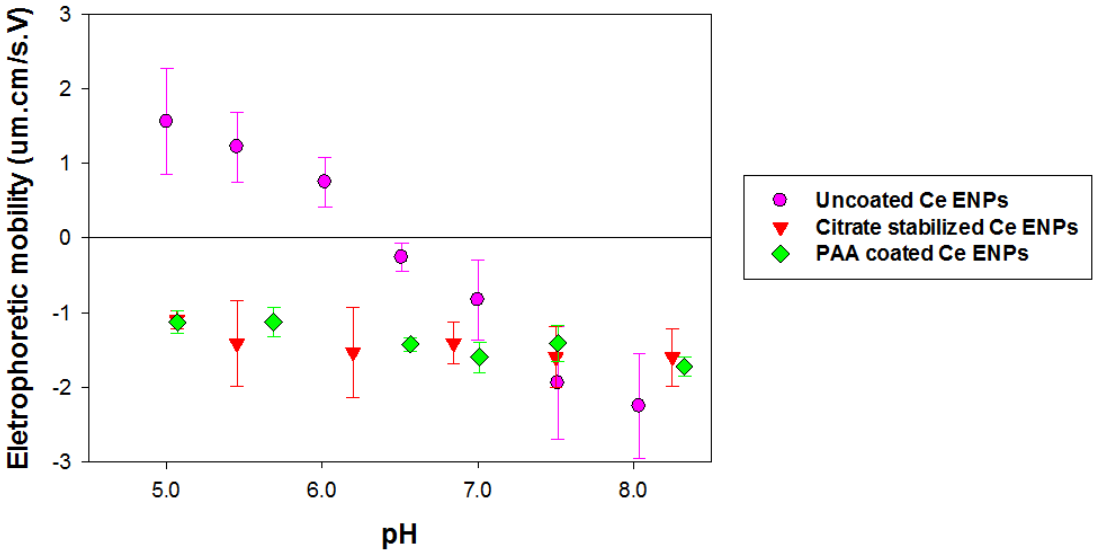

Figure S6. Electrophoretic mobility (µm.cm/s.V) of 40-50 mg.L^{-1} of the uncoated (pink circle), citrate stabilized (red triangle) and PAA coated (green square) Ce ENPs as function of pH in media buffered by NaMES between pH 5.0 and 6.0 and NaHEPES for pH 6.5 to 8.5. For the coated ENPs, these electrophoretic mobilities corresponded to zeta potentials of ~ -20 mV, which appeared to be sufficient to stabilize the ENP suspensions via electrostatic repulsions. The pH_{zpc} of the uncoated Ce ENPs was ~ 6.3. Errors correspond to the standard deviations; n= 2 to 4.

Ce valency

The redox characteristics of Ce at the ENP surface are thought to be major determinants of the effects of Ce ENP on organisms,[72,81] with generally higher toxicity for higher proportions of Ce(III) at the particle surface.[79] According to the manufacturers, the Ce ENPs used in this study were composed mostly of Ce(IV) (i.e. CeO_2 ENPs). However, analysis of Ce(III)/Ce(IV) ratios by XPS revealed that the uncoated Ce ENPs had 12% Ce(III) whereas the PAA coated Ce ENPs had nearly 100% Ce(III) (**Figure S4)**. Indeed, XPS measurements for the PAA coated Ce ENPs suggested that they were largely organic with a mixture of Ce_2O_3 and Ce bound to the carboxylate groups (polyacrylate, oxalate). The results contrast with XRD (x-ray diffraction) data provided by the manufacturer, which suggested a crystalline CeO_2 structure. This discrepancy could be explained by an expected structural transformation from CeO_2 to Ce_2O_3 that is observed

for small (< 20 nm) Ce ENPs.[162,163] Nonetheless, an underestimation of the core Ce(IV) cannot be excluded for these ENPs. Finally, while the citrate stabilized Ce ENPs were obtained in a suspension and could not be analyzed, earlier work by Auffan et al. (2014) on the same ENPs from the same producer, concluded that they contained ≤10% Ce (III).[112]

RNA-Seq data

Overview

Table SII. Mapping statistics (mean ± standard deviation, n = 3 (for treatments) to 4 (for controls) resulting from the TopHat2 alignment on *C. reinhardtii* reference genome (version 5.3) and analysis of differential gene expression (DeSeq2, padj < 0.001, Log2FC > |1|).

Treatment	Concentration ($\mu g\ L^{-1}$)	Number of sequenced reads ($\times 10^6$)	% of read alignment	Number of DEGs		
				Up-regulated	Down-regulated	Total (% detected)
Ionic	60.65 ± 3.87	66.2 ± 2.3	93.4 ± 0.4	71	67	138 (0.8)
Uncoated	39.33 ± 10.02	61.6 ± 3.3	92.7 ± 0.6	485	202	687 (4.1)
Citrate	33.15 ± 5.58	65.3 ± 3.8	92.9 ± 0.3	21	2	23 (0.1)
PAA	70.72 ± 2.15	66.0 ± 6.7	92.7 ± 0.2	239	76	315 (1.9)
Control	Q.L.	62.2 ± 5.5	94.1 ± 0.5	-	-	-

Q.L.: under quantification limit, DEGs: differentially expressed genes.

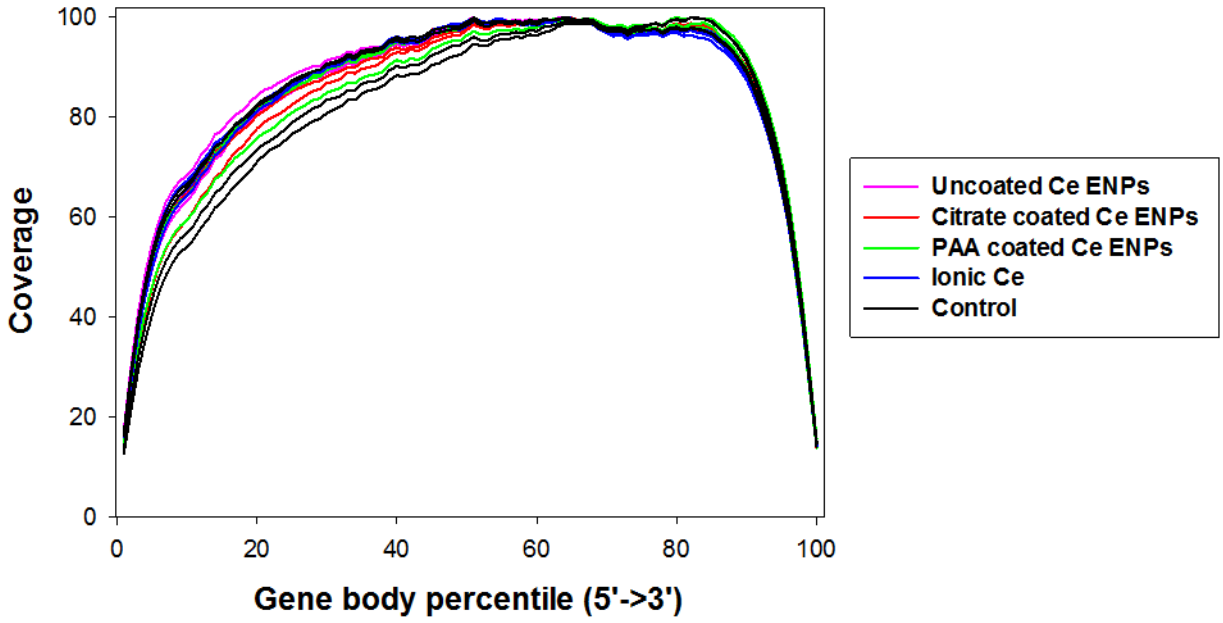

Figure S7. Spatial repartition of normalised read numbers obtained by RNA-Seq over the gene length (5'->3') for each biological replicate (n=3 for treatments or n=4 for controls) of the uncoated Ce ENPs (pink), the citrate stabilized Ce ENPs (Red), the PAA coated Ce ENPs (green) and the ionic Ce (blue) treatments and the control (black) (geneBodyCoverage).

Principal component analysis (PCA)

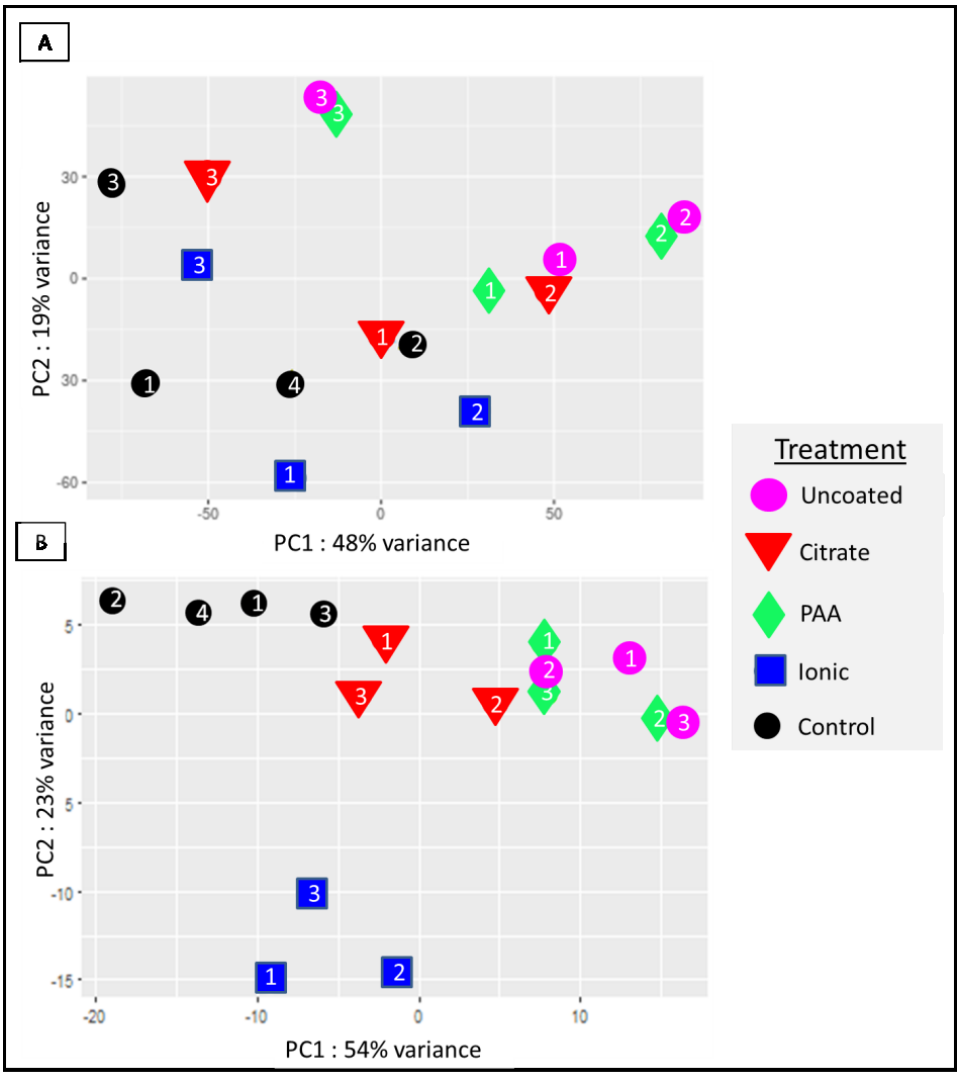

Figure S8. PCA scores from analysis of (A) entire transcriptome (16,808 transcripts, RNA-Seq) or (B) DEGs with the respect to control (848 genes, DeSeq2, $Log_2FC > |1|$, $p_{adj} < 0.001$) for *C. reinhardtii* after a 2 h exposure: uncoated Ce ENPs (pink circles, 39.3 ± 10.0 µg L^{-1}), citrate stabilized Ce ENPs (red triangles, 33.2 ± 5.6 µg L^{-1}), PAA coated Ce ENPs (green diamonds, 70.7 ± 2.2 µg L^{-1}), ionic Ce (blue squares, 60.7 ± 3.9 µg L^{-1}), and control (black circles).

When differential expression levels of the entire transcriptome were compared, PCA was unable to identify clear covariances among the treatments (**Figure S8.A**). With the false discovery threshold adjusted was 0.001 and with a minimal cutoff of 15 reads, 848 genes showed a minimum of 2-fold change with respect to their control values in one or more of the treatments **(Supplementary Data 2)**. When those DEGs were analyzed by principal component analysis, data were grouped around the Ce ENPs (associated with PCA1, 54% of variance) and ionic Ce (associated with PCA2, 23% of variance) (**Figure S8.B**).

Functional annotation analyses

Table SIII. Number of DEGs (with respect to control) in different metabolic pathways (MapMan) for *C. reinhardtii* following a 2 h exposure to uncoated Ce ENPs, citrate stabilized Ce ENPs, PAA coated Ce ENPs and ionic Ce. In the final two columns, ionic Ce was compared to the uncoated ENPs with respect to the number of common genes or the number of DEGs.

Metabolic pathways	Versus Control				Ionic versus Uncoated	
	Uncoated	Citrate	PAA	Ionic	Common	DEGs
Amino acid	6	0	1	2	0	2
Degradation	2	0	1	0	0	0
Synthesis	4	0	0	2	0	1
Cell	37	3	25	4	2	13
Cycle	2	0	1	0	0	1
Mobility	18	3	14	1	0	7
Organisation	11	0	9	0	0	4
Vesicle transport	6	0	1	3	2	1
Cell wall	1	0	0	0	0	1
Cofactor and vitamin synthesis	2	0	0	0	0	0
Development	2	0	1	3	0	3
DNA	10	0	5	2	1	5
Repair	1	0	1	1	0	2
Synthesis	9	0	4	1	1	3
Glycolysis	0	0	0	1	0	1
Hormones	1	1	0	1	0	0
Abscisic acid	1	0	0	0	0	0
Gibberellin	0	0	0	1	0	0
Jasmonate	0	1	0	0	0	0
Lipid	7	0	3	3	0	5
"exotics"	2	0	1	1	0	2
FA synthesis and FA elongation	0	0	0	2	0	2
Glycolipid synthesis	1	0	0	0	0	1
Lipid degradation	1	0	0	0	0	0
Phospholipid synthesis	3	0	2	0	0	0
Major carbohydrates	1	0	0	0	0	0
Metal handling	1	0	0	0	0	0
Minor carbohydrates	1	0	1	3	0	1
Callose	0	0	0	2	0	1
Others	1	0	1	1	0	0
Miscellaneous enzyme families	10	3	4	3	1	2
Acid and other phosphatases	1	1	1	0	0	0
Calcineurin-like phosphoesterases	1	0	0	0	0	0
Cytochrome P450	1	0	0	0	0	0
GCN5-related N-acetyltransferase	0	1	0	0	0	0
GDSL-motif lipase	1	0	0	0	0	0
Other	2	0	1	0	0	1
Rhodanese	0	0	0	1	0	0
Short chain dehydrogenase/reductase	2	1	2	2	2	0
UDP glucosyl and glucoronyl transferases	2	0	0	0	0	1
Mitochondrial electron transport/ATP synthesis	4	0	1	0	0	1
Alternative oxidase	1	0	0	0	0	0

Cytochrome c oxidase	2	0	1	0	0	1
NADH-DH type II	1	0	0	0	0	0
Nitrogen assimilation	2	0	0	0	0	1
Nucleotide	0	0	1	1	0	1
Deoxynucleotide metabolism cytosine deaminase	0	0	1	0	0	0
Deoxynucleotide metabolism pseudouridine synthase	0	0	0	1	0	1
OPP cycle	0	0	0	1	0	0
6-phosphogluconate dehydrogenase	0	0	0	1	0	0
Photosynthesis	1	0	1	1	0	2
Light reaction, hydrogenase, FeFe-hydrogenase	1	0	1	1	0	2
Protein	85	0	41	24	3	40
Activation	4	0	0	2	0	5
Assembly	0	0	0	1	0	0
Degradation	20	0	12	6	0	8
Folding	4*	0	1	7	1	5
Glycosylation	1	0	1	0	0	1
Post-translational modification	43	0	21	5	1	15
Synthesis	5	0	2	0	0	3
Targeting	8	0	4	5*	1	5
Redox	2	0	2	3	0	4
Ascorbate and glutathione	1	0	1	2	0	2
Thioredoxin	1	0	1	1	0	2
RNA	30	1	10	4	1	10
RNA processing	13	0	3	0	0	4
Regulation transcription	15	1	6	3	1	5
RNA binding	2	0	1	1	0	1
Secondary metabolism	3	0	2	0	0	1
Signalling	17	0	7	3	0	8
Calcium	6	0	3	0	0	2
G-proteins	6	0	3	2	0	3
Light	2	0	0	0	0	1
MAP kinases	1	0	0	0	0	1
Phosphoinositide	2	0	1	1	0	1
Stress	4	2	2	2	0	1
Abiotic	3	0	1	1	0	2
Biotic	1	2	1	1	0	0
TCA / organic acid transformations	3	0	3	1	0	2
Carbonic anhydrases	0	0	1	0	0	0
Other organic acid transformations	2	0	1	0	0	1
TCA, fumarase	1	0	1	1	0	1
Tetrapyrrole synthesis	2	0	0	0	0	1
Porphobilinogen deaminase	1	0	0	0	0	0
Uroporphyrin-III C-methyltransferase	1	0	0	0	0	1
Transport	39	5*	13	8	2	13
ABC transporters	13	0	5	0	0	4
Metabolites	2	0	0	1	0	2
Metals	7	0	2	1	0	3
Nitrates	0	0	0	1	1	0
Nucleotide	1	0	1	0	1	0
Others	5	1	1	1	0	2
P- and V-ATPases	2	0	1	0	0	0
Phosphates	2*	3*	1	1	1	0
Potassium	3	0	1	0	0	0
Sugars	0	0	0	1	0	1
Sulphates	1	1	0	0	0	1
Unspecified anions and cations	3	1	1	2	1	0
Unknown/Not assigned	427	7	197*	73	8	124

Numbers in bold red accompanied by a star (*) are associated with enriched pathways and sub-pathways (Wilcoxon test, $p < 0.05$).

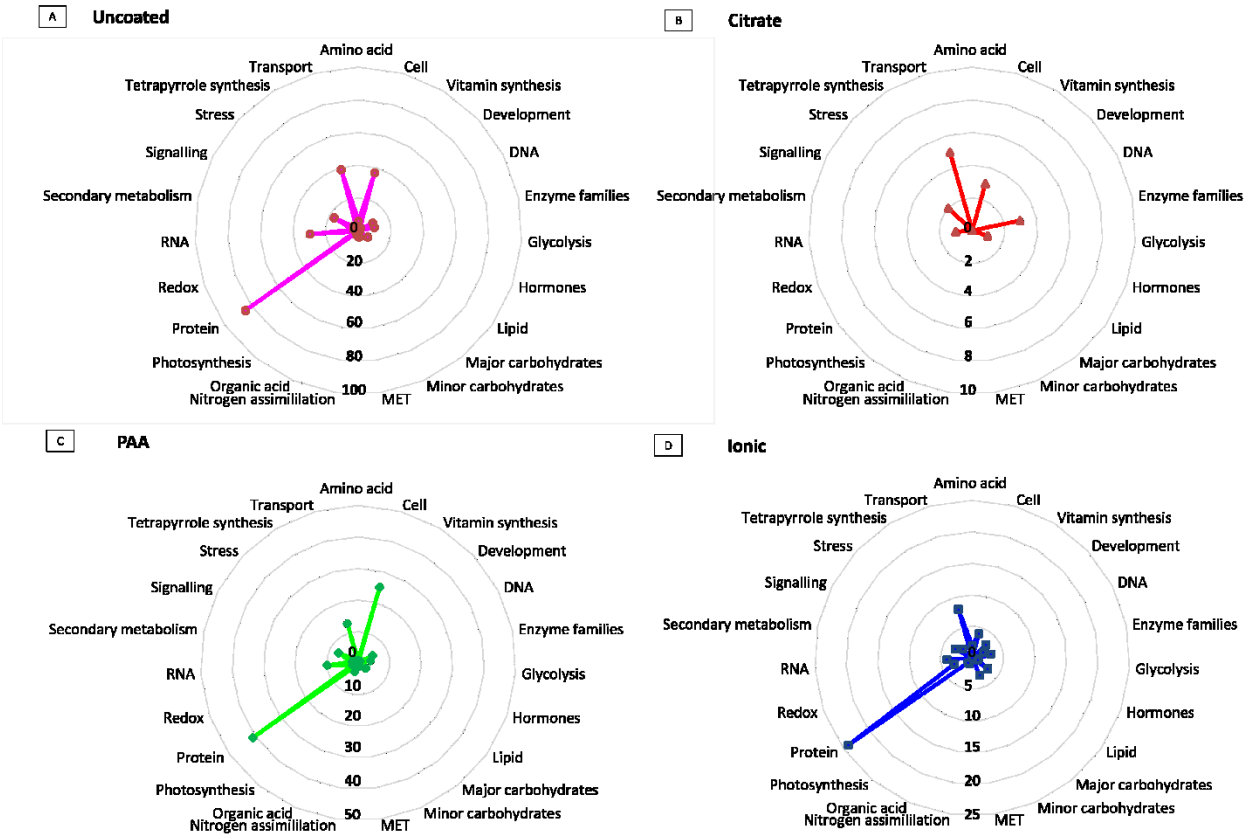

Figure S9. Radar plot showing the number of DEGs relative to the controls (DeSeq2, Log2FoldChange > |1|, p_{adj} < 0.001) according to their metabolic pathways (MapMan). Measurements were performed on *C. reinhardtii* following a 2 h exposure to (A) uncoated Ce ENPs (pink, scale=0 to 100 DEGs), (B) citrate stabilized Ce ENPs (red, scale=0 to 10 DEGs), (C) PAA coated Ce ENPs (green, scale=0 to 50 DEGs)) and (D) ionic Ce (blue, scale=o to 25 DEGs). MET:Mitochondrial electron transport.

Identification of exposure biomarkers

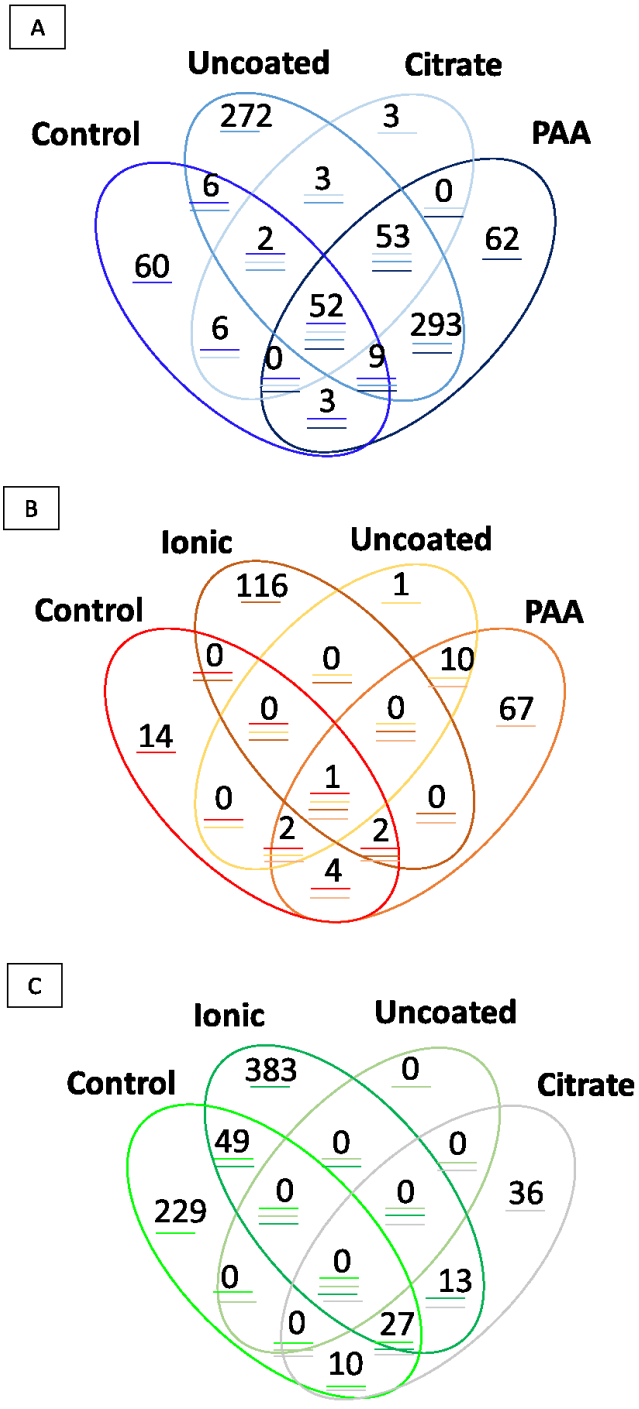

Figure S10. Differentially expressed genes with respect to (A) ionic Ce, (B) citrate stabilized Ce ENPs and (C) PAA coated Ce ENPs following a 2 h exposure of *C. reinhardtii*.

Supplementary Data

Morel, Elise, 2020, "Données supplémentaires thèse 'Biodisponibilité et effets transcriptomiques du cérium chez Chlamydomonas reinhardtii'", https://doi.org/10.5683/SP2/TIGPFS, Scholars Portal Dataverse, VERSION PROVISOIRE, UNF:6:TvtqXzilz/657ZwytFToiQ== [fileUNF]

Supplementary Data 1. Gene expression estimates

Supplementary Data 2. Differential gene expression analysis and MapMan ontology for all the differentially expressed genes

Supplementary Data 3. Differential gene expression analysis, MapMan ontology and functional complementary information for selected cell processes related genes.

Supplementary Data 4. Differential gene expression analysis, MapMan ontology and functional complementary information for transport-related genes.

Supplementary Data 5. Differential gene expression analysis, MapMan ontology and functional complementary information for signaling-, hormones-, DNA-, RNA- and protein-related genes.

Supplementary Data 6. Differential gene expression analysis and MapMan ontology for redox homeostasis and stress related genes.

Supplementary Data 7. Differential gene expression analysis and functional complementary information for not assigned genes according to MapMan analysis.

Supplementary Data 8. Identification of exposure biomarkers specific to ionic Ce, uncoated and PAA coated Ce ENPs, and citrate stabilized Ce ENPs.

Chapitre 2 – Distinguishing the effects of Ce nanoparticles from their dissolution products-Identification of transcriptomic biomarkers that are specific for ionic Ce in *Chlamydomonas reinhardtii*

Elise Morel[1], Jessica Dozois[1], Vera I. Slaveykova[2] and Kevin J. Wilkinson[1,Ψ]

[1]Biophysical Environmental Chemistry Group, University of Montreal, P.O. Box 6128, Succ. Centre-Ville, Montreal, QC

[2] Environmental Biogeochemistry and Ecotoxicology, Department F.-A. Forel for Environmental and Aquatic Sciences, School of Earth and Environmental Sciences, Faculty of Science, University of Geneva, Uni Carl Vogt, 66, boulevard Carl-Vogt, CH-1211 Genève 4, Switzerland

[Ψ]corresponding author

Submitted to Environmental Toxicology and Chemistry in March 2020

Abstract

With the growing number of applications using engineered nanoparticles (ENPs), increased environmental contamination is inevitable. Cerium (Ce) is a rare earth element that is incorporated in numerous consumer products, either in its cationic form or as ENPs. Given the propensity of small oxide particles to dissolve, it is unclear if biological responses induced by the ENPs will be due to the nanoparticles themselves or rather to the dissolved Ce fraction that co-occurs. This study provides the foundation for the development of transcriptomic biomarkers that are specific for ionic Ce in the freshwater alga, *Chlamydomonas reinhardtii.* exposed either to ionic Ce or to two different types of small Ce ENPs (uncoated, ~10 nm or citrate coated, ~ 4 nm). Quantitative reverse transcription PCR was used to analyse mRNA levels of four ionic Ce specific genes (*Cre17g.737300*, *MMP6*, *GTR12* and *HSP22E*) that were previously identified by whole transcriptome analysis in addition to two oxidative stress biomarkers (*APX1* and *GPX5*). Expression was characterized for exposures to 0.03 to 3 μM Ce, for 60 to 360 minutes and for pH 5.0-8.0. Near linear concentrations-responses curves were obtained for the ionic Ce. Distinct patterns of mRNA expression were observed as a function of exposure time, based upon the corresponding metabolic pathways of the genes. Some variability in the transcriptomic response was observed as a function of pH, which was attributed to the formation of metastable Ce species in solution. Oxidative stress biomarkers analysed at transcriptomic and cellular levels confirmed that different effects were induced for dissolved Ce in comparison to Ce ENPs. The measured expression levels confirmed that changes in Ce speciation and the dissolution of Ce ENPs greatly influence Ce bioavailability.

Introduction

Approximately one consumer product containing engineered nanoparticles (ENPs) is created every day.[164] Their increasing use and diversity of applications (biology, medicine, electronics, optics, cosmetics, textiles, painting, etc.) is largely explained by their unique properties, including a high specific surface area.[76] Nonetheless, once emitted into environmental matrices, their properties change. In order to decrease their excess surface energy, they will undergo modifications such as agglomeration, adsorption, dissolution or even changes to their crystal structure.[70] These modifications will dictate the intrinsic properties of the ENPs and their interfacial reactivities.[165]

One of the major difficulties in evaluating the environmental effects of the metal-based ENPs is distinguishing between the effects of dissolution products and the nanoparticles themselves.[166,167,97] Indeed, many of the metal-based nanoparticles dissolve significantly, especially at environmentally relevant (i.e. low) concentrations.[168,169] Several authors have postulated that the effects of dissolved Ce to phytoplankton could be neglected with respect to the ENPs.[110,58,111] Others have shown Ce ENPs to have a lower acute toxicity than ionic Ce.[72,81] One of the difficulties is that it is technically difficult to quantify ENP dissolution at low particle concentrations.[169] An alternate strategy would be to distinguish dissolved metal and ENPs at the level of the cell by using biomarkers that are specific to one form or the other of the metal. The use of biomarkers has the added advantage of contributing to our mechanistic understanding of the bioavailability of the toxic species, which can be helpful for assessing environmental risk via an adverse outcome pathways approach.

Ideally, a biomarker should give a sensitive and specific molecular signal in response to an environmentally relevant exposure condition.[80] In reality, biomarkers typically respond over a limited concentration range and in some cases, non-linearly with respect to environmental stressors. In addition, environmental media are generally complex and variable, with physicochemical factors such as temperature, pH, water hardness, organic matter content having the potential to influence the activation and intensity of the biomarkers. Therefore, in ecotoxicology, multiple biomarkers are generally used in order to identify effects concentrations.[170] As much as possible, targets should be related to a relevant biological pathway and induction should be related to the dose of the stressor. Nonetheless, it is necessary to keep the

number of molecular targets included in the bioassay low enough so that analysis is both affordable and practical.

Whole transcriptomic analysis (RNA-Seq) has been used previously to distinguish the effects of different metal oxide nanoparticles,[150] the effects of particle size,[94] the effects of particle coatings[171] and nanoparticles at different stage of their life cycle.[117] The present study contributes to the development of a transcriptomic bioassay for ionic Ce, by quantifying mRNA levels of genes that were identified as potential ionic Ce biomarkers in the freshwater eukaryotic green alga *Chlamydomonas reinhardtii*.[171] Quantitative reverse transcription PCR (RT-*q*PCR) was performed on a number of promising biomarkers as a function of exposure time, dose and pH.[172] The specificity of the response to ionic Ce was validated by analyzing mRNA levels of selected targets in response to uncoated and citrate stabilized Ce ENPs.

Materials and Methods

Ce forms of interest

$Ce(NO_3)_3$ (ionic Ce) was purchased from Inorganic Ventures (1.0 g L^{-1}; ICP-MS standard). Uncoated Ce ENPs (nominally 15 - 30 nm) were purchased from Nanostructured & Amorphous Materials as a powder (1406RE). Triammonium citrate stabilized Ce ENPs (nominally 10 nm) were obtained from Byk (Nanobyk®-3810). The measured Ce concentration of the stock suspension of the citrate coated Ce ENPs was 187.6 ± 2.7 g L^{-1} Ce ENPs. Detailed characterization and preparation of the Ce ENPs can be found in Morel *et al.* (2019).[171]

Culture and preparation of the microalgae

C. reinhardtii is a green microalga that is ubiquitous to fresh waters and is often used for water quality monitoring and studies examining the toxicology of pollutants in natural waters. Details on its specific culture and preparation for experiments involving trace metals can be found in Zhao and Wilkinson (2015).[56] In brief, wild type CC-125 (aka 137c) from the *Chlamydomonas* resource center was grown at 20°C under conditions of 12 h light/12 h dark (60 mmol s^{-1} m^{-2}) using orbital shaking (100 rpm), until algae reached their mid-exponential growth phase in 4×diluted TAP. The cells were then washed 3x with a simplified exposure medium (see below) that contained no Ce. Cell concentrate was added to the exposure solutions in order to

obtain 6.5-10 x 10^4 cells mL^{-1} (i.e. 0.15 $cm^2.mL^{-1}$). Cell concentrations and cell surface areas were measured using a Multisizer 3 particle counter (50 mm aperture; Beckman Coulter).

Algal exposures

Simplified experimental media were used during the exposure so that the chemical speciation of Ce could be precisely controlled. For example, phosphates can precipitate Ce and thus were removed from the exposure media. The absence of phosphates for short time experiments has been shown to not induce any deleterious effects to the microalgae.[130] Furthermore, 10^{-5} M $Ca(NO_3)_2$ was added to the exposure media in order to help preserve cell wall integrity.[130] Exposures were conducted in triplicate (at least) with independent batches of microalgae and fresh exposure media that were prepared daily. Control treatments were conducted in similar exposure medium than treated cells but without the addition of any Ce forms.

For the time series exposures, cells were exposed to 0.5 µM of Ce (70.1 µg L^{-1} for the ionic standard; 86.1 µg L^{-1} for the Ce ENPs) in a medium containing 10.0 mM NaHEPES (pH 7.0) and 10^{-5} M $Ca(NO_3)_2$. Cells were sampled at 3, 10, 20, 40, 60, 120 and 360 minutes for the determination of Ce biouptake and at 60, 120, 240 and 360 minutes for the analysis of mRNA expression. Cells were pelleted by centrifugation (2000×g, 2 min., 4°C) from 200 mL of the exposure solution. Cell pellets were then resuspended in 1 mL of nuclease-free water before being transferred into 1.5 mL microtubes where they were again separated (2000×g, 1 min., 4°C), prior to being frozen on dry ice for 10 min. and stored at −80°C until RNA extraction.

For the concentration-response exposures, *C. reinhardtii* was exposed for 2 hours to 0.03, 0.05, 0.3, 0.5 or 3 µM Ce (nominal Ce concentrations for both ionic Ce and Ce ENPs) in 10.0 mM NaHEPES (pH 7.0) and 10^{-5} M $Ca(NO_3)_2$. For exposures examining the effect of pH, Ce was held constant (0.5 µM Ce) while pH was varied by changing the pH buffer: 10.0 mM NaHEPES (pH 7.0, pH 8.0); 10.0 mM NaMES (pH 5.0, pH 6.0). Cell pellets were isolated as described above, for the analysis of mRNA expression.

Ce determinations

Cerium concentrations in the exposure media were quantified by inductively coupled plasma mass spectrometry (ICP-MS, Perkin Elmer Nexion 300X).[171] Dissolved Ce was distinguished from colloidal (ENP) forms using centrifugal ultrafiltration (Amicon ultra-4, 3 kDa molar mass cutoff) by centrifuging 4 mL samples for 20 min. at 3700×g. In order to minimize adsorptive losses to the ultrafiltration membrane, the filtrate was collected and analyzed only after the third centrifugation cycle. Mass balances were determined from Ce concentrations that were measured: (i) in the filtrate; (ii) in the solution remaining above the filter; and (iii) in an acid (69% v/v HNO_3) extraction of the filter. Ce speciation in the exposure media was calculated with Visual Minteq (v3.1) using measured Ce concentrations and a partial pressure of $4.0x10^{-4}$ atm for CO_2 (to take into account atmospheric contributions of carbonate/bicarbonate).

Ce biouptake

For the analysis of Ce biouptake, 5 mL of 0.1 M EDTA was added to 45 mL of the exposure medium in order to stop biouptake and to simultaneously wash the adsorbed Ce from the cell wall, presumably leaving only internalized Ce.[173] After 1 min. in EDTA, the solution was filtered through a nitrocellulose filter (pore size 3.0 μm, Millipore), which was then rinsed three more times with 5 mL of 0.01 M EDTA. A similar filtration protocol was carried out on exposure solutions without added algae, in order to quantify adsorptive losses to the filter. Furthermore, 1 mL of the exposure medium was sampled immediately before and during algal exposition. Algal cells and filters were digested by adding 400 μL of ultrapure HNO_3 (67–70%) and 300 μL of ultrapure H_2O_2 (30%), prior to heating the mixture at 80° C for 5 h (DigiPREP, SCP science).

Digests were diluted in MilliQ water and analyzed by ICP-MS. During ICP-MS analysis, a Ce calibration curve was run every 20 samples while blanks and quality control standards were run every 10 samples. Indium was used as an internal standard to correct instrumental drift. All analyses were conducted at least in duplicate.

RNA extraction

Frozen cell pellets were thawed and then immediately resuspended in freshly prepared lysis buffer (0.3 M NaCl, 5.0 mM EDTA, 50 mM Tris-HCl (pH 8.0), 2.0% SDS (wt/v), 3.3 U mL^{-1} proteinase K), where they were incubated at 37°C for 15 min. with orbital shaking (300

rpm). Total RNA was isolated by extracting the sample 3x with phenol:chloroform:isoamyl alcohol (25:24:1, pH 6.8), followed by 1x with chloroform:isoamyl alcohol (24:1). At each step, samples were centrifuged (12,000xg, 10 min., 4°C) and supernatants were transferred into new tubes. Total RNA was precipitated from the final aqueous phase by isopropanol addition, then washed with 75% ethanol. After a final centrifugation, the pellet was resuspended in 20-30 µL of nuclease-free water. An aliquot (3 µL) was analyzed by automated electrophoresis for RNA quality (RIN number > 7, 1.8 < ratio 260/280 < 2.1, ratio 260/230>1.8; Bioanalyzer, Agilent) and spectroscopy (OD260) in order to determine the concentration of RNA (Nanodrop). RNA samples were stored at −80°C until RNA RT-*q*PCR analysis.

Reverse transcriptase quantitative real-time PCR (RT-*q*PCR)

Real-time PCR procedures and analysis followed MIQE guidelines.[174] Primers and fluorescent probe sets for the Taqman assay were designed using the Roche Universal Probe Library website (www.universalprobelibrary.com). Specificity of the probes was verified using the grep function of the Linux exploitation system with primer sequences searched in two annotation files containing either the transcript or the gene sequences of *C. reinhardtii* (genome v5.3 assembly), allowing for exon overlaps. Exon positions and transcript isoforms were determined for each gene using the JGI Comparative Plant Genomics Portal.[139] Total extracted RNA was converted into cDNA using the High Capacity cDNA Reverse Transcription Kit (Applied Biosystems). Controls without reverse transcriptase were prepared in order to verify the absence of contaminating DNA. *q*PCR reactions were performed using the Taqman Fast *q*PCR MasterMix (Applied Biosystems) with a 1/5 dilution of reverse transcription products and primer and probe concentrations of 250 nM and 100 nM, respectively, in a final volume of 10 µL. 'No template' controls were also prepared in order to control for contamination. Enzyme activation was conducted for 20 s at 95°C and followed by 40 dual temperature amplification cycles (1 s at 95°C and 20 s at 60°C) using the QuantStudio 7 Flex Real-Time PCR Systems (IRIC Genomics Platform). For each primer pair and probe set, amplification efficiency was assessed using a standard curve and validated when >85%.

To generate the standard curve, *q*PCR reactions were performed using cDNA from a mix of RNA samples using a serial dilution of 1/5, 1/25, 1/125 and 1/625. Data were analyzed using the QuantStudio Real-Time PCR software (v1.3). Relative mRNA levels were analyzed using the

$2^{-\Delta\Delta CT}$ method with the threshold cycle (CT). Non-induced control genes: *RACK1*[175] (CT around 20) and *APG6* (CT around 27 and no observable changes in intensity[171]) were used for normalisation of the *q*PCR data (**Table S1**). The fold changes between 0.5 and 2.0 were related to technical and biological variability rather than treatment effect.

Reactive oxygen species (ROS) production and oxidative stress

Flow cytometry was employed to follow the oxidative stress and membrane damage in microalgae exposed under similar conditions as described above, except that nominal concentrations were 0, 0.05, 0.1, 0,5, 1 and 5 µM for the ionic Ce and 0, 0,5, 1 and 10 µM for the Ce ENPs. Three 1 mL or 0.5 mL aliquots were taken from each of algal suspensions following 30, 90, 210 or 330 min. of exposure. The 1 mL aliquot was directly analyzed using flow cytometry (BD Accuri C6 Plus, BD) equipped with a 488 nm argon excitation laser and a CSampler (Accuri cytometers Inc., Michigan). A flow rate of 35 µL min^{-1} was used to measure cell density and biological parameters including: (i) size and granularity of *C. reinhardtii* using either forward laser scattering (0 ± 15°, forward scatter, FSC) or side scattering (90 ± 15°, side scatter, SSC); (ii) autofluorescence of chlorophyll (> 670 nm, FL3). Oxidative stress and membrane damage of the exposed algae were determined following staining with CellROX green and propidium iodide (PI). Two 0.5 mL aliquots were stained with 5 µM of CellROX green (Life Technologies Europe BV, Zug, Switzerland) or 7 µM propidium iodide (PI; Sigma – Aldrich, Buchs, Switzerland) in the dark for 30 min. Negative controls ([Ce] = 0 M) were performed for each exposure time and for each type of measurement. Positive controls were prepared from 0.5 mL of an algal aliquot that was: (i) not exposed to Ce; (ii) incubated for 30 min. in the dark with cumene hydroperoxide (1.2 mM) or (iii) placed in warm water (T°> 50°C) for 30 min., prior to incubation with the fluorescent markers (CellROX, PI). CellROX green stained cells were followed using green fluorescence channel (530 ± 15 nm, FL1) and PI stained cells via yellow / orange fluorescence channel (585 ± 20 nm, FL2). Analyses were conducted in triplicate with independent batches of algae and exposure media that were prepared on different days.

For each acquisition, a threshold of 10,000 events in the gate corresponding to algal cells was selected. Details on the flow cytometry gating strategy can be found in the Supplemental information (**Figure S1** and **Figure S2**), however, it mainly followed procedures described in Cheloni et *al.* (2013, 2014).[103,104] The proportions of cells that were present in the different gates

of interest were retrieved with the CFlow Plus program, in addition to the average values of the different parameters of interest.

Statistical analyses

Statistical analyses were performed in SigmaPlot (v12.0). Data points presented are determined from biological replicates (i.e. independent cultures), while error bars show the standard deviations. A one way analysis of variance (ANOVA) paired with the Holm-Sidak test were used to compare measured fold change to the threshold values (i.e. RT-qPCR) or to compare treated and untreated microalgae (i.e. cytometry data) with significance defined by * for $p<0.05$, ** for $p<0.01$ and *** for $p<0.001$. This method was also applied for all pairwise multiple comparisons with significant differences highlighted by the different letters when $p<0.05$.

Results and Discussion

Identification of exposure biomarkers for ionic Ce

Based upon RNA-Seq analysis,[171] a number of candidate transcripts were identified as being specific to ionic Ce. Among the 57 transcripts that were shown to be clearly regulated by Ce,[171] 8 were selected based on the magnitude of their regulation by ionic Ce in regards to controls (i.e. the 4 most up-regulated and the 4 most down-regulated). Further filtering based upon the analysis of their raw expression profiles (**Figure S3**) and their functional annotations led to the selection of four transcripts: three that were induced following exposure to ionic Ce (*Cre17.g737300*, *MMP6* and *GTR12*) and a single transcript (*HSP22E*) that was repressed in its presence (**Table I**). Transcript levels of ROS-induced genes *APX1*[176] and *GPX5*[177] were added in order to test for occurrence of oxidative stress.

RNA-Seq results were first validated using RT-*q*PCR assays (**Table SI**), that were conducted on independent samples of cells, which were exposed to similar exposure conditions (i.e. 0.5 µM Ce in HEPES, pH 7.0, 120 min. exposure). While the direction of regulation (induction or repression) was similar using RNA-Seq and RT-*q*PCR, the magnitude of the regulation (i.e. fold change values) generally differed (**Table I**). Differences were attributed to both technical and biological variabilities in the experiments.

Table I. Functional information (MapMan ontology[137],[138] and JGI Comparative Plant Genomics Portal (Phytozome)[139]) and fold change in mRNA levels for selected differentially expressed genes (Fold-change > |2.0|) after a 120 min. exposure of C. reinhardtii to 0.5 µM of ionic Ce (pH 7.0), as determined using RNA-Seq (n=3) and RT-qPCR (n=5 to 7). Four potential ionic Ce exposure biomarkers (*Cre17.g737300, MMP6, GTR12, HSP22E*), 2 oxidative stress biomarkers (*APX1, GPX5*) and 2 endogen controls (*APG6, RACK1*) were examined.

Identification		**Functional information**		**Fold change**	
ID	**Symbol**	**Mapman**	**Phytozome**	**RNA-Seq**	**RT-*q*PCR**
Cre17.g737300	-	Not assigned	Ultrahigh sulfur keratin-associated protein	10.7 ± 0.8	5.7 ± 1.0
Cre16.g692200	*MMP6*	Protein degradation	Metalloproteinase of VMP family	7.3 ± 0.8	13.9 ± 7.0
Cre06.g302050	*GTR12*	Minor CHO metabolism	1,3-beta-D-glucan synthase	4.9 ± 0.8	17.6 ± 8.2
Cre14.g617450	*HSP22E*	Protein folding	Heat shock protein 22E	0.3 ± 0.9	0.3 ± 0.1
Cre02.g087700	*APX1*	Redox	Ascorbate peroxidase	-	0.4 ± 0.2
Cre10.g458450	*GPX5*	Not assigned	Glutathione peroxidase	-	-
Cre01.g020250	*APG6*	Protein degradation/Cell organization	Beclin 1	-	-
Cre06.g278222	*RACK1*	Development	Receptor of activated protein kinase C	-	-

Ce biouptake and the induced transcriptomic signals as a function of time

Ce biouptake increased over the first two hours of exposure but appeared to stabilize at longer times (**Figure 1**), consistent with prior results with this microalga.[30] Given that Ce concentrations in the medium were constant over the entire exposure period (**Figure S4)**, the decreased uptake flux (decrease in slope in Fig. 1) was likely due to biological regulation of the uptake (resulting from an increased efflux or decreased influx) as opposed to chemical effects (precipitation of Ce, depletion of Ce in the medium, etc.).

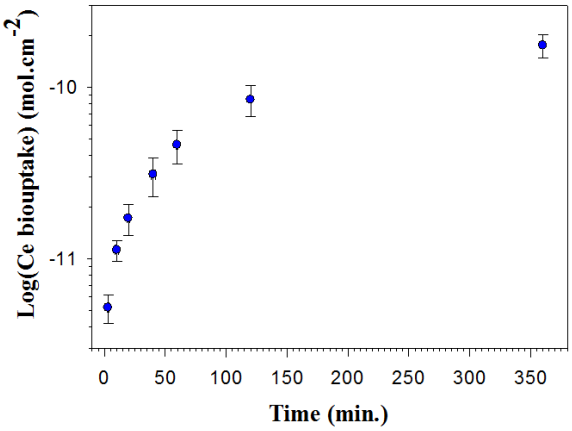

Figure 1. – Ce biouptake by *C. reinhardtii* as a function of exposure time for *C. reinhardtii* exposed to 0.5 µM of ionic Ce (n=2 to 3).

The mRNA levels of the four most sensitive biomarkers (**Table 1**) were quantified during an exposure to 0.5 µM Ce over 360 min. **(Figure 2)**. Three patterns of mRNA expression were observed: *Cre17.g737300* increased over time to reach a plateau at 240 min. (**Figure 2a**); the expression level of *HSP22E* was repressed over time (**Figure 2d**); whereas the expression levels remained fairly stable for *GTR12* and *MMP6*, over the entire exposure period (**Figure 2b, 2c**). For the oxidative stress marker genes, a significant repression of *APX1* was observed at very short exposure times (Holm-Sidak test, $p<0.01$) but then values returned to control levels by 120 min. (**Figure S5a**). Expression levels of *GPX5* were stable and showed no sign of being regulated by ionic Ce (**Figure S5b**).

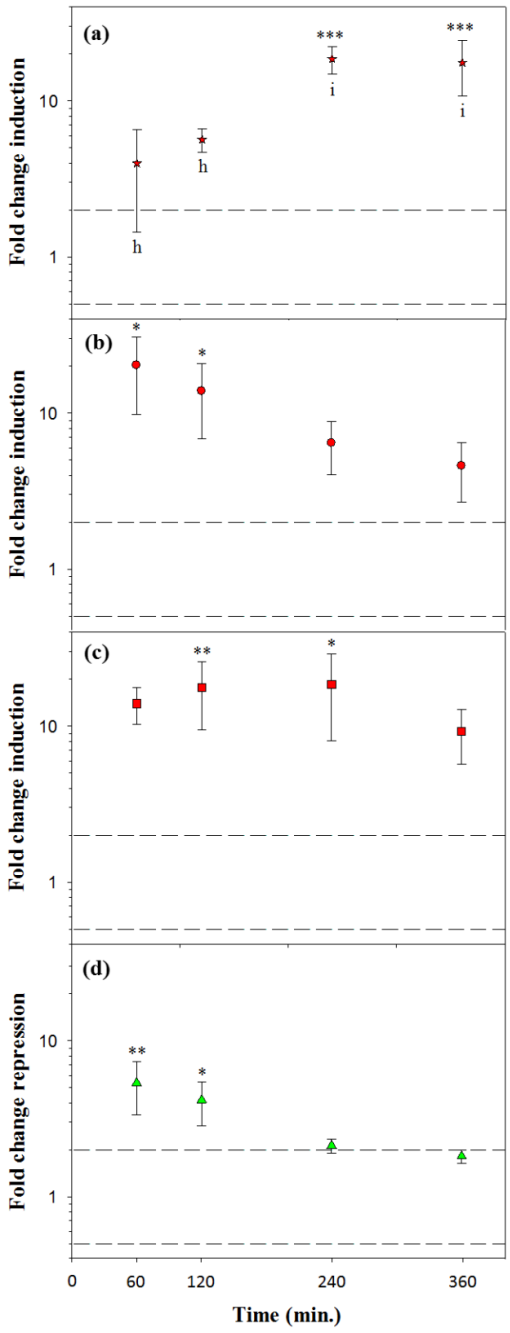

Figure 2. – Fold change induction of (a) *Cre17.g737300*, (b) *MMP6*, (c) *GTR12*, and fold change repression of (d) *HSP22E* as a function of exposure time for *C. reinhardtii* exposed to 0.5 µM of ionic Ce. Induced biomarkers are indicated by red points, while repressed biomarker (=1/fold change induction) is represented by the green points (n=2 to 7). The dotted lines define the area in which the fold changes of mRNA levels are considered to occur randomly due to technical and biological variability (0.5>fold change<2.0).

Concentration-response relationship

For a 120 min. exposure to ionic Ce, biomarker expression was examined as a function of the measured concentrations of Ce (from 0.03 to 3 µM nominally). Increased expression was observed as a function of concentration for all potential biomarker genes, up to 2-3 µM Ce (**Figure 3**). *APX1* appeared to be repressed only for the highest exposure concentration (ionic Ce ~ 3 µM) (**Figure S6a**), whereas expression levels of *GPX5* were stable and showed no sign of being regulated by ionic Ce over the entire tested concentration range (**Figure S6b**).

The no effects (mRNA) concentration[170] for a 120 min. exposure was between 0.2 µM and 0.5 µM Ce for *MMP6* (Holm-Sidak test, $p<0.05$) and *HSP22E* (Holm-Sidak test, $p<0.05$) and between 0.5 and 1 µM for *Cre17.g737300* (Holm-Sidak test, $p<0.001$) and *GTR12* (Holm-Sidak test, $p<0.05$) (**Figure 3**). As expected, these values are lower than the values required to observe significant biological effects at the cellular level. For example, an EC_{10} of 9.4 µM was observed for a 72 hours fluorescence inhibition assay for *Pseudokirchneriella subcapitata*.[73] The predicted "no-effects" concentration (PNEC) estimated for a Ce salt was around 0.4 µM for an ecosystem level study by the same authors, which is in good agreement with the transcriptomic results obtained in this study.[73] Finally, Collin *et al.* (2014) estimated a PNEC value of 5.8 nM for Ce ENPs (cerium dioxide).[72]

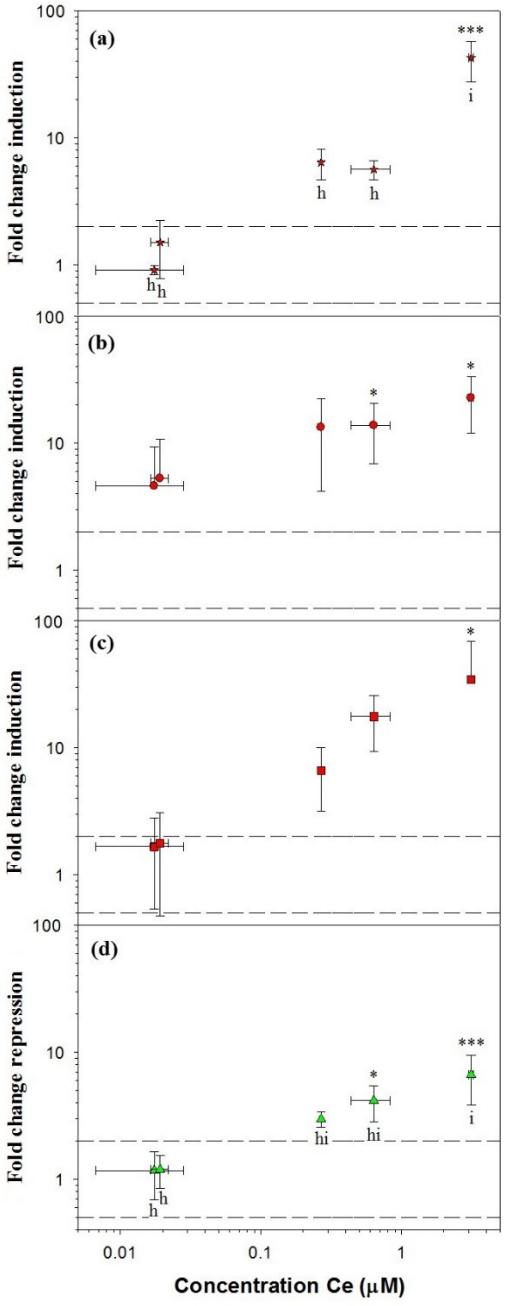

Figure 3. – Fold change induction of (a) *Cre17.g737300*, (b) *MMP6*, (c) *GTR12*, and fold change repression of (d) *HSP22E* as a function of concentration for a 120 min. exposure of *C. reinhardtii* to ionic Ce (n= 2 to 7). Induced biomarkers are indicated by red points, while the repressed biomarker (=1/fold change induction) is represented by green points. The dotted lines define the area in which fold changes of mRNA levels are considered to occur randomly due to technical and biological variability (0.5>fold change<2.0).

Role of pH on the transcriptomic signal

Transcript levels of the biomarkers were evaluated for pH variations from 5.0 to 8.0 for 0.5 µM ionic Ce and a 120 min. exposure time. Based upon thermodynamic calculations (Visual Minteq), free Ce in solution will vary from 99.9% to 5.9% of the total Ce in solution, over the pH range of 5.0 to 8.0. Measured Ce concentrations and calculated ionic Ce were fairly constant between pH 5.0 and 7.0 (**Figure 4**), however, metastable colloidal species, not predicted by equilibrium calculations, are thought to form, especially at the higher pH.[171,30] For example, significant decreases of 20% of the total Ce (Holm-Sidak test, $p<0.01$) and nearly all of the dissolved Ce (Holm-Sidak test, $p<0.001$) were observed when increasing the pH from 7.0 to 8.0 (**Figure 4**), suggesting losses by adsorption on the flask walls and/or the formation of sedimenting precipitates at pH 8.0. Indeed, the near absence of dissolved Ce at pH 8.0 broadly agreed with the transcriptomic responses observed for all of the biomarkers, which were not different from control values at pH 8.0 (**Figure 5, Figure S7**).

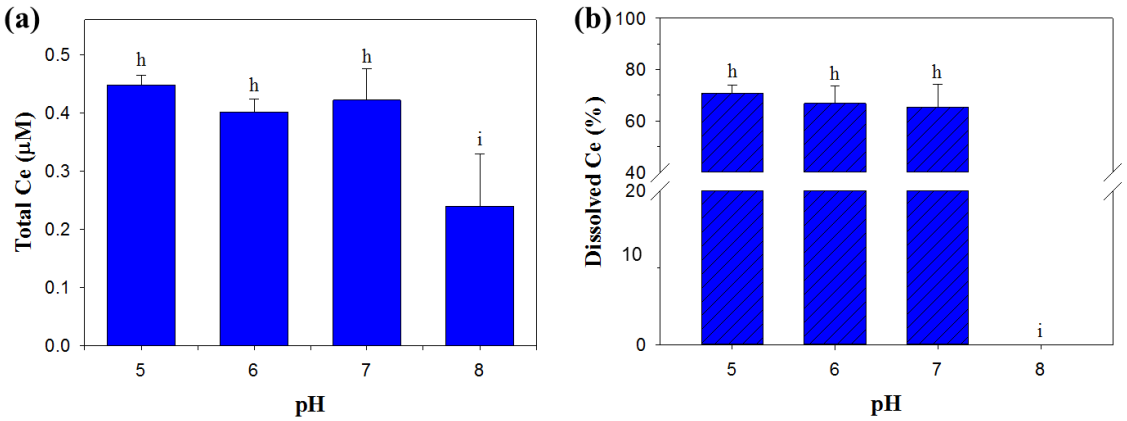

Figure 4. – (a) Total Ce concentration in the exposure media and (b) proportion of dissolved Ce as a function of pH for a 120 min. exposure of *C. reinhardtii* to 0.5 µM ionic Ce (n= 2 t 6).

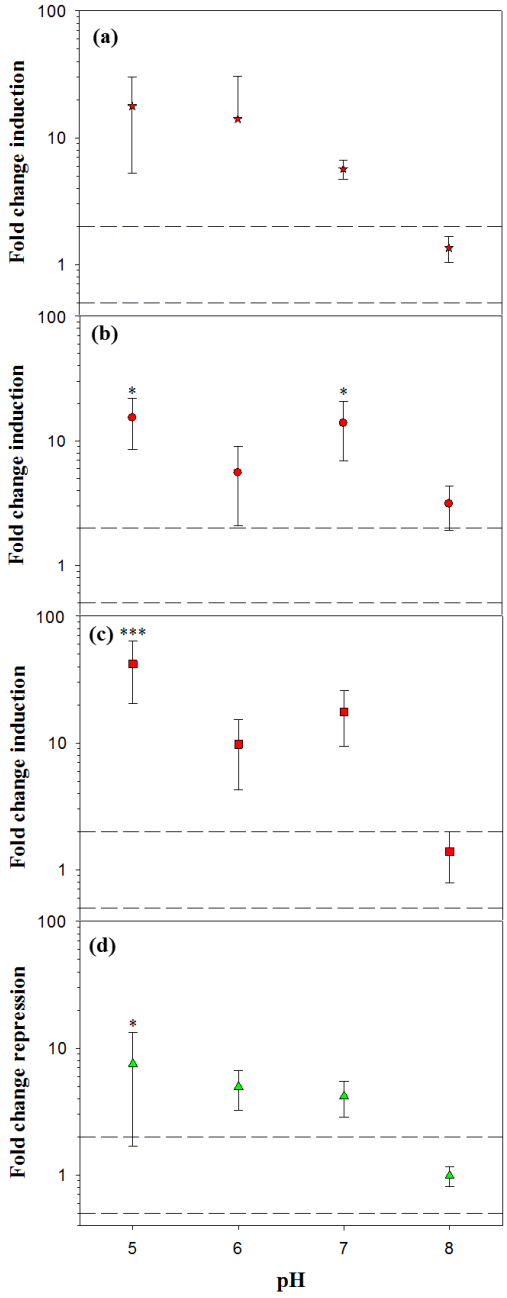

Figure 5. – Fold change induction of (a) *Cre17.g737300*, (b) *MMP6*, (c) *GTR12*, and fold change repression of (d) *HSP22E* as function of pH for a 120 min. exposure of *C. reinhardtii* to 0.5 µM of ionic Ce. Induced biomarkers are indicated by red points, while repressed biomarker (=1/fold change induction) is represented by the green points (n= 2 to 7). The dotted lines define the area in which fold changes of mRNA levels are considered to occur randomly due

to technical and biological variability (0.5>fold change<2.0). Biomarker responses for the Ce ENPs

Biomarker responses for the Ce ENPs

Very little or no dissolved Ce could be detected in the Ce ENPs suspensions at pH 7.0 (**Table II)**, though this fraction did appear to increase at the lower pH for the citrate coated ENPs. In spite of these very low concentrations (and proportions) of dissolved Ce, biouptake was ~10x higher for the ENPs than it was for dissolved Ce (**Figure S8**), for a similar total concentration of Ce in the exposure medium.

In spite of a much greater biouptake in the presence of ENPs, induction did not differ from control responses for any of the selected biomarkers, either as a function of time (**Figure 6**) or concentration (**Figure 7**), strongly indicating a specificity for dissolved Ce. This result is important as it shows that these biomarkers could be used to distinguish between the effects of the ENPs and the effects of dissolved Ce. It also demonstrates that there is a clear mechanistic difference between the effect of dissolved Ce and that of Ce ENPs. Note that in spite of our efforts, no specific biomarkers for the Ce ENPs were identified to date. *GTR12* did respond to the citrate coated Ce ENPs, but only at the most acidic pH (pH 5.0, Holm-Sidak test, $p<0.01$) (**Figure S9**). As postulated earlier,[171] some of the transcriptomic effects observed for the citrate coated Ce ENPs may have come from increased citrate in the medium, rather than from a specific ENP effect, however, this result implied that the effects of these Ce ENPs were due to their dissolution products rather than to the ENP themselves. Admittedly, this point would require a more thorough examination of all potential biomarkers (*Chlamydomonas* has 19,526 predicted transcripts).[178],[142]As expected, based upon the weak response for the ENPs, little variation in the transcriptomic response was observed for the oxidative stress biomarkers (**Figure S10**).

Table II. Total Ce concentrations and percentages of dissolved Ce as a function of pH after 120 min. exposure of C. reinhardtii to 0.5 µM Ce in the form of either citrate coated Ce ENPs or uncoated Ce ENPs (n= 2 to 6).

pH	Total Ce concentration (µM)		Dissolved Ce (%)	
	Citrate coated	Uncoated	Citrate coated	Uncoated
5.0	0.28 ± 0.09	0.35 ± 0.09	10.0 ± 8.9	ND
6.0	0.42 ± 0.07	0.42 ± 0.04	1.4 ± 1.7	1.1 ± 0.4
7.0	0.38 ± 0.02	0.42 ± 0.07	0.2 ± 0.2	ND
8.0	0.28 ± 0.09	0.39 ± 0.04	ND	ND

ND= Not detected.

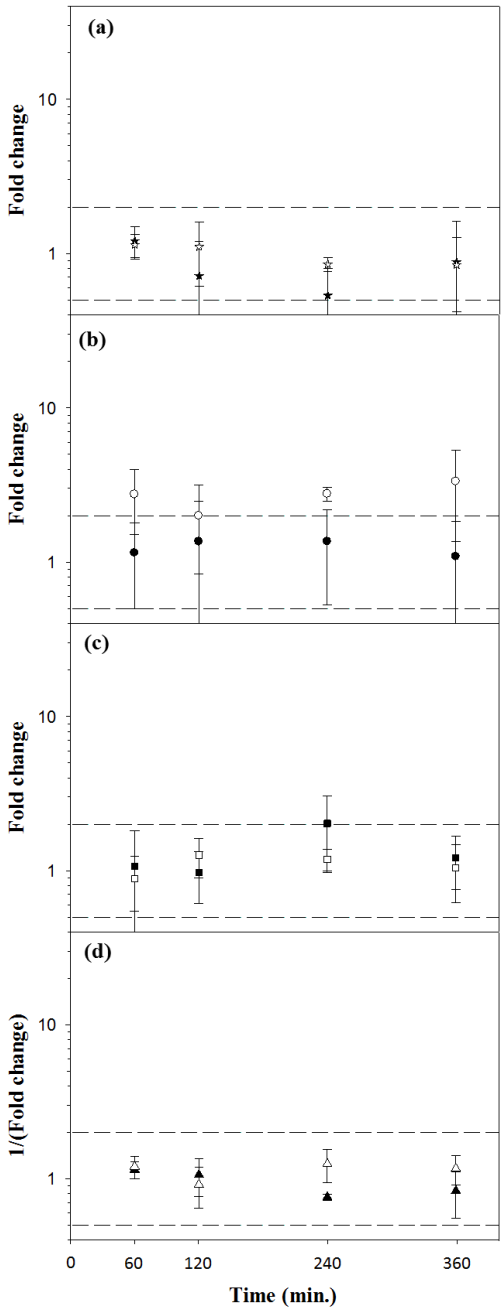

Figure 6. – Fold change in mRNA levels of (a) *Cre17.g737300*, (b) *MMP6*, (c) *GTR12*, and reciprocal of fold change in mRNA levels of (d) *HSP22E* as a function of exposure time for *C. reinhardtii* exposed to 0.5 µM of total nominal Ce (dissolved and ENP) for citrate coated Ce ENPs (empty symbols) and uncoated Ce ENPs (full symbols) (n=2 to 7). The dotted lines define an area in which the fold change mRNA levels are considered to occur randomly due to technical and biological variability (0.5>fold change<2.0).

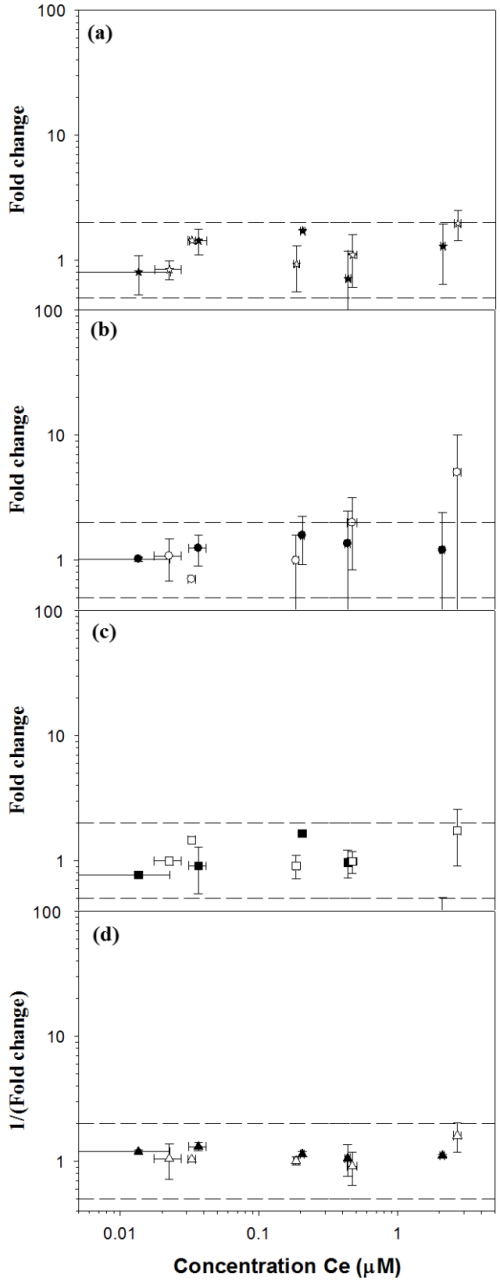

Figure 7. – Fold change in mRNA levels of of (a) *Cre17.g737300*, (b) *MMP6*, (c) *GTR12*, and reciprocal of fold change in mRNA levels of (d) *HSP22E* as a function of the Ce concentration for a 120 min. exposure of *C. reinhardtii* to citrate coated Ce ENPs (empty symbols) and uncoated Ce ENPs (full symbols) (n=2 to 7). The dotted lines define the area in which fold changes of mRNA levels are considered to occur randomly due to technical and biological variability (0.5>fold change<2.0).

Validation of the transcriptomic signatures

mRNA levels generally changed in a single direction as a function of both exposure time and Ce concentration, which is an important point when identifying useful biomarkers. It also suggests that the conditions that were employed in this study did not induce important changes in the metabolism of *C. reinhardtii*. This observation was reinforced by the absence of induction in the mRNA levels of the oxidative stress biomarkers (*APX1*, *GPX5*) at these concentrations of ionic Ce. Nonetheless, this result does not exclude the response of other stress biomarkers to Ce since similar exposure conditions have led to an overexpression of the reactive oxygen species (ROS) and a modification in the membrane permeability of *C. reinhardtii*, when determined by the flow cytometry (**Figure S11 a, d**). For example, after a 120 min. exposure to 1 µM ionic Ce, 10% (Holm-Sidak test, $p \leq 0.001$) of the microalgae presented an excess in ROS and while 7% (Holm-Sidak test, $p \leq 0.05$) showed signs of membrane damage. For the short exposure times used here, similar effects were not observed when the microalgae were exposed to Ce ENPs, even at higher concentrations (> 1 µM Ce) (**Figure S11 b, c, e, f**). Indeed, ROS generation and membrane damages have really only been reported in *C. reinhardtii* for much longer exposure times (> 12h) and high concentrations of Ce ENPs.[59]

Nonetheless, not all of the biomarkers were affected in the same manner by exposure time, which may have been related to the specific biological pathways within which the investigated genes were involved. For example, in the case of *HSP22E* and *APX1,* both were induced at early exposure times (i.e. maximum of down-regulation was observed at 60 min.) and both encode chloroplast-targeted proteins that are induced during oxidative stress.[179] Given the significant modifications to cell size were observed within 60 min. following the exposure of *C. reinhardtii* to 1 µM ($p \leq 0.05$) and 5 µM ($p \leq 0.001$) of Ce (**Figure S12a**), the induction of *Cre17g.737300* that was observed as a function of time and concentration may have reflected perturbations in cell turgor at the higher concentrations of ionic Ce. Indeed, while no precise biological function for the protein that is encoded by *Cre17g.737300* has been yet identified in *C. reinhardtii*, high sulfur keratin-associated transmembrane proteins have been reported to be up-regulated in maize during hydric stress.[180] The absence of such an effect (at both the transcriptomic and cellular levels) when the microalgae were exposed to environmentally relevant concentrations of Ce ENPs (**Figure S12 b,c**) suggests that the regulation of genes related

to cellular processes[171] may allow *C. reinhardtii* to adapt well to short-term and low concentration exposures of the ENPs.

Summary and environmental implications

Due to their high specificity and relative linearity with the respect the concentration of ionic Ce (over an environmentally relevant concentration range), four biomarkers (*Cre17.g737300*, *GTR12*, *MMP6* and *HSP22E*) were identified as being specific to dissolved Ce (likely Ce^{3+}) in *C. reinhardtii*. With their different sensitivities, their simultaneous use could be an appropriate strategy for identifying bioavailable Ce to *C. reinhardtii* and perhaps other biological species. Indeed, the low concentrations of dissolved Ce that co-occurred in the suspensions of citrate coated Ce ENPs at pH 5.0 were likely signaled from the induction of *GTR12*. One caveat should be noted. A much greater variability in mRNA levels was observed when the pH of media varied. This result likely reflected the complexity of Ce speciation, even in simple aqueous media, resulting from the formation of metastable species, which are likely highly charged and likely to sorb to multiple surfaces including cell walls and exposure container walls. Finally, the specificity of this transcriptomic signature will need to be validated in the presence of other rare earth metals since in nature, they are almost always found as metal mixtures.[2] The presence of ligands such as phosphate or natural organic matter should also be validated as they are both likely to attenuate the bioavailability of Ce[181] and/or the metabolism of the microalgae.[159]

Acknowledgments

Funding for this work was provided by the Natural Sciences and Engineering Research Council of Canada (NSERC Discovery and Strategic projects grants) and the Fonds de Recherche du Québec - Nature et Technologies (FRQNT). Special thanks go to Raphaëlle Lambert and Pierre Melançon at IRIC genomic platform (*Université de Montréal*) for their advices and support with RT-*q*PCR analyses and to Yanxia Wu (Concordia University) for sharing her expertise in *C. reinhardtii* RNA extraction. Acknowledgements are also addressed to Giuila Cheloni and Rebecca Beauvais-Flueck (University of Geneva) for their technical support and expert advice during realization of flow cytometry analysis.

Supplementary information

Supplementary materials and methods

RT-*q*PCR optimization assay results

Table SI. RT-qPCR probe efficiencies for ionic Ce exposure biomarkers (*MMP6*, *GTR12*, *Cre17.737300* and *HSP22E*), oxidative stress biomarkers (*GPX5* and *APX1*) and 2 endogen controls (*APG6* and *RACK1*). Probe numbers refer to Roche Universal Probe Library numbers. CT 1st and CT 4th correspond respectively to the cycle threshold (CT) obtained after the first dilution (1/5) and the last dilution (1/625) used to test amplification efficiencies of RT-*q*PCR assays (i.e. standard curves, n=2, technical duplicates). No CT was obtained for the 'no reverse transcriptase' controls.

ID transcript	Gene Symbol	Probe	Forward	Reverse	CT 1st	CT 4th	Efficiency
Cre16.g692200.t1.1	*MMP6*	92	CCAGGATGACA CGACACTTG	CGAAATGTCCGT GTACTCAAAA	28	35	98.0
Cre06.g302050.t1.2	*GTR12*	70	CAACTACACCGT CGACATGG	CAGGAACAGCAC AATCACCA	24	31	98.6
Cre17.g737300.t1.1	-	43	TCTGCTGCTTTG GACTGCT	AGCAGCAGGTGG AGTTCG	27	34	99.1
Cre14.g617450.t1.2	*HSP22E*	61	GCCTAGTGCTGA GGAGCTGT	CCGACACGGCAC ATATTGTA	19	26	91.2
Cre10.g458450.t1.1	*GPX5*	25	TAGCAAGTGCG GCTTTACG	CCGGTCCTTGTAC TGTTGGT	23	30	91.9
Cre02.g087700.t1.1	*APX1*	44	TCAAGGAGATC AAGGCCAAG	ACGCAGTAGTCG GCGAAG	23	30	97.8
Cre01.g020250.t1.2	*APG6*	22	GGCGCAGCTGTT TGAACT	CTGCCCCACACA GTCCAT	27	34	94.4
Cre06.g278222.t1.1	*RACK1*	80	CACCCAGTCCTC CATCAAG	GCCTTCTTGCTGG TGATGTT	20	28	88.7

Flow cytometry data acquisition and data treatment

For each acquisition, a threshold of 10,000 events occurring in the P2 window associated with the algal cells (**Figure S1, b**) was set, after exclusion of any doublets located outside the P1 window (**Figure S1, a**). In view of the complexity of certain suspensions containing Ce ENPs, the chlorophyll autofluorescence signal from algal cells (FL3) was preferred to signals of size and granularity (FSC and SSC) when defining the "algal" gate (M1, **Figure S1, c**), which is then applied to all of the data dealing with the biological parameters of interest. The V2-L window (**Figure S1, c**) was used to measure the proportion of the FL3 signal that was associated with background noise and/or cellular debris, particles or aggregates of the Ce ENPs. For the cellular oxidative stress and damages to membrane permeability, windows of positive or negative responses were defined by comparing the profiles obtained for the positive and negative controls (**Figure S2**).

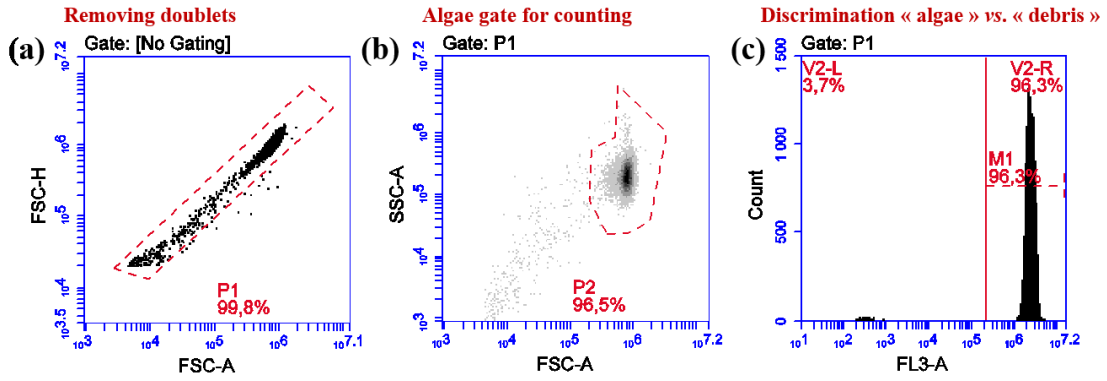

Figure S1. Gates defined from a negative control and used on flow cytometry data in order to (a) allow the exclusion of doublets; (b) set a counting threshold for 10,000 events; (c) separate the signal for the algae (V2-R) from that for the cellular debris or other particles (V2-L).

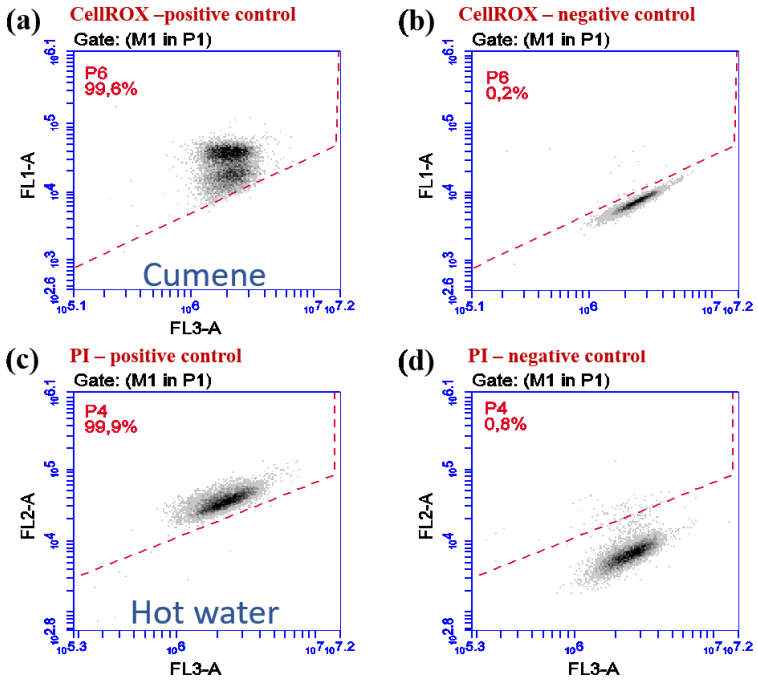

Figure S2. Windows of positive biological responses defined from positive (a, c) and negative (b, d) control samples whose FL1 and FL2 fluorescence were measured after incubation with CellROX (a and b) and PI (c and d).

Supplementary results

Selection of the biomarkers

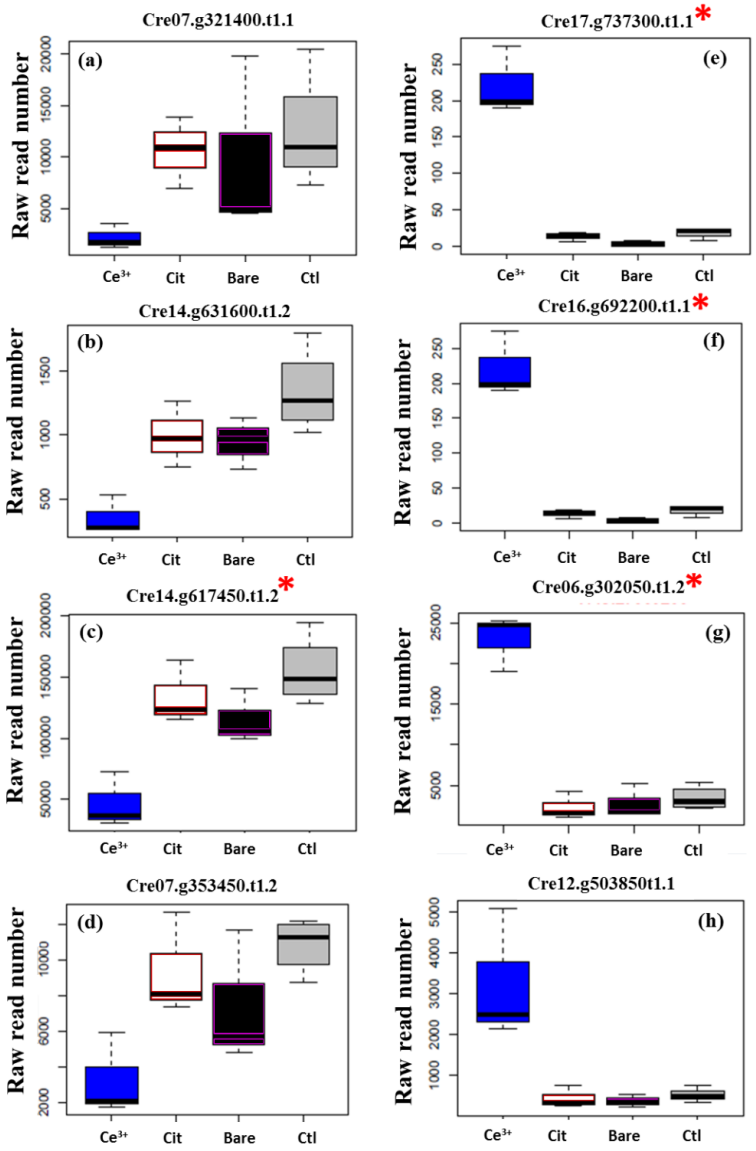

Figure S3: Raw read numbers obtained using RNA-Seq[171] for 8 pre-selected transcripts after a 120 min. exposure of *C. reinhardtii* to 0.5 µM Ce: ionic Ce (Ce^{3+}), citrate coated Ce ENPs (Cit), uncoated Ce ENPs (Bare) or no cerium (Ctl) (n=3 for treatments, n=4 for control).The transcripts identified by a red star were selected for use as exposure biomarkers.

Exposure to ionic Ce

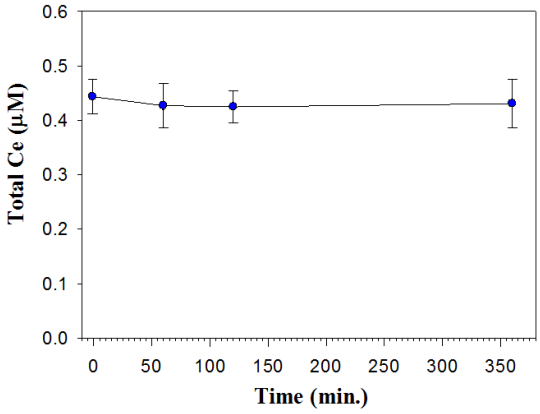

Figure S4: Concentration of ionic Ce in the exposure medium (nominally 0.5 µM) as a function of exposure time (min) in the presence of *C. reinhardtii* (n=2 to 3).

mRNA levels following exposure to Ce

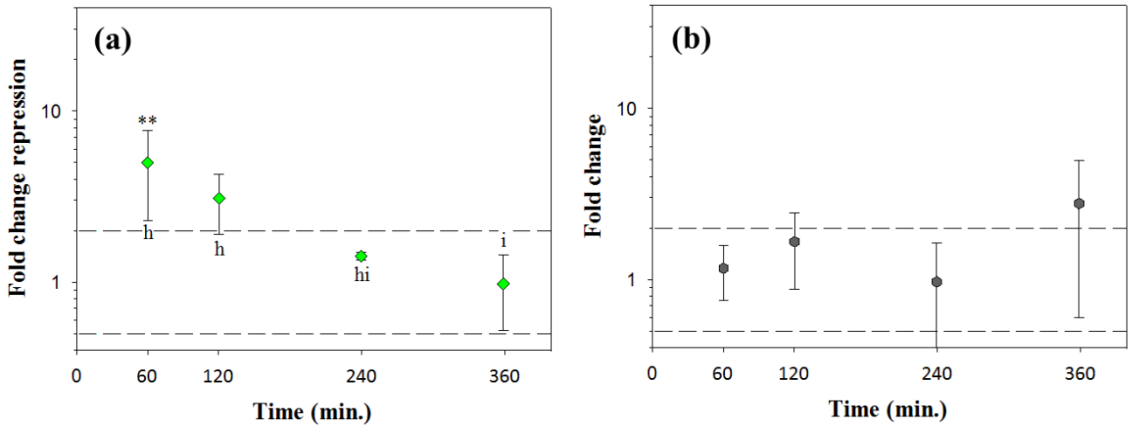

Figure S5: Fold change repression of (a) *APX1* and fold change in mRNA levels of (b) *GPX5* as a function of exposure time for *C. reinhardtii* exposed to 0.5 µM of ionic Ce (n=2 to 7). *APX1* initially showed a repression of mRNA levels and was thus plotted as 1/fold change induction (green points) while *GPX5* did not appear to be affected by time (grey points). The dotted lines define the area in which fold changes of mRNA levels are considered to occur randomly due to technical and biological variability (0.5>fold change<2). ANOVA paired with Holm-Sidak test were used to compare measured fold changes to the threshold value (i.e. 2.0) with significance defined by * for $p<0.05$, ** for $p<0.01$ and *** for $p<0.001$. This

method was also applied for all pairwise multiple comparisons between treatments with significant differences highlighted by different when $p<0.05$.

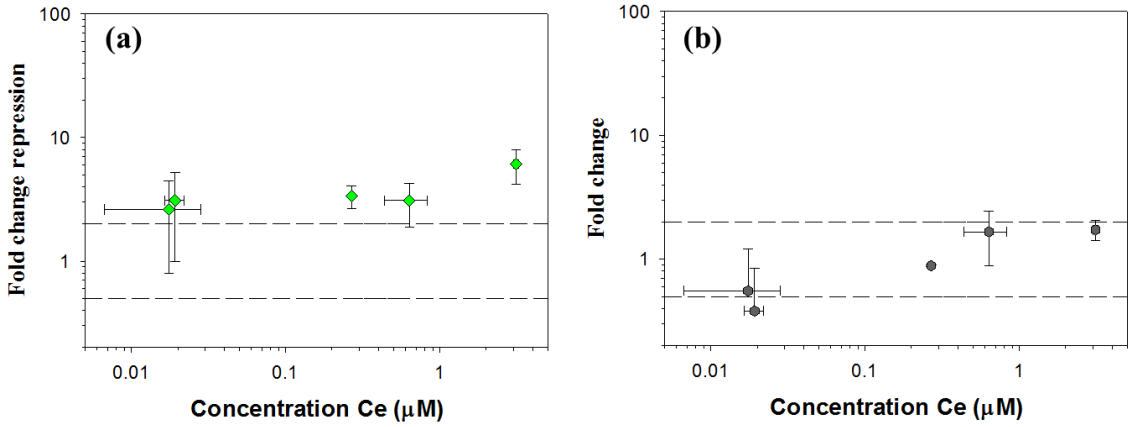

Figure S6: Reciprocal of fold change of mRNA levels for (a) *APX1* and fold change for (b) *GPX5* as a function of Ce concentration for a 120 min. exposure of *C. reinhardtii* to ionic Ce (n=2 to 7). *APX1* showed a repression of expression levels with time and was thus plotted as 1/fold change induction (green points) while *GPX5* did not appear to be affected by time (grey points). The dotted lines define the area in which fold changes in mRNA levels are considered to occur randomly due to technical and biological variability (0.5>fold change<2.0). ANOVA paired with Holm-Sidak test were used to compare measured fold changes to the threshold value of 2.0 and between treatments although no significant differences were observed ($p<0.05$).

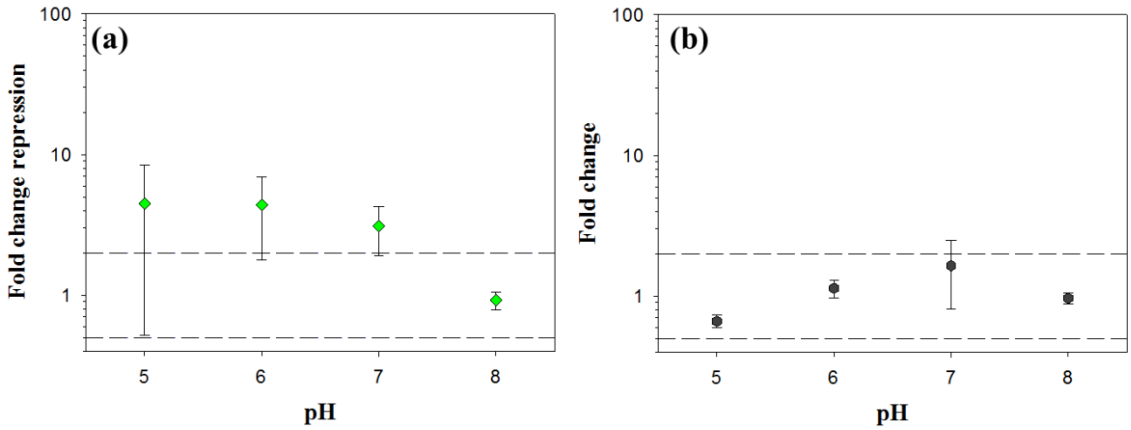

Figure S7: Reciprocal fold change in mRNA levels of (a) *APX1* and fold change in mRNA levela of (b) *GPX5* as a function of pH for *C. reinhardtii* exposed to 0.5 µM of ionic Ce. *APX1* showed a repression of expression levels with time and was thus plotted as 1/fold change induction (green points) while *GPX5* did not appear to be affected by time (grey points) (n=2 to 7). The dotted lines define the area in which fold changes of mRNA levels are considered to occur randomly due to technical and biological variability (0.5>fold change<2.0). ANOVA paired with Holm-Sidak test were used to compare measured fold changes to the threshold value of 2.0 and between treatments although no significant differences were observed ($p<0.05$).

Ce ENP biouptake

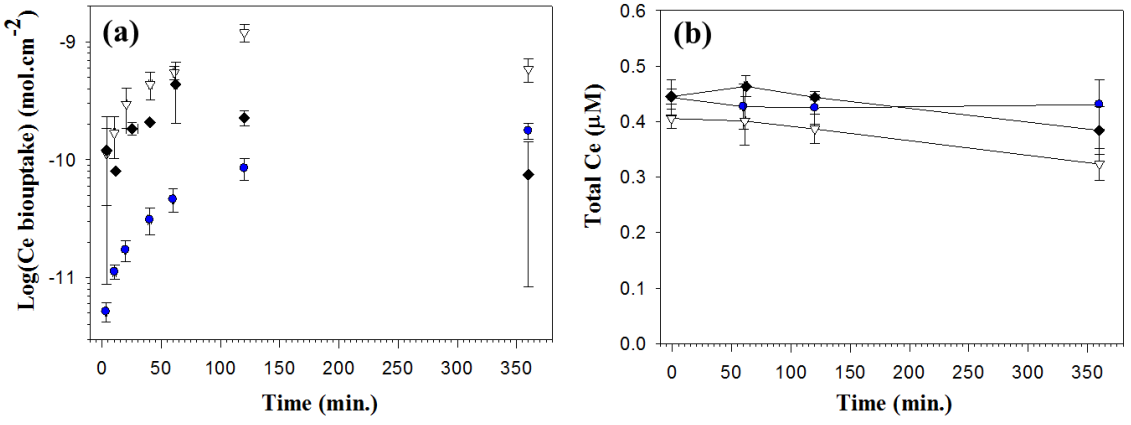

Figure S8: (a) Ce biouptake by *C. reinhardtii* and (b) total Ce concentration measured in the exposure medium as a function of exposure time for *C. reinhardtii* exposed nominally to 0.5

µM Ce: ionic Ce (blue circles); citrate coated Ce ENPs (white triangles); uncoated Ce ENPs (black diamonds) (n=2 to 3).

Ce ENP transcriptomic effects

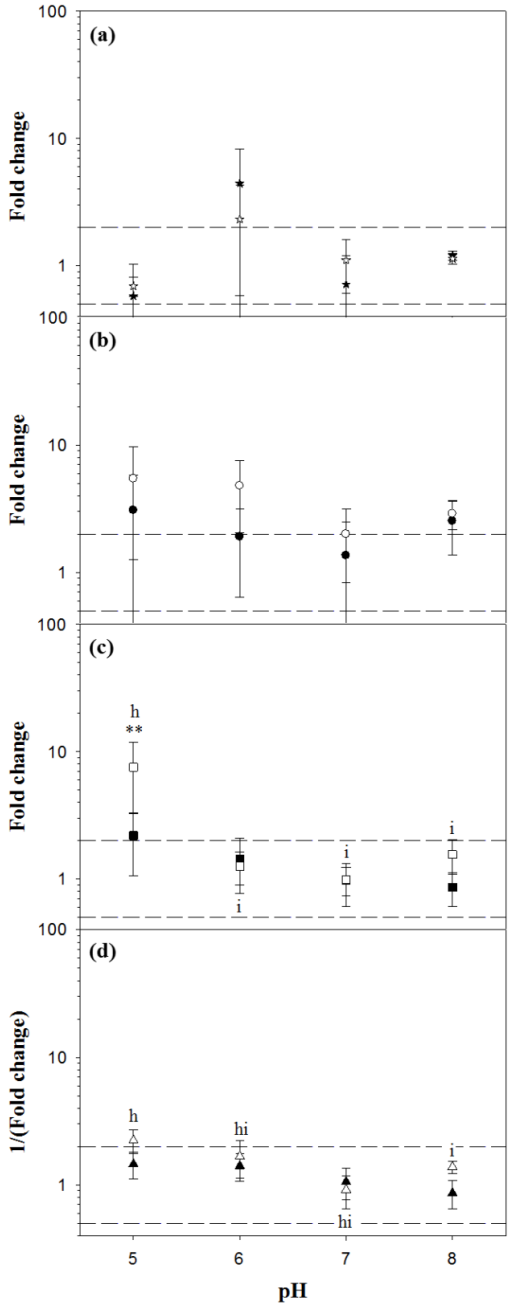

Figure S9: Fold change in mRNA levels of (a) *Cre17.g737300*, (b) *MMP6,* (c) *GTR12*, and reciprocal of fold change in mRNA level of (d) *HSP22E* as function of pH for a 120 min.

exposure of *C. reinhardtii* to 0.5 µM Ce: citrate coated Ce ENPs (empty symbols); uncoated Ce ENPs (full symbols) (n=2 to 7). The dotted lines define the area in which fold changes of mRNA levels are considered to occur randomly due to technical and biological variability (0.5>fold change<2.0). ANOVA paired with Holm-Sidak test were used to compare measured fold changes to the threshold value of 2.0 with significance defined by * for $p<0.05$,** for $p<0.01$ and *** for $p<0.001$. This method was also applied for all pairwise multiple comparisons between treatments with significant differences highlighted by different letters when $p<0.05$.

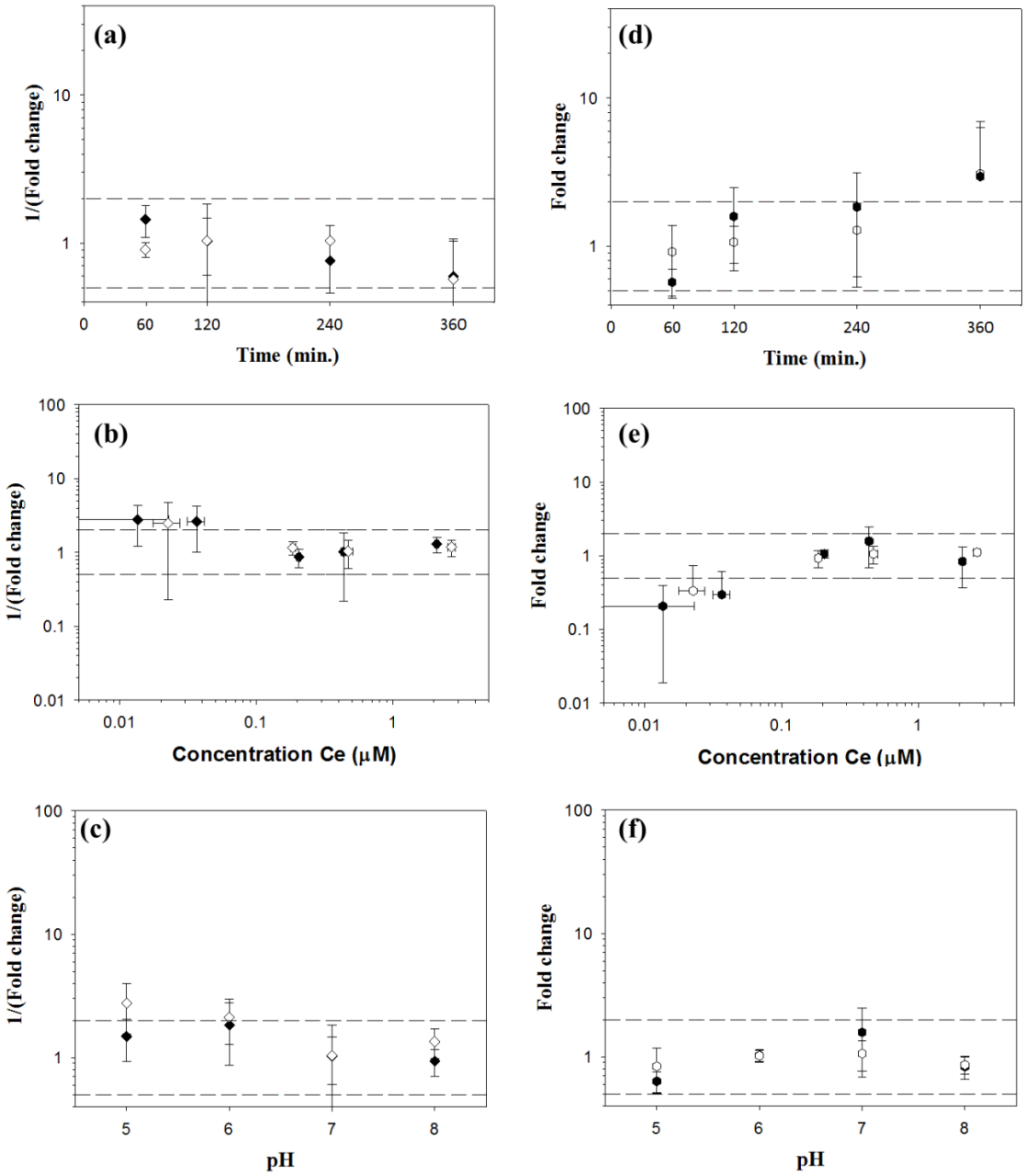

Figure S10: Reciprocal of fold change in mRNA levels of (a, b, c) *APX1* and fold change in mRNA level of (d, e, f) *GPX5* as a function of (a, d) exposure time, (b, e) concentration and (c, f) pH for *C. reinhardtii* exposed to citrate coated Ce ENPs (empty symbols) and uncoated Ce ENPs (full symbols) (n=2 to 7). The dotted lines define the area in which fold changes of mRNA levels are considered to occur randomly due to technical and biological variability (0.5>fold change<2.0). ANOVA paired with Holm-Sidak test were used to compare

measured fold changes to the threshold value of 2.0 and between treatments although no significant differences were observed ($p<0.05$).

Oxidative stress analyses at a cellular level (flow cytometry)

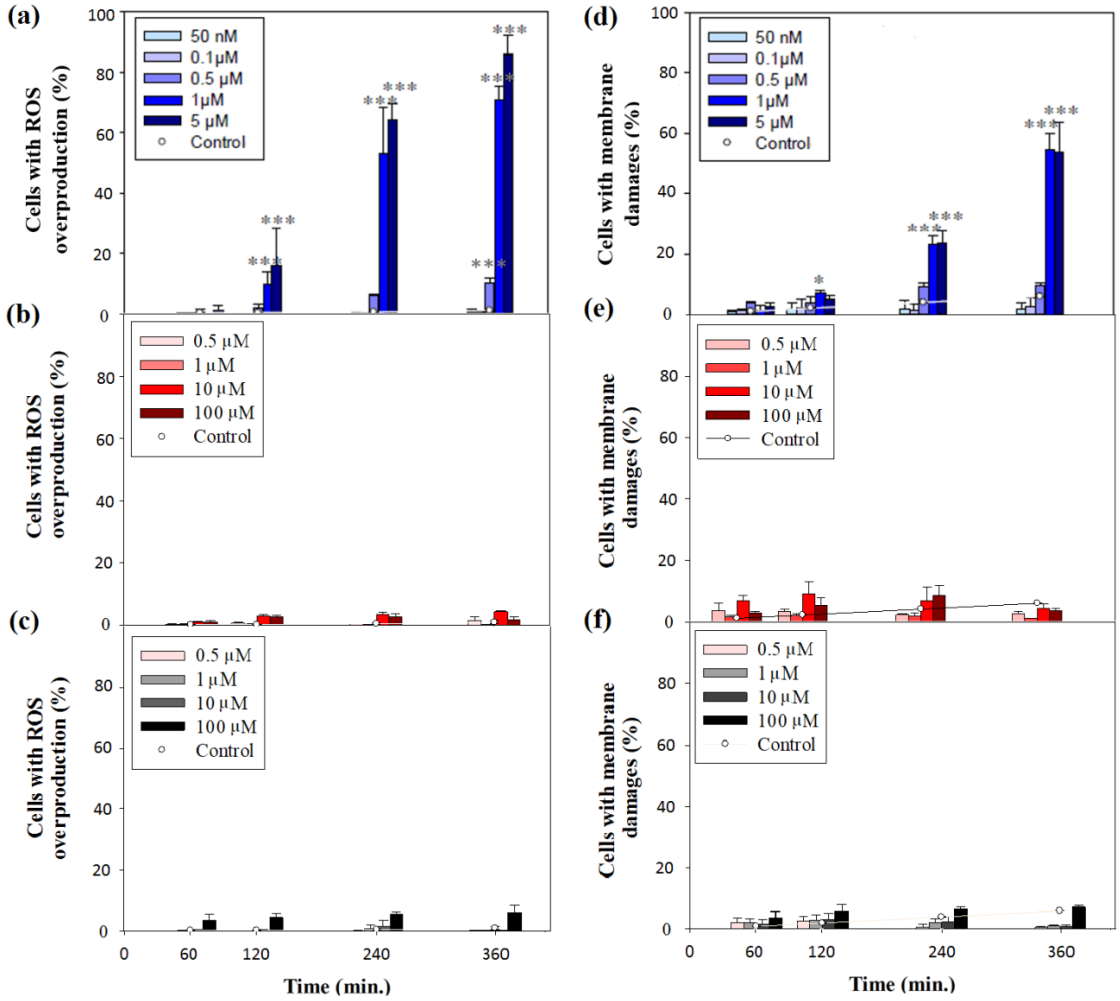

Figure S11: (a, b, c) ROS overproduction and (d, e, f) membrane damage for *C. reinhardtii* as a function of time and concentration for exposures to (a, d) ionic Ce, (b, e) citrate coated Ce ENPs and (c, f) uncoated Ce ENPs at pH 7.0 (n=2 to 3). ANOVA paired with Holm-Sidak test were used to compare treated and untreated microalgae, with significance defined by * for $p\leq0.05$,** for $p\leq0.01$ and *** for $p\leq0.001$.

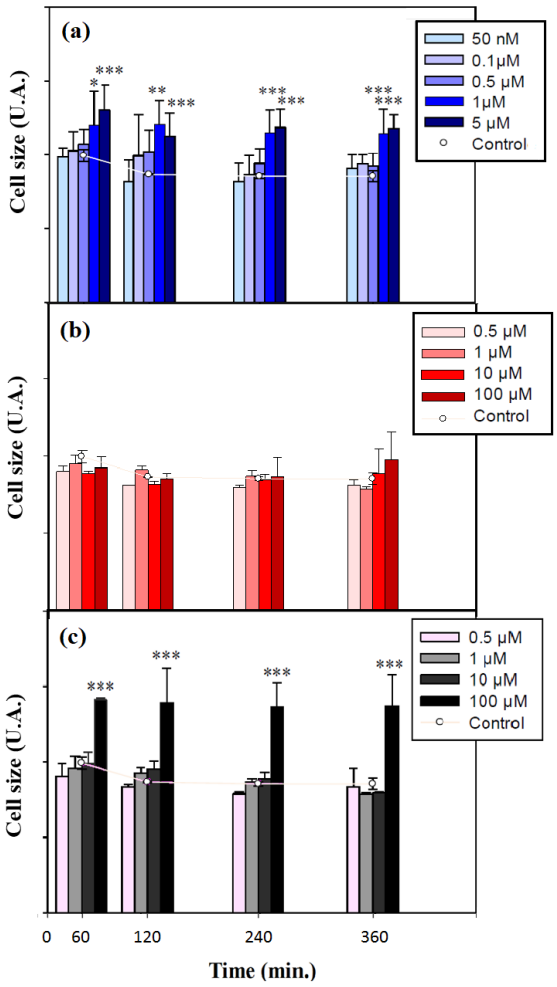

Figure S12. - Cell surface area/size (FSC signal) as function of time and concentration for (a) ionic Ce, (b) citrate coated Ce ENPs and (c) uncoated Ce ENPs at pH 7.0 (n=2 to 3). ANOVA paired with Holm-Sidak test were used to compare treated and untreated microalgae, with significance defined by * for $p \leq 0.05$,** for $p \leq 0.01$ and *** for $p \leq 0.001$.

Chapitre 3 – Whole transcriptome profiling (RNA-Seq) of a rare earth metal mixture in *Chlamydomonas reinhardtii* shows mainly antagonistic interactions among the metals.

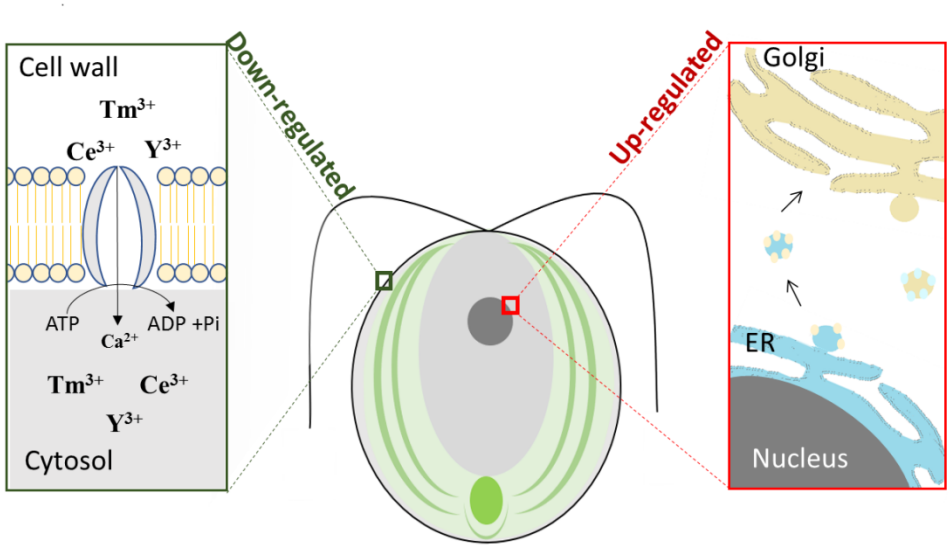

Elise Morel[1], Lei Cui [1], William Zerges[2] and Kevin J. Wilkinson[1,Ψ]

[1]Biophysical Environmental Chemistry Group, University of Montreal, P.O. Box 6128, Succ. Centre-Ville, Montreal, QC

[2]Dept. of Biology, Concordia University, 7141 Sherbrooke W., H4B 1R6, Montreal, QC, Canada

[Ψ]corresponding author

Modified after its submission to Environmental Science & Technology in February 2020

Abstract

In order to better understand the risks of rare earth elements (REEs), it is necessary to determine their fate and biological effects under environmentally relevant exposure conditions (e.g. low concentrations, REE mixtures). Contradictory results have been reported with respect to REE bioavailability to aquatic microorganisms. Here, the unicellular freshwater microalga, *Chlamydomonas reinhardtii*, was exposed for 2 h to one of three soluble REEs (Ce, Tm, Y) salts at 0.5 μM or to an equimolar mixture of the REEs. Relative bioavailabilities were deduced from whole transcriptome profiling analysis and results have been interpreted with respect to REE speciation. Common biological targets related to a protein secretory pathway were identified when the REEs were applied individually. Potential REE competition with calcium was also highlighted. When exposed to ionic Ce, *C. reinhardtii* appeared to acclimate by stimulating arginine synthesis and regulating protein folding. When REEs were applied as a mixture, antagonistic effects were overwhelmingly observed. These results suggest that the approach of government agencies to regulate the REEs using biological effects data from a single metal is largely a conservative approach.

.

Introduction

Rare earth elements (REEs) are strategic metals in the development of the low-carbon energy sector.[7,8] They include the lanthanide metals, in addition to Y and Sc. In the aquatic environment, REE concentrations vary from ng.L^{-1} in non-contaminated waters[25] to mg.L^{-1} in the more contaminated ones.[182] Nonetheless, REE contamination levels appear to be increasing in the environment, due largely to increasing e-waste discharges[183] and agricultural applications, such as REE enriched fertilizers.[184, 185] In addition, REE contamination has been observed in streams close to REE mines.[17]

In natural systems, the light lanthanides (La to Eu) are generally found at higher concentrations than the heavy lanthanides (Gd to Lu), largely due to their differing solubilities.[186] Heavy REEs are generally more strongly complexed than light REEs,[2] potentially decreasing their free ion concentration (and thus their bioavailability). Although there are relatively few exposure data available to define the risk of REEs to environmental and human health, early reports indicated that the heavy REEs are more toxic than the light ones.[187] Nonetheless, complicating interpretation on the risk of REEs is work suggesting that REE speciation cannot be predicted solely from thermodynamic considerations;[188,189] work from our lab showing that some (small, hydrophilic) REE complexes were bioavailable;[56,55] and the observation of significant variations of toxicity data among biological species.[2] In addition, numerous toxicological experiments that have been performed in the presence of phosphates, which are known to precipitate the REEs.[73]

Organisms inhabiting metal-contaminated natural waters are almost always exposed to metal mixtures.[190] This is especially true for metals within the REE series, which are nearly always found together in natural systems.[191-27] In metal mixtures, uptake may be both competitive and non-competitive, resulting in biological uptake and toxicological impacts that can be antagonistic, additive or even synergistic.[190, 192-194] For algae, biouptake experiments have shown antagonistic effects for binary mixtures of REEs,[55] however, biological effects measurements are rare, especially for environmentally relevant concentrations of REE mixtures. Generally speaking, the interpretation of bioaccumulation or toxicity results for REE mixtures is complex due to interactions at the site(s) of toxicity, interactions among physiological processes and potential chemical interactions with constituents in the media, affecting chemical speciation.[2]

In order to understand the biological effects of REEs, at low concentrations and in mixtures, transcriptome profiling (RNA-Seq) analysis was performed on *Chlamydomonas reinhardtii* exposed to Ce (light lanthanide), Tm (heavy lanthanide), Y and a mixture of these metals. Transcriptomic effects of the REEs were inferred from the known functions of the differentially regulated genes in comparison to unexposed microalgae. Expression levels for an equimolar mixture of REEs were then compared to predictions based upon the single metal exposures.

Materials and methods

Materials

All experiments were performed in polymerware (polypropylene or polycarbonate), which was first soaked in 2% v/v HNO_3 for 24 hours, rinsed 7x with Milli-Q water (total organic carbon < 2 µg L^{-1}; resistivity > 18 MΩ cm) and dried under laminar flow conditions. Chemicals were molecular biology grade or higher, including acetic acid (analytical grade, Fisher Scientific); chloroform (99,8%, Acros organics); nuclease-free water (Qiagen); K_2HPO_4 and KH_2PO_4 (ACS reagent grade, Fisher Chemical); Tris (Tris-(hydroxymethyl)-aminomethane, USP/EPgrade, BDH); EDTA disodium salt (Bioultra grade, Sigma-Aldrich); Isotone (VWR); HNO_3 (67–70%; Aristar Ultra, BDH), NaOH (Acros Organics), NaMES (2-(N-morpholino)ethanesulfonic sodium salt, Acros Organics); NaHEPES (4-(2-hydroxyethyl)-1-piperazineethanesulfonic sodium salt, Acros Organics). Single element (1.0 g.L^{-1}; $Ce(NO_3)_3$, $Tm(NO_3)_3$, $Y(NO_3)_3$) and multielement (10 mg.L^{-1}; CMS-1) ICP-MS standards were acquired from Inorganic Ventures.

Culture and exposure conditions

C. reinhardtii is a green microalga that is ubiquitous to fresh waters and often used for studies examining the toxicology of pollutants in natural waters. Details on its specific culture conditions and preparation for experiments involving trace metals have been published previously.[56] In brief, the wild-type strain CC-125 (aka 137c, *Chlamydomonas* resource center) was cultured in 4×diluted TAP at 20°C under conditions of 12 h light/12 h dark (60 mmol s^{-1} m^{-2}) using orbital shaking (100 rpm), until algae reached their mid-exponential growth phase. Cells were then washed 3 times as follows: pelleting by centrifugation (2000xg for 3 min) followed by

resuspension in an exposure medium (see below) that contained no Ce. The concentrated cell suspension was then diluted to 6.5-10 x 10^4 cells mL^{-1} (i.e. 0.15 $cm^2.mL^{-1}$) in an exposure solution containing the appropriate metal concentration. Culture densities and cell surface areas were measured using a Multisizer 3 particle counter (50 mm aperture; Beckman Coulter).

Cells were exposed for 2 h to 0.5 µM of **Ce**, **Tm**, **Y** or their equimolar mixture (**Mix**) in 10.0 mM NaHEPES (pH 7.0 in a solution also containing 10.0 µM $Ca(NO_3)_2$).[130] This simplified experimental medium was used so that the chemical speciation of REEs could be precisely controlled. The latter was modeled using Visual MINTEQ v3.1, under the assumption that the solutions were in equilibrium with 14.0 µM $CO_{2(aq)}$. In order to evaluate adsorptive losses and/or contamination, dissolved (< 0.45 µm, nitrocellulose membrane, Millipore) metal concentrations in the experimental media were measured: (i) after preparation of solutions but before the addition of the cells; (ii) following the addition of the cells and (iii) at the end of the 2h exposure of the algae to the REEs. Four hundred µL of HNO_3 (67–70%) was added to 1 mL of sample followed by 5 h of heating at 80° C (DigiPREP, SCP science). Samples were then diluted in 10 mL and analyzed by inductively coupled plasma mass spectrometry (ICP-MS, PerkinElmer; NexION 300X). A calibration curve for each element was run every 20 samples while blanks and quality control standards were run every 10 samples. Indium was used as the internal standard to correct for instrumental drift.

Cell densities were low enough to ensure that REE concentrations did not decrease significantly over the duration of experiment (**Figure S1**). Following the 2 h exposure, cells were pelleted from 200 mL of the exposure solution by centrifugation (2000×g, 2 min, 4°C). Cell pellets were resuspended in 1 mL nuclease-free water before being transferred into 1.5 mL microtubes where cells were again pelleted by centrifugation. Cell pellets were frozen on dry ice and stored at −80 °C.

Total RNA extraction

Frozen cell pellets were thawed and immediately resuspended in freshly prepared lysis buffer (0.3 M NaCl, 5.0 mM EDTA, 50 mM Tris-HCl (pH 8.0), 2.0% (w/v) SDS, 3.3 U mL^{-1} proteinase K) and then incubated at 37°C for 15 min with orbital shaking (300 rpm). Total RNA was isolated by extracting the sample 3x with phenol:chloroform:isoamyl alcohol (25:24:1, pH

6.8), followed by 1x with chloroform:isoamyl alcohol (24:1). At each step, samples were centrifuged (12000xg, 10 min, 4°C) and supernatants were transferred into new tubes. Total RNA was precipitated from the final aqueous phase by isopropanol, then washed with 75% ethanol. After a final centrifugation, the pellet was resuspended in 20-30 µL of nuclease-free water. A 3 µL aliquot was analyzed by automated electrophoresis for RNA quality (RIN number > 7; 1.8 < ratio 260/280 < 2.1; ratio 260/230>1.8; Bioanalyzer, Agilent) and spectroscopy (OD260) in order to determine the concentration of RNA (Nanodrop). RNA samples were stored at −80°C until RNA RNA-Seq analysis.

RNA-Seq analysis

DNase treatment, mRNA selection, library preparation (NEB/KAPA mRNA stranded library preparation) and Illumina sequencing were carried out at the Genome Quebec facilities (www.gqinnovationcenter.com). Two lanes on a HiSeq (v.4) were used for the paired-end sequencing (2 × 100 base pairs) of 25 samples (5 replicates for each treatment: Ce; Tm; Y; Mix; Controls). All replicates were from independent algal cultures.

For each sample, *ca.* 55 million of reads with their sequences, identification and quality scores were stored in two FastQ files. Read quality was explored with FastQC[131], while filtering quality and adapter trimming were carried out with Trim Galore!.[132] Only paired reads obtained after the cleaning step (phred >20, length > 21 bp) were conserved. Reads were aligned to the *C. reinhardtii* genome v5.3 assembly using TopHat2 with standard presets except that intron size was between 30 and 28000 bbp.[133] Approximately 45 million reads were mapped for each sample (around 82% of raw data) with concordant pair alignment accounting for 85% of the total mapped reads in each sample. GeneBody coverage python script (RSeQC) was used to calculate the number of reads for each nucleotide position and to generate a plot illustrating the coverage profile along the gene (**Figure S2**).[134] The number of reads per gene was determined using the Python package HTSeq.[135] Differentially expressed genes (DEGs) were identified using DESeq2[136] for $\log_2$ fold change (Log_2FC) values exceeding |3| and false discovery rates (p_{adj}) < 0.001. Gene annotations were retrieved from MapMan ontology.[137,138] The JGI Comparative Plant Genomics Portal was also used to explore the function of gene sets of interest, such as the "not assigned" gene list obtained from MapMan.[139] The Fisher exact test (FET) was used to

identify enriched metabolic pathways. The Algal Functional Annotation Tool was used to convert gene and transcript IDs, when necessary.[140]

Combined effect modeling

Due to limitations in the applicability of the addition concentration model for transcriptomic data[195], an Independent Action (IA) model was used to predict transcriptomic effects associated with the mixture. The conceptual approach depicted by Song *et al.* in the case of binary toxicant mixture[196] was adapted to a ternary mixture and the combined effects of the mixture treatments were evaluated for each differentially expressed gene (DEG). Additive interactions among the REEs were obtained when the Log_2FC (fold change) observed for a given gene in the mixture treatment was equal to the Log_2FC predicted by the IA model (Eq. 1), defined as the sum of the Log_2FC of individual REE treatments (x_i represents the different REE: Ce, Tm or Y). Gene expression was considered to be synergistic for $|Log_2FC_{observed}\ (Mix)| > |Log_2FC_{predicted}\ (Mix)|$ and antagonistic when $|Log_2FC_{observed}\ (Mix)| < |Log_2FC_{predicted}\ (Mix)|$. Different patterns of combined effects were also discriminated by taking into account the direction of the transcriptional regulation.[196]

$$Log_2FC_{observed}\ (Mix) = Log_2FC_{predicted}\ (Mix) = \Sigma\ Log_2FC_{observed}\ (x_i) \qquad \textbf{(Eq. 1)}$$

Results and discussion

Chemistry of the exposure solutions

Speciation calculations indicated that the REEs should exist mainly as free metal ions in the simplified exposure solutions (72% to 85% of the total metal), with small contributions of carbonate and hydroxide complexes (**Figure S3**). Nonetheless, in preliminary filtration controls of solutions containing the individual metals or the mixtures, important losses of REE were observed when filtering over 0.45 µm nitrocellulose membranes (91 ± 4% of Ce; 84 ± 4% of Tm and 70 ± 18% of Y). Losses were attributed to the adsorption of the trivalent metals to the flasks or filters, potentially following the formation of metastable (non-equilibrium) particles.[2,30] In spite of a thorough acid wash prior to use, losses were much more important when re-using older polycarbonate flasks, again reinforcing the hypothesis that adsorptive losses were occurring. In order to ensure consistency between added and measured concentrations in the exposure

solutions: new flasks were employed; solutions were pre-equilibrated at least 24 hours prior to exposure; and concentrations were measured at the start and the end of the exposure period (**Figure S4**). In this manner, REE concentrations were stabilized, ranging from 4.5 to 4.9x10^{-7} M prior to the introduction of the algae (nominal concentration = 5x10^{-7} M).

Overview of the RNA-Seq data

Transcriptome profiling with RNA-Seq was used to compare effects of Ce, Tm, Y or an equimolar mixture of the three metals (2 h exposure to a nominal REE concentration of 5.0x10^{-7} M). Of the 19,526 predicted transcripts in *Chlamydomonas reinhardtii*,[142] 16,855 (86%) were detected, indicating sufficient coverage of the genome. Principal component analysis (PCA), performed on expression levels of the detected transcripts, revealed that samples exposed to Tm, Y and the mixture could be distinctly grouped from those exposed to Ce (PC2, 33% of variance) (Figure 1A). PCA also indicated that the mixture effect was most strongly influenced by Tm (and to a lesser extent by Y).

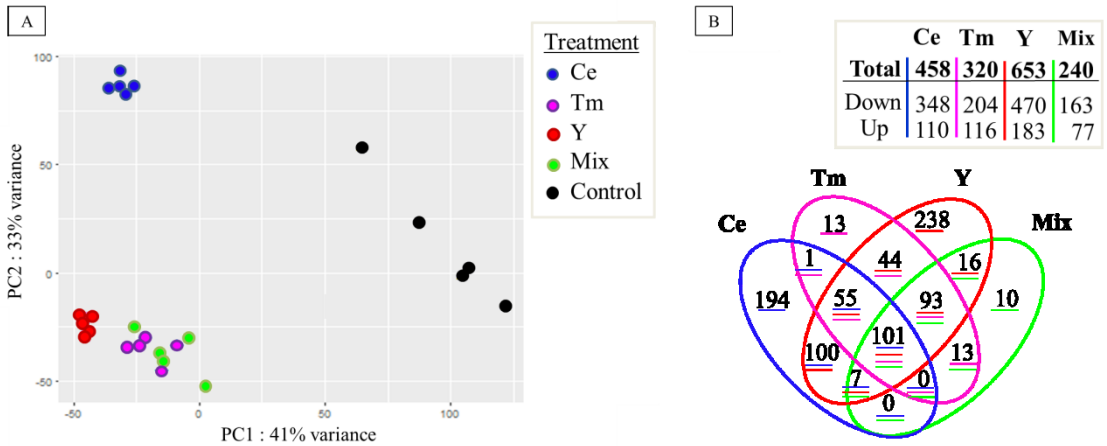

Figure 1. – (A) PCA scores from RNA Seq analysis resulting in 16,855 detected transcripts following a 2 h exposure of *C. reinhardtii* to 5.0x10^{-7} M of: Ce (blue), Tm (pink), Y (red), Mixture (green) and control (i.e. no added metal, black). (B) Differentially expressed genes (DEGs) with respect to the control ($Log_2FC > |3|$, $p_{adj} < 0.001$), following a 2 h exposure of *C. reinhardtii* to 5.0x10^{-7} M of Ce, Y, Tm or their mixture at pH 7.0.

In comparison to control values obtained for unexposed cells, 884 genes showed at least an 8-fold change (FC) due to one or more of the treatments ($Log_2FC > |3|$, $p_{adj} < 0.001$) **(Supplemental Data 1)**. Direct comparison of the numbers of differentially expressed genes (DEGs) suggested that bioavailability decreased in the order Y (653 DEGs) > Ce (458 DEGs) > Tm (320 DEGs) > Mix (240 DEGs) (Figure 1B). These differences can only partly be attributed to free ion concentrations in solution ($[Ce^{3+}]>[Y^{3+}]>[Tm^{3+}]$) and are thus again indicative of distinctive transcriptomic effects of the 3 metals. The proportion of up-regulated and down-regulated DEGs was similar in all treatments, with about 70% down-regulated genes (76% for Ce; 72% for Y; 64% for Tm and 68% for the mixture; **Figure 1B**). Below, we first explore the common biochemical effects of the REEs. Second, we discuss the results that led us to believe that some of the biological effects are distinct for the REEs. Finally, we examined the nature of the interactions for REEs in a common exposure solution.

Common biological targets for the REEs

Of the 884 genes that were differentially expressed with respect to the controls, 156 (18%) were regulated by all three of the REEs (**Figure 1B**, **Supplemental Data 2)**. Functional annotation revealed that an important fraction of the commonly induced genes (14 of the 40 up-regulated DEGs) encoded proteins that were involved in protein processing in the endoplasmic reticulum (ER) (**Table SI**). Genes involved in protein targeting to secretory pathways were significantly enriched for all treatments (FET, $p < 0.05$) **(Table I**). Since protein modifications and trafficking via the endomembrane system which begins at the ER are associated with many diverse cellular processes, the significance of this observation is unclear. However, given that Ca^{2+}-binding chaperone proteins in the ER, such as *BIP1* and *DNJ3*,[197] were up-regulated by the REEs, a potential competition of the REEs with calcium was suspected. This result is consistent with results obtained for *Desmosdesmus quadricauda*, another green microalgae, where lanthanides were shown to alleviate the effects of a calcium deficiency.[198] Interestingly, a few genes that encode calcium-related proteins, acting outside the ER, were down-regulated by the REEs (**Supplemental Data 2**). Among them, a gene encoding a primary active calcium transporter located in the plasma membrane (*Cre16.g681750*) was down-regulated, consistent with an observed decrease in Ce biouptake in the presence of Ca^{2+}.[30] The regulation of calcium-related

targets may also occur at other biological levels. As an example, metal-dependent conformational changes in calreticulin, a key Ca^{2+} signaling protein in the ER, have been observed[199] (though no transcriptomic effect was observed here in the presence of the REEs). The nature of the interactions between the REEs and Ca^{2+} in *C. reinhardtii* (i.e. direct competition or modulation of Ca^{2+} signaling) will require future investigation.

The expression of genes encoding stress-related proteins acting in the cytosol or other cellular organelles (e.g. genes involved with xenobiotic resistance, redox stress and osmotic stress) were down-regulated by REEs (**Supplemental Data 2**). Finally, several genes related to DNA replication and regulation of gene expression, including different transcription regulators (TRs) and transcription factors (TFs) or genes encoding proteins involved in chromatin structure or ribosome biogenesis, appeared to be regulated by the REEs (**Supplemental Data 2**).

In summary, most of the DEGs common to the REEs were related to biological responses that function in stress tolerance or the regulation of metabolism. No clear evidence of acute toxicity was observed. This was expected given the sub-lethal exposure concentrations (0.5 μM) and the short exposure times (2 h) that were used in order to reveal more environmentally relevant effects. Indeed, higher REE concentrations and longer exposure times are generally required to observe toxic endpoints such as growth inhibition in microalgae (e.g. EC_{50} of > 2000 μM Ce for *Pseudokirchneriella subcapitata* in a medium containing phosphates).[73]

Table I. Number of DEGs (with respect to control conditions) for several important metabolic pathways and sub-pathways (MapMan) following a 2 h exposure of *C. reinhardtii* to Ce, Tm, Y and their mixture. Numbers in red are associated with enriched pathways/sub-pathways (FET, $p < 0.05$).

Metabolic pathways	Versus Control			
	Ce	Tm	Y	Mix
Amino acid	**5**	4	6	3
Degradation	0	0	1	0
Synthesis	**5**	3	5	2
Cellular processes	6	6	10	4
Cell development	5	3	7	3
DNA	7	3	12	4
Hormone	1	2	2	1
Lipid	4	5	9	3
Major CHO	1	0	3	0
Minor CHO	4	1	2	1
Miscellaneous enzyme families	6	6	8	4
Not assigned	**317**	224	451	175
Nucleotide	2	1	4	1
Protein	**41**	32	**67**	16
Activation	1	0	3	0
Degradation	9	6	14	2
Folding	6	7	11	5
Posttranslational modification	13	12	23	6
Synthesis	4	0	5	0
Targeting	**8**	**7**	**11**	**3**
Photosynthesis	2	2	7	3
Redox	3	2	2	1
RNA	20	11	28	9
Signaling	8	8	10	5
Stress	**5**	2	4	1
Abiotic	**4**	2	4	1
Biotic	1	0	0	0
Organic acid transformation	1	2	3	2
Tetrapyrrole	1	0	3	1
Transport of metals and small molecules	24	11	25	6

Ce anomaly among the REEs

Among the common annotated functions for all three metals, a large number of DEGs were related to protein metabolism, RNA metabolism and the transport of metals and small molecules (**Table I, Figure S4**). In contrast, genes involved in amino acid metabolism, stress and numerous non assigned genes were only enriched as a result of the Ce exposures (FET, $p < 0.05$). Further analyses at the level of specific pathways, indicated that Ce stimulated glutamate metabolism and regulated abiotic stress related genes, though genes responded to a lesser extent than the other REEs **(Table I, Supplemental Data 3).** Indeed, genes encoding enzymes in arginine synthesis (i.e. glutamate metabolism) were up-regulated by 9 to 11-fold following exposure to Ce and protein folding (i.e. abiotic stress) was either up- or down-regulated by 11 to 18-fold. Ce specifically down-regulated two genes encoding stress-induced heat shock proteins (HSPs): a putative HSP70 (*Cre02.g141186*) and a chloroplast targeted *HSP22C* (**Supplemental Data 3**), in addition to *HSP90B* and *BIP1* that were up-regulated by all of the tested REEs (as mentioned above - Common biological targets for the REEs). Most of the Ce specific genes have no annotated function (FET, $p < 0.05$) (**Table I**).

Interestingly, despite its distinctive redox properties among the REEs, no significant enrichment in redox-related pathways was found for the cells exposed to Ce. For example, genes encoding a protein disulfide isomerase (*PDI1*) and a superoxide dismutase (*MSD5*) were regulated by exposure to all three of the metals.

Finally, although PCA analysis and the Venn's plot strongly indicated a unique response of *Chlamydomonas* to Ce, differences among the REEs represented only 8% of the explained variance when PCA analysis was restricted to the 884 DEGs (PC2: 8% of variance) (**Figure S5**). This indicates that much of the difference between Ce and the two other REEs (Tm and Y) is found in the overall gene expression and not the simply within the subset of DEGs.

Antagonistic effects in the REE Mixture

For cells exposed to an equimolar mixture of Ce, Tm and Y, only 240 DEGs were significantly up- or down-regulated and among those, 101 were common to DEGs that were seen during the treatments with the individual metals (**Figure 1B**). Given that for any given REE, the mixture contained the same concentration of metal in addition to the two complementary metals, the observation that there were far fewer DEGs in the mixture (i.e. 240 DEGs) than for any of the individual REE treatments (i.e. > 320 DEGs) is strong evidence that competitive interactions are occurring among the metals. Furthermore, cells exposed to the mixture had far more DEGs in common with the Tm exposed cells (207 out of 320 DEGs, 64%) than with those exposed to Y (217 out of 653 DEGs, 33%) or Ce (108 out of 420 DEGs, 25%) (**Figure 1B**).

The expression profiles of the 240 DEGs induced by the mixture were compared to predictions of an IA model. The results strongly indicated antagonistic interactions among the three REEs with 162 DEGs showing antagonistic downregulation, 76 showing antagonistic upregulation, one showing a synergistic interaction (i.e. enhanced downregulation) and one showing a contradicted regulation (i.e. reverse upregulation) (**Supplemental Data 4**). For example, none of the stress and/or damage biomarkers showed additive or synergistic interactions among the REEs in the mixture (**Table 2**). Similar results were obtained for entire dataset of 884 DEGs with >99% of the genes displaying antagonistic interactions among Ce, Tm and Y.

Given the high proportion of DEGs that were common between the mixture and the individual REE (25% to 64%, Figure 1B and above**)** and the paucity of DEGs that were specific to the mixture (i.e. 10 DEGs, **Figure 1B**); the near absence of additive or synergistic interactions is surprising. Biouptake experiments in the presence of binary REE mixtures have generally shown that as the concentration and biouptake of one REE is increased, biouptake of the secondary REE is reduced.[55] Furthermore, affinity constants for the binding of REE to the biological uptake sites are similar, with only a small apparent increase as one goes from left to right in the periodic table (i.e. K_{La} of $10^{6.8}$ M^{-1}; K_{Ce} of $10^{6.9}$ M^{-1}; K_{Sm} of $10^{7.0}$ M^{-1}; K_{Eu} of $10^{7.0}$ M^{-1}).[55] The similarity of the affinity constants suggests that the sum of accumulated REEs should remain nearly constant, although Tm might outcompete Ce to a small extent. The observation that fewer genes were significantly differentially expressed and that fold changes were generally lower in the mixture as compared to the individual metal exposures suggests that competitive

interactions between REEs might occur for their biouptake (common transporter, perhaps related to Ca uptake, e.g. Cre16.g681750) and/or for their interactions with common intracellular targets (18% of the DEGs identified in this study). On the other hand, the presence of DEGs that were specific to a single metal treatment (i.e. 194 of 458 DEGs for Ce and 238 of 653 DEGs for Y; Figure 1B) suggests some independent targets of independent REE once inside the cells.

Table II. Annotated functions and log_2FC of several stress-related genes that were differentially expressed in response to treatments with the individual REEs or the mixture (Mix). Metal interactions (synergistic or antagonistic) for a specific gene were deduced from a deviation of the calculated log_2FC value with respect to the expected value obtained for the mixture using an independent action model.

Gene		**Annotated function**	**Observed Log_2 FC**				**Expected Log_2FC**	**Interaction**
ID	**Symbol**	**MapMan**	**Ce**	**Tm**	**Y**	**Mix**	**IA**	
g17702		Biodegradation of xenobiotics	-1.7	-5.2	-4.6	-4.9	-11.5	A. up
cre12.g518200	*PDI1*	Thioredoxin	-4.2	-3.6	-4.5	-3.1	-12.2	A. up
cre02.g090850	*CLPB3*	Stress abiotic	2.2	3.3	4.2	3.3	9.7	A. down
g17150	*HEP2*	HSP70s co-chaperones	2.9	3.5	3.6	3.4	10.1	A. down
cre07.g327450	*DNJ34*		2.7	2.9	3.2	3.1	8.7	A. down
g4407	*DNJ31*		2.6	3.4	3.8	3.2	9.8	A. down
cre07.g327800		ABC transporter	5.6	4.3	5.4	3.7	15.2	A. down
g1850	*MFT10*	Major facilitator transporter	3.5	3.3	3.9	3.4	10.7	A. down
g4500		Osmotic stress potassium transporter	4.5	4.6	4.8	4.3	14.0	A. down
cre08.g367400	*LHCSR 3*	Light harvesting for photosynthesis	2.8	3.4	3.8	3.2	10.0	A. down

Log_2FC <-1 represent the genes that were induced by the treatment while Log_2FC >1 represents those that were repressed, ABC= ATP Binding Cassette, A.= antagonistic interaction.

Implications for regulatory agencies and metals researchers

Based on the above observation that antagonistic interactions largely predominated in the REE mixture, it follows that the approach of governmental agencies to derive toxicity and effects data from single metal mixtures will be largely conservative for the rare earth metals. Given that nearly all contamination of the REE occurs as mixtures, these results suggest that the use of the single metal data will be overprotective. Moreover, our results diminish concern for potential synergistic effects or emergent toxicity of REE mixtures in natural waters. Nonetheless, two caveats need to be noted: data were obtained for a single organism and all exposures were performed at sub-lethal exposure levels. The (initial) observation of adsorptive losses to container walls and untested role of REE complexes, strongly suggests that great care should be made when extrapolating results obtained in the laboratory to real world conditions.

Acknowledgements

Funding for this work was provided by the Natural Sciences and Engineering Research Council of Canada (NSERC Discovery and Strategic project grants) and the *Fonds de Recherche du Québec - Nature et Technologies* (FRQNT). Special thanks go to Yanxia Wu (Concordia University) for sharing her expertise with the RNA extraction of *C. reinhardtii*. The authors declare no competing financial interest.

Supplementary information

Supplementary materials and methods

Exposure optimization

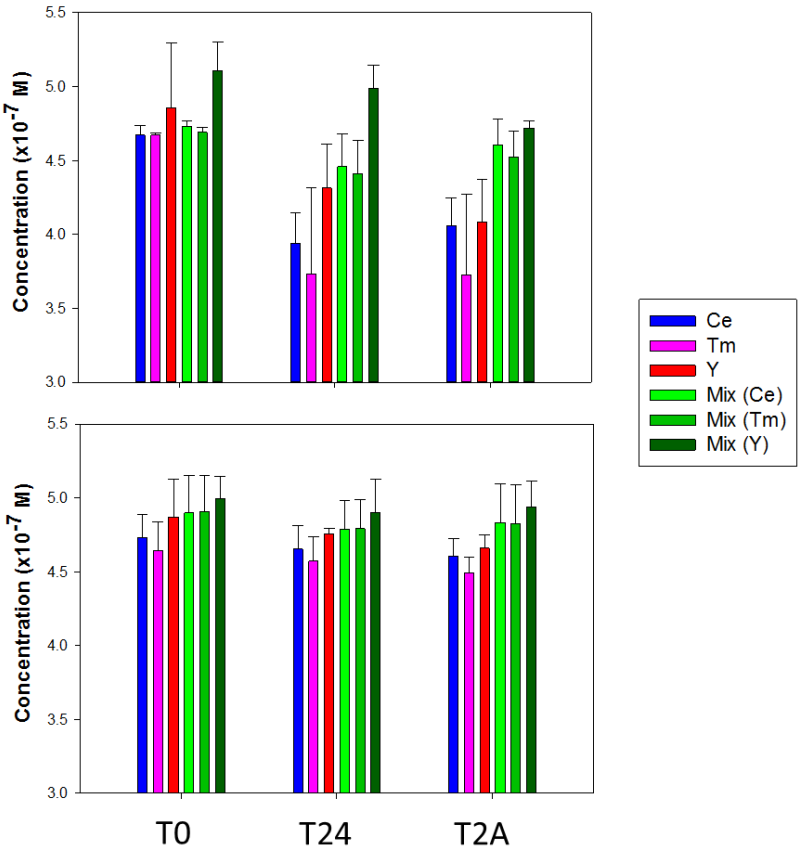

Figure S1. Total REE concentrations measured in the exposure media immediately following preparation (T0), after 24 hours of equilibration (T24) and after 2 hours of exposure to the algae (T2A) for exposure solutions nominally containing $5.0x10^{-7}$ M of Ce, Tm, Y or their mixture in 10^{-2} M NaHEPES. pH 7.0. Experiments were performed in old polymerware (A) and new polymerware (B).

Coverage profile along genes

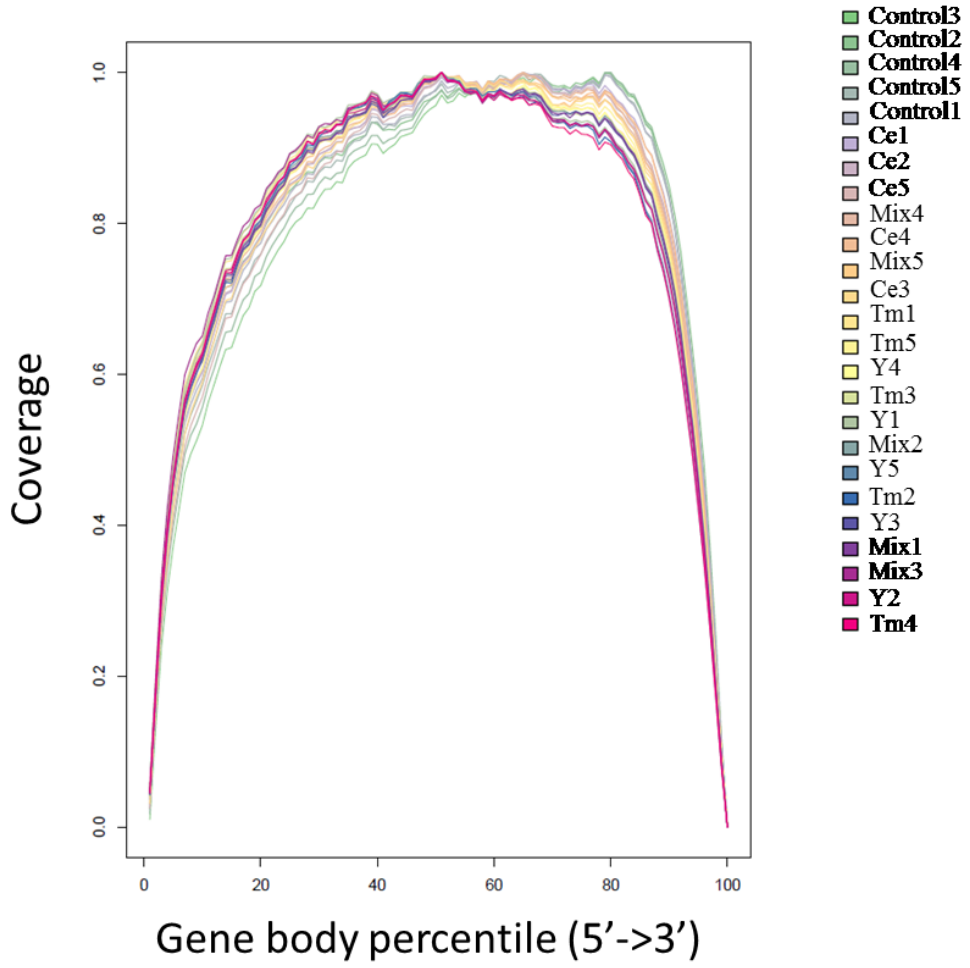

Figure S2: **S**patial repartition of normalized read numbers obtained by RNA-Seq over the gene length (5'->3') for each biological replicate (n=5) of the control or Ce, Y, Tm treatments or their mixture (Mix). Data generated by GeneBodyCoverage.

Supplementary results

REE speciation modelling

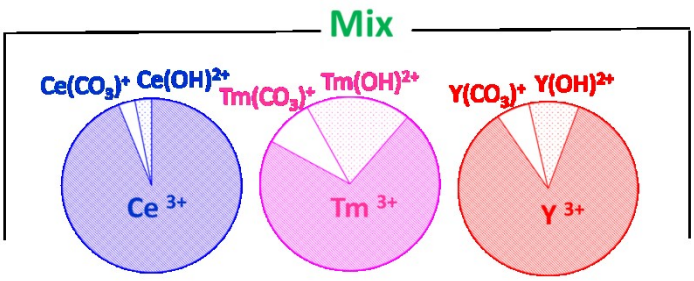

Figure S3: Species distribution for Ce, Tm, Y in the exposure media as predicted by Visual Minteq (in the presence of 10^{-2} M HEPES, 10^{-5} M $Ca(NO_3)_2$ and $1.4x10^{-5}$ M $CO_{2(aq)}$). Data were generated for 4.5 to $4.9x10^{-7}$ M of the REE. Free ion concentrations represented 94% of Ce, 72% of Tm and 85% of Y, in both the individual solutions and the mixtures.

Table SI. Functional information and induction levels of genes (Log_2FC) related to protein processing in the endoplasmic reticulum and which were commonly induced by individual REE treatments. ER: endoplasmic reticulum, PM: plasma membrane.

Gene identification		Functional information			Log_2 (FC)			
ID	**Symbol**	**MapMan**	**Phytozome**	**Cellular component**	**Ce**	**Tm**	**Y**	**Mix**
Cre12.g524200	SPC25	Not assigned	Signal Peptidase (25 kDa)	ER, protein complex, peptidase complex, PM, vacuole	-4.7	-5	-5.9	-4.4
g7473		Not assigned	Protein folding regulator	ER, PM, vacuole	-4.2	-4.5	-5.5	-3.9
Cre11.g467726		Not assigned	Oligosaccharide translocation protein (RFT1)	ER, PM, vacuole	-3.3	-3.1	-4.4	
Cre05.g244950		Not assigned	Translocon-associated protein subunit beta (SSR2)	ER, PM, vacuole	-4.1	-3.3	-4.3	
Cre09.g415400		Not assigned	Neuroblastoma amplified sequence		-3.3	-3.4	-4.1	-3.1
Cre06.g299750		Not assigned	Predicted membrane protein	COPII-coated ER to Golgi transport vesicle, PM, vacuole	-3.4	-3.3	-4	
Cre02.g080700	BIP1	Protein folding	ER associated Hsp70 protein	Cytoplasm	-4.1	-3.1	-4	
Cre02.g080650	HSP90B	Protein folding/stress abiotic	ER associated heat shock protein 90B		-4.2	-3.2	-4.2	
Cre03.g170350	SEC12	Protein targeting	Regulator of COP-II vesicle coat	Golgi, ER, PM, vacuole	-4.7	-4.5	-5.6	-3.8
Cre14.g620400	SPC22	Protein targeting	Signal Peptidase, 22 kDa subunit	ER, protein complex, peptidase complex, PM, vacuole	-3.7	-3.9	-4.7	-3.5
Cre07.g318450	SEC61B	Protein targeting	SEC61-beta subunit of ER-translocon	ER, protein complex, PM, vacuole	-4	-3.2	-4.3	
Cre01.g068150	SEC61G	Protein targeting	SEC61-gamma subunit or ER translocon	Cytoplasm, ER	-3.7	-3.2	-4	
Cre12.g518200	DNJ3	Redox thioredoxin	Protein disulfide isomerase	Cytosol	-4.2	-3.5	-4.5	-3.1
Cre01.g032050	UAA1	Transport. P-sugars at the	UDP-galactose transporter related	Golgi, ER, PM, vacuole	-3.5	-3.1	-3.7	

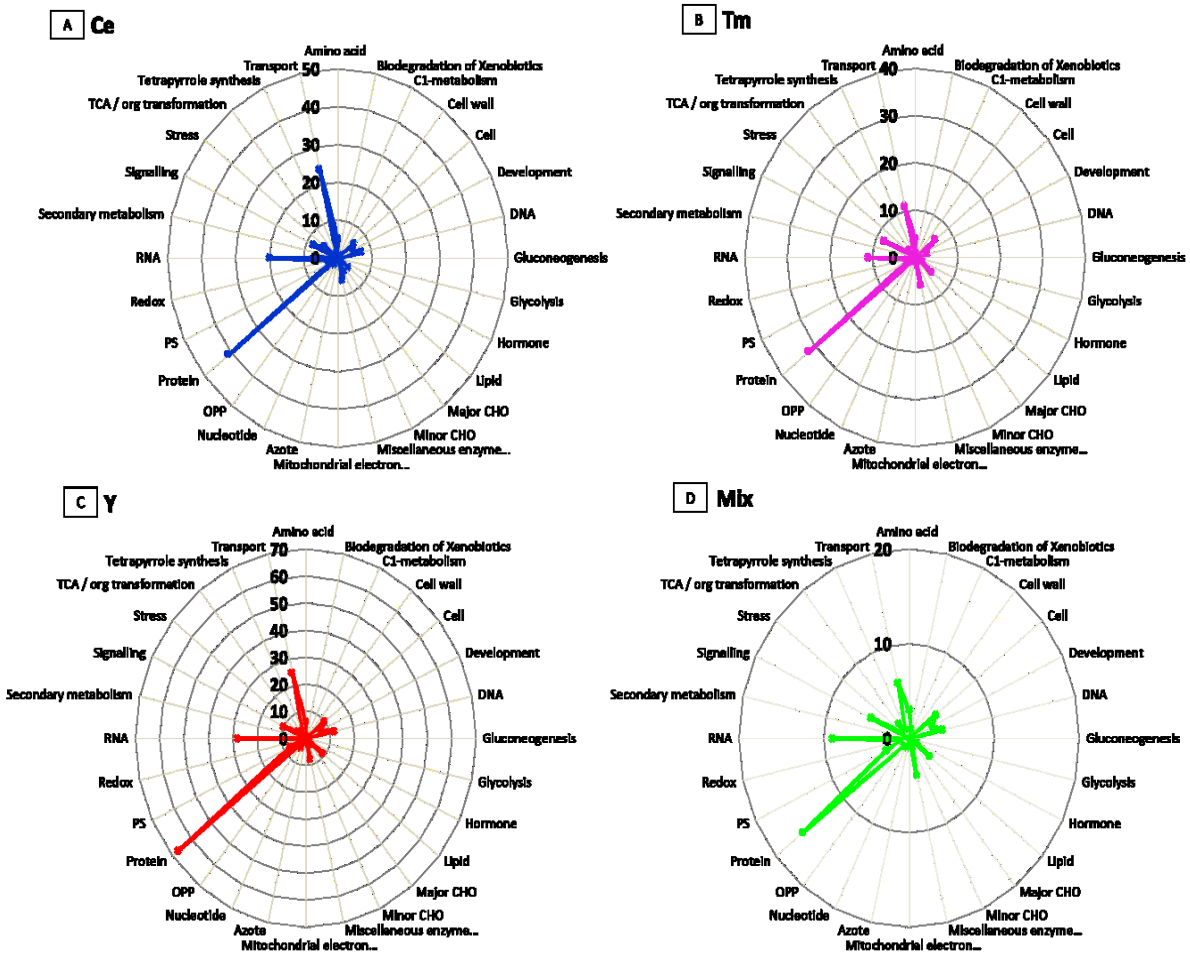

Figure S4. Radar plot showing the number of DEG relative to controls (DeSeq2, Log2FoldChange > |3|, $p_{adj} < 0.001$) according to the metabolic pathways (MapMan) for a 2 h exposure of *C. reinhardtii* to (A) Ce (blue, scale=0 to 50 DEGs), (B)Tm (pink, scale=0 to 40 DEGs), (C)Y (red, scale=0 to 70 DEGs) and (D) their mixture (green, scale=0 to 20 DEGs).

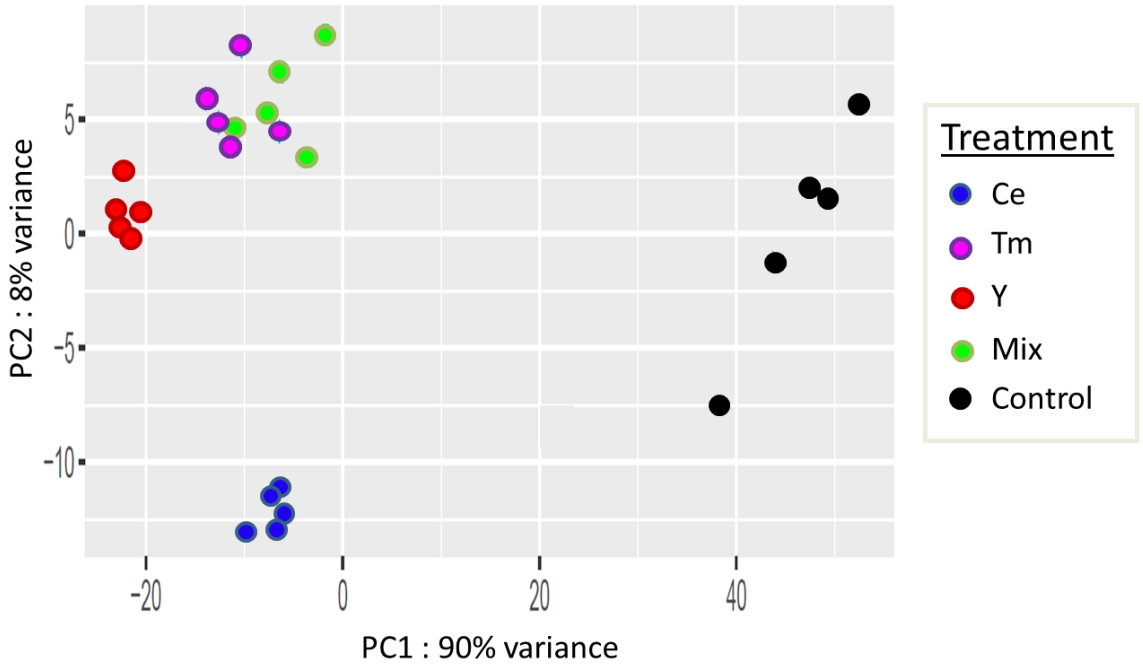

Figure S5. PCA scores for the analysis of DEGs (884 genes, $Log_2FC > |3|$, $p_{adj} < 0.001$) for *C. reinhardtii* after a 2 h exposure to Ce (blue), Tm (pink), Y (red), Mixture (green), and control (black). Differential expression is relative to the control (no metal) solutions. This figure looks at only DEGs (as opposed to Fig. 1A in the main body of the paper, which shows all examined genes).

Supplementary Data

Morel, Elise, 2020, "Données supplémentaires thèse 'Biodisponibilité et effets transcriptomiques du cérium chez Chlamydomonas reinhardtii'", https://doi.org/10.5683/SP2/TIGPFS, Scholars Portal Dataverse, VERSION PROVISOIRE, UNF:6:TvtqXzilz/657ZwytFToiQ== [fileUNF]

Supplementary Data 1. Differential gene expression analysis and MapMan ontology for all the differentially expressed genes

Supplementary Data 2. Differential gene expression analysis, MapMan ontology and functional complementary information for genes commonly regulated by REE treatments.

Supplementary Data 3. Differential gene expression analysis, MapMan ontology and functional complementary information for Ce responding genes.

Supplementary Data 4. Combined effects modelling for genes responding to the mixture.

Conclusions

Biodisponibilité relative du Ce anthropique chez *C. reinhardtii*

Dans ce projet, la biodisponibilité relative du Ce ionique par rapport aux nanoparticules d'oxydes de cérium et au Tm et à l'Y a été déduite des transcriptomes de *C. reinhardtii*. Il ne s'agit pas d'analyses quantitatives de la biodisponibilité de ces éléments comme le seraient des mesures de bioaccumulation, par exemple. Cependant, cette approche permet de se placer directement du point de vue de l'organisme exposé, et donc de s'affranchir de la quantité de Ce bioaccumulé, qui ne reflète pas forcément l'intensité des effets biologiques produits. Par exemple, les Ce NMs peuvent induire des effets biologiques par simple contact avec les membranes biologiques (sans être forcément internalisées).

Des effets transcriptomiques généralement distincts entre les Ce NMs et le Ce ionique ont été observés dans les études menées soit à un temps fixé suite à l'exposition des microalgues à une concentration unique de Ce s'intéressant à caractériser plus de 16 000 signaux biologiques (**Chapitre 1**) ou soit pour des conditions d'exposition variées (temps, concentrations, pH) ne mesurant que quelques signaux biologiques (**Chapitre 2**). Des niveaux de transcrits plus importants de *GTR12* ont été observés chez les cellules de *C. reinhardtii* exposées aux Ce NMs enrobées de citrate à pH 5.0, ce qui témoigne de l'importance de la stabilité des Ce NMs produites, même si généralement, la dissolution des Ce NMs dans des conditions environnementales des eaux douces de surface semble négligeable (<10% pour des pH 5.0). Ensemble ces résultats révèlent que la biodisponibilité des Ce NMs pour *C. reinhardtii* ne dépend pas uniquement de leur dissolution, contrairement à l'hypothèse 1.

Des analyses approfondies des caractéristiques physico-chimiques initiales des Ce NMs ont révélé des différences importantes dans l'état d'oxydation des Ce NMs sélectionnées, supplémentaires à la présence ou non d'un enrobage organique. En effet, toutes les Ce NMs sélectionnées devaient être composées principalement de CeO_2 (Ce(IV)) selon les informations des producteurs. Cependant, les analyses de spectroscopie photoélectronique à rayons X ont révélé que les Ce NMs enrobées de PAA étaient majoritairement composées d'atomes de Ce réduits (Ce(III)). Cependant, en dépit de leurs différentes distribution de tailles, différents rapports de Ce(III)/Ce(IV) et différents enrobages, les Ce NMs non enrobées et celles enrobées

de PAA présentaient peu de différences par rapport aux cibles moléculaires qu'elles affectaient. Alors que les Ce NMs enrobées de citrate qui présentaient la même stabilité colloïdale que les Ce NMs enrobées de PAA et le même rapport Ce(III)/Ce(IV) que les Ce NMs non enrobées, ont eu un impact particulièrement atténué comparé à celui des deux autres. La biodisponibilité des Ce NMs n'était donc pas limitée aux petites NMs dispersées en suspensions.

Des analyses ayant trait à la bioaccumulation et à la spéciation intracellulaire du Ce, nous permettraient de valider certaines différences mises en évidence dans les **chapitres 1 et 2,** entre les formes ioniques et les formes nanoparticulaires du Ce. Pour exemple, elles permettraient d'identifier si les cellules de *C. reinhardtii* isolent les Ce NMs dans des compartiments cellulaires spécifiques (ex. espace périplasmique, vacuole) ou si elles les transforment (dissolution, réduction, complexation).[201]

Défis des analyses transcriptomiques

L'analyse de profilage du transcriptome entier a permis d'identifier des gènes et voies métaboliques mobilisées chez les populations algales de *C. reinhardtii* pour s'adapter à leurs expositions à des nanoparticules d'oxydes de cérium ou à des sels d'éléments de terres rares pour des concentrations d'exposition de 0,5 µM Ce, Tm et/ou Y en milieux contrôlés à pH 7.0. Cette technique très quantitative est actuellement préférée à la méthode des puces à ADN. Cependant, l'analyse des données issues du séquençage haut-débit est complexe. De grandes quantités de données sont générées, un niveau d'expertise important est nécessaire pour assurer la bonne qualité du traitement bio-informatique de ces dernières, tout comme, leur interprétation (ex. identification des voies métaboliques).

Valeurs seuils

Le seuil qui définit la significativité des variations des quantités d'ARNm entre les échantillons traités et les échantillons contrôles (Log_2FC) doit respecter une certaine cohérence entre le nombre de réplicas biologiques et les taux de faux et de vrais positifs attendus. Le choix du programme utilisé pour identifier les gènes différentiellement exprimés est également important. Ainsi, selon une étude de Schurch *et al.* si l'on dispose de 3 réplicas biologiques, qu'on utilise le programme DESeq2, comme tel a été le cas dans les **chapitre 1 et 3**, il est nécessaire d'appliquer au moins un seuil de log_2FC de |0,5| avec un taux de faux positif corrigé

pour le test multiple d'hypothèse, p_{adj}, de 0,05.[200] Dans le **chapitre 1**, nous avons utilisé un seuil de Log_2FC de |1,0| et un p_{adj} de 0,001, ce qui semble donc conservatif en vue des recommandations de l'article précédemment cité. Un Log_2FC de |1.0| équivaut à une induction ou une répression de 2 par rapport au contrôle, seuil généralement considéré lorsque les quantités de ARNm sont mesurées par RT-*q*PCR. L'application de paramètres trop conservatifs peut toutefois limiter l'identification de vrais positifs, et surtout limiter la mise en évidence des voies métaboliques dans lesquelles interviennent les protéines encodées par ces gènes vraiment différentiellement exprimés mais non détectés. Par exemple, si un log_2FC minium de |2.0| avait été fixé seulement une dizaine de gènes différentiellement exprimés aurait été identifiée chez les microalgues exposées en tripliquas aux nanoparticules d'oxydes de cérium (**Tableau I**). Dans le **chapitre 2**, possédant plus de réplicas biologiques indépendants (n=5), au moins trois fois plus de gènes différentiellement exprimés auraient été obtenus si un Log_2FC de |2.0| avait été fixé (**Tableau II**).

Tableau I. Nombre de gènes différentiellement exprimés en fonction des seuils fixés pour l'estimation des taux de faux positifs (p_{adj}) et la variation de la quantité d'ARNm (Log_2FC) par rapport aux contrôles chez *C. reinhardtii* après 2 h d'exposition à du Ce ionique, des Ce NMs enrobées de citrate, enrobées de PAA et non-enrobées (**chapitre 1, n= 3**). Les valeurs en gras et en rouge sont issues des seuils sélectionnés pour l'étude.

	Ce ionique	$Log_2FC > \|1\|$	$Log_2FC > \|2\|$	$Log_2FC > \|3\|$
Ce ionique	$p_{adj} < 0.01$	262	17	1
	$p_{adj} < 0.001$	**138**	17	1
Cit-Ce NMs	$p_{adj} < 0.01$	33	8	3
	$p_{adj} < 0.001$	**23**	7	3
PAA-Ce NMs	$p_{adj} < 0.01$	819	6	0
	$p_{adj} < 0.001$	**315**	6	0
Ce NMs non enrobées	$p_{adj} < 0.01$	1414	14	0
	$p_{adj} < 0.001$	**688**	14	0

Tableau II. Nombre de gènes différentiellement exprimés en fonction des seuils fixés pour l'estimation des taux de faux positifs (p_{adj}) et la variation de la quantité d'ARNm (Log_2FC) par rapport aux contrôles chez *C. reinhardtii* après 2 h d'exposition à du Ce, Tm, Y et leur mixture équimolaire (**chapitre 3, n= 5**). Les valeurs en gras et en rouge sont issues des seuils sélectionnés pour l'étude.

		$Log_2FC > \|1\|$	$Log_2FC > \|2\|$	$Log_2FC > \|3\|$	$Log_2FC > \|4\|$
Ce	$p_{adj} < 0.01$	5540	1785	458	120
	$p_{adj} < 0.001$	5486	1785	**458**	120
Tm	$p_{adj} < 0.01$	4480	1436	320	60
	$p_{adj} < 0.001$	4348	1436	**320**	60
Y	$p_{adj} < 0.01$	5056	1956	653	177
	$p_{adj} < 0.001$	4943	1956	**653**	177
Mix	$p_{adj} < 0.01$	4339	1299	240	27
	$p_{adj} < 0.001$	4210	1298	**240**	27

Sur les 338 gènes différentiellement exprimés identifiés à la suite d'une exposition de *C. reinhardtii* à 0,5 µM de Ce ionique pendant deux heures à pH 7.0 dans le **chapitre 1**, 22 ont été similairement identifiés dans le **chapitre 2** (**Figure 1**). Ils sont associés à des $Log_2FC > |1,4|$ pour le chapitre 1 et $Log_2FC > |3,0|$ pour le chapitre 3. Il est possible que cette faible répétabilité entre les deux analyses ARN-Seq pour une même condition soit attribuée à l'augmentation à la fois du nombre de réplicas biologiques et des seuils de Log_2FC pour le deuxième batch d'expériences. Il est également à noter que du fait d'une contamination bactérienne des cultures solides de microalgues, une nouvelle culture avait dû être débutée entre la réalisation de ces deux expériences de séquençage aléatoire du transcriptome entier de *C. reinhardtii*.

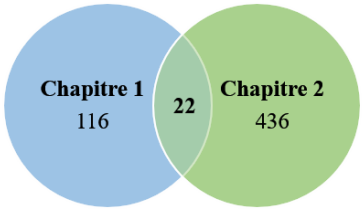

Figure 1. – Diagramme de Venn obtenu pour les gènes différentiellement exprimés dans le chapitre 1 (n=3, $Log_2FC > |1|$, $p_{adj} < 0.001$) et dans le chapitre 2 (n=5, $Log_2FC > |3|$, $p_{adj} < 0.001$) suite à une exposition de *C. reinhardtii* à 0,5 µM de Ce ionique pendant deux heures à pH 7.0.

Identification de biomarqueurs

Bien que peu nombreux, les 22 gènes différentiellement exprimés communs entre les deux chapitres contiennent notamment *GTR12, Cre17g.737300, MMP6* et *HSP22E* qui composent la signature transcriptomique spécifique d'une exposition de *C. reinhardtii* à du Ce ionique relativement aux Ce NMs, validée en milieu aqueux simplifié (**chapitre 2**). Les quantités d'ARNm de ces quatre biomarqueurs transcriptomiques identifiés par ARN-Seq ont été reproduites avec succès par RT-qPCR, et ont présenté une variation monotone suivant le temps et la concentration d'exposition des microalgues au Ce ionique (hypothèse 2 validée). Ils avaient été initialement sélectionnés sur la base de l'intensité de leur régulation parmi les gènes spécifiques au Ce ionique (i.e. Log_2FC les plus importants en valeurs absolues). Cependant, l'analyse des quantités d'ARNm suite à une exposition des microalgues à d'autres ETRs (**Chapitre 3**) a démontré que *GTR12* était également induit par le Tm, l'Y et la mixture équimolaire composée de 0,5 µM de Ce, Y, Tm (**Tableau III**) et que les trois autres biomarqueurs transcriptomiques analysés (*MMP6, Cre17g.737300* et *HSP22E*) ne répondent plus à la présence de Ce lorsque ce dernier est mélangé avec d'autres ETRs (en milieu contrôlé) (**Tableau III**).

Leur applicabilité dans le contexte de développement d'un bio-essai permettant la détection de forme dissoute et nanoparticulaire du Ce dans les matrices environnementales est donc compromise puisque les ETRs sont très souvent retrouvés ensemble dans la nature. Aussi, ces effets compétitifs permettent d'infirmer l'hypothèse 4 selon laquelle la réactivité redox atypique du Ce ionique induirait une biodisponibilité différente de celles des autres ETRs. Une précipitation des ions Ce en nanoparticules a été observée par SP-ICP-MS donnant un signal de la fraction particulaire du Ce représentant environ 20% du Ce total à pH 7.0 (**Chapitre 1 et chapitre 2**). Des analyses similaires dans les milieux d'exposition contenant la mixture d'ETRs permettraient de vérifier si de tels particules sont également formées en présence d'autres ETRs (ex. Tm et Y), comme suggèrent les expériences de filtration (**Chapitre 3**).

Tableau III. Informations fonctionnelles (MapMan)[137,138] et changements des quantités d'ARNm (*fold change*) des 4 biomarqueurs transcriptomiques validés dans le **chapitre 2** (*GTR12, Cre17g.737300, MMP6* et *HSP22E*) après 120-min. d'exposition de *C. reinhardtii* à 0,5 µM of Ce, Tm, Y ou leur mixture (pH 7.0) déterminés par ARN-Seq (n=5).

ID	Mapman	Ce	Tm	Y	Mixture
GTR12	Carbohydrate mineur	9.4	9.6	9.8	12.8
Cre17.g737300	-	12.9			
MMP6	Dégradation des protéines	30.1			
HSP22E	Repliement des protéines	0.3			

L'identification de biomarqueurs transcriptomiques d'exposition de *C. reinhardtii* aux différentes formes du Ce anthropique demandera donc des efforts de recherches supplémentaires dans l'optique du développement d'un bio-essai. Les deux bases de données de ARN-Seq obtenues dans ce projet sont sources de nombreuses découvertes sur les effets transcriptomiques du Ce, du Tm et de l'Y.

Informations mécanistiques

Par exemple, les transcrits de *SEC12, ARL9* et *ARL12* ont été fortement induit (Log_2FC > |1,5| pour **chapitre 1**, Log_2FC > |4,5| pour **chapitre 3**) par le Ce ionique et les autres ETRs. Ces gènes encodent des protéines impliquées dans le transport vésiculaire vers une direction encore inconnue (***Supplementary Data* des chapitres 1 et 3**). Il est possible que ces vésicules se dirigent vers la vacuole, qui est le compartiment cellulaire principal de détoxification chez les cellules algales.[201] Aussi, des gènes reliés au complexe d'exocyste ont été communément induits chez les microalgues exposées au Ce ionique et aux Ce NMs non enrobées ou enrobées de PAA (**Chapitre 1, *Supplementary Data* 4**). L'exocytose serait donc potentiellement un autre mécanisme de détoxification entrepris par les microalgues pour s'acclimater à la présence de Ce ionique ou nanoparticulaire. Il s'agit maintenant de confirmer de telles hypothèses par des analyses complémentaires soit à d'autres échelles biologiques (ex. moléculaire et cellulaire, **Chapitre 2**) soit via d'autres analyses bio-informatiques (ex. analyses de réseaux).

Dans le **chapitre 2**, les analyses par RT-*q*PCR ont mis en évidence que des biomarqueurs de stress oxydatifs (*GPX5, APX1*) étaient soit peu affectés soit réprimés lors d'une exposition de *C. reinhardtii* à du cérium, ionique ou nanoparticulaire. Le cérium n'induit donc pas dans les conditions d'exposition la génération en excès de H_2O_2, une espèce réactive de l'oxygène induisant l'expression *GPX5* et *APX1*. Cependant, des marqueurs fluorescents non spécifiques ont révélé la présence d'espèces oxydantes en excès chez les cellules de *C. reinhardtii* traitées dans des conditions d'exposition similaires, ainsi que des modifications significatives de leur perméabilité membranaire (**Chapitre 2 - Figure S11**). Ensemble, ces résultats pourraient indiquer que le stress oxydant souvent rapporté chez les organismes exposés au cérium ne passe pas par la génération de H_2O_2 mais ne permettent pas de conclure sur l'effet anti- ou pro-antioxydant des différentes formes de cérium testées. L'interprétation du niveau d'expression de quelques gènes en termes d'effets biologiques chez les cellules est donc limitée, infirmant ainsi l'hypothèse 3.

Les analyses transcriptomiques effectuées dans ce projet fournissent donc une quantité importante d'informations sur les potentiels effets biologiques des ETRs, mais seules, elles présentent une interprétation limitée. Il incombe ainsi d'effectuer des analyses complémentaires afin de pouvoir intégrer de telles observations dans un contexte d'évaluation du risque environnemental de ces éléments, via par exemple, des approches émergentes telles que l'*Adverse Outcome Pathway*.[202] La reproductibilité des résultats devrait être préalablement établie pour des échantillons indépendants de ceux analysés par les techniques 'omiques' en tant que telle avant que les données ne soient intégrées aux modèles d'évaluation des risques. Aussi, la sélection des seuils permettant d'établir l'importance biologique des réponses obtenues par de telles techniques devrait faire l'objet de justifications approfondies.

De l'évaluation des profils d'expression de gènes à l'évaluation du risque écologique

La diversité des propriétés physicochimiques des nanoparticules produites implique que ce ne sont pas tous les types de nanoparticules utilisés qui vont pouvoir être évalués par les organisations gouvernementales. Il incombe donc de définir les propriétés essentielles qui déterminent la biodisponibilité et les effets des Ce NMs. Selon nos résultats, l'état d'agglomération des Ce NMs et l'état d'oxydation des atomes de Ce présents à leurs surfaces ne sont pas des indicateurs suffisants de leurs biodisponibilités et effets chez les microalgues. L'enrobage des Ce NMs semble être un facteur clef pour leur biodisponibilité chez *C. reinhardtii* comme cela a été montré chez certaines plantes cultivées (e.g. maïs[67], blé[69] et concombre[203]). Les réglementations pourraient s'orienter dans le sens de l'utilisation d'enrobages biocompatibles, par exemple, le citrate, qui a atténué les effets transcriptomiques des Ce NMs.

De nombreux projets d'exploitations minières des ETRs sont actuellement en cours d'évaluation pour contrer la réduction des exportations chinoises de ces métaux.[19] Aussi l'efficacité des Ce NMs est maintenant étudiée dans une perspective de sécurité alimentaire.[108] C'est donc sans conteste que les concentrations de ces substances, dont le risque environnemental reste à évaluer, vont augmenter dans les années à venir. La perte de la majorité des ETRs par adsorption sur les contenants expérimentaux utilisés pour les expositions et la biodisponibilité suspectée des complexes d'ETRs indiquent qu'il faut faire attention lors de l'extrapolation des résultats obtenus en laboratoire au monde réel. Les effets compétitifs observés entre les ETRs suggèrent par exemple, que les concentrations maximales permissives estimées via des tests d'écotoxicité réalisés un contaminant à la fois, seraient donc conservatrices et protectrices pour les écosystèmes aquatiques. Cependant, la spéciation de ces éléments peut être complexe même en milieu simplifié et n'a pas forcément été suffisamment considérée lors de tels tests.

Dans nos milieux d'exposition simplifiés, les concentrations en ions libres ont été favorisées pourtant aucun biomarqueur transcriptomique de dommages (ex. apoptose) n'a été induit par les cellules de *C. reinhardtii* exposées durant 2h à 70 µg L^{-1} de Ce, de Tm et/ou d'Y. Cette faible réactivité des éléments de terres rares à court terme se veut rassurante mais doit être vérifier pour des scénarios d'exposition plus réalistes (ex. sur plusieurs générations).

Références bibliographiques

1. Alonso, E.; Sherman, A. M.; Wallington, T. J.; Everson, M. P.; Field, F. R.; Roth, R.; Kirchain, R. E., Evaluating rare earth element availability: A case with revolutionary demand from clean technologies. *Environmental Science & Technology* **2012,** *46*, (6), 3406-3414.

2. Gonzalez, V.; Vignati, D. A.; Leyval, C.; Giamberini, L., Environmental fate and ecotoxicity of lanthanides: are they a uniform group beyond chemistry? *Environment International* **2014,** *71*, 148-157.

3. Perullini, M.; Bilmes, S. A. A.; Jobbágy, M., Cerium oxide nanoparticles: structure, applications, reactivity, and eco-toxicology. In *Nanomaterials: A Danger or a Promise?*, Springer: 2013; pp 307-333.

4. Kulaksız, S.; Bau, M., Contrasting behaviour of anthropogenic gadolinium and natural rare earth elements in estuaries and the gadolinium input into the North Sea. *Earth and Planetary Science Letters* **2007,** *260*, (1), 361-371.

5. Castor, S. B.; Hedrick, J. B., Rare earth elements. *Industrial Minerals volume, 7th edition: Society for Mining, Metallurgy, and Exploration, Littleton, Colorado* **2006**, 769-792.

6. Klee, R.; Graedel, T., Elemental cycles: a status report on human or natural dominance. *Annu. Rev. Environ. Resour.* **2004,** *29*, 69-107.

7. Chu, S. *Critical Materials Strategy*; US Department of Energy: December 2011, 2011.

8. Moss, R.; Tzimas, E.; Willis, P.; Arendorf, J.; Thompson, P.; Chapman, A.; Morley, N.; Sims, E.; Bryson, R.; Peason, J. *Critical metals in the path towards the decarbonisation of the EU energy sector*; EUR 25994 EN European commission, 2013.

9. Park, B.; Donaldson, K.; Duffin, R.; Tran, L.; Kelly, F.; Mudway, I.; Morin, J.-P.; Guest, R.; Jenkinson, P.; Samaras, Z., Hazard and risk assessment of a nanoparticulate cerium oxide-based diesel fuel additive-a case study. *Inhalation Toxicology* **2008,** *20*, (6), 547-566.

10. Lu, C.-H.; Hong, H.-C.; Jagannathan, R., Sol–gel synthesis and photoluminescent properties of cerium-ion doped yttrium aluminium garnet powders. *Journal of Materials Chemistry* **2002,** *12*, (8), 2525-2530.

11. Stambouli, A. B.; Traversa, E., Solid oxide fuel cells (SOFCs): a review of an environmentally clean and efficient source of energy. *Renewable and Sustainable Energy Reviews* **2002,** *6*, (5), 433-455.

12. Auffan, M.; Rose, J.; Bottero, J. Y.; Lowry, G. V.; Jolivet, J. P.; Wiesner, M. R., Towards a definition of inorganic nanoparticles from an environmental, health and safety perspective. *Nature Nanotechnology* **2009,** *4*, (10), 634-641.

13. Reed, K.; Cormack, A.; Kulkarni, A.; Mayton, M.; Sayle, D.; Klaessig, F.; Stadler, B., Exploring the properties and applications of nanoceria: is there still plenty of room at the bottom? *Environmental Science: Nano* **2014,** *1*, (5), 390-405.

14. Dhall, A.; Self, W., Cerium oxide nanoparticles: a brief review of their synthesis methods and biomedical applications. *Antioxidants* **2018,** *7*, (8), 97.

15. Gilbertson, L. M.; Wender, B. A.; Zimmerman, J. B.; Eckelman, M. J., Coordinating modeling and experimental research of engineered nanomaterials to improve life cycle assessment studies. *Environmental Science: Nano* **2015**.

16. Weng, Z.; Jowitt, S. M.; Mudd, G. M.; Haque, N., A detailed assessment of global rare earth element resources: opportunities and challenges. *Economic Geology* **2015,** *110*, (8), 1925-1952.

17. Liang, T.; Li, K.; Wang, L., State of rare earth elements in different environmental components in mining areas of China. *Environmental Monitoring and Assessment* **2014,** *186*, (3), 1499-1513.

18. Park, B.; Martin, P.; Harris, C.; Guest, R.; Whittingham, A.; Jenkinson, P.; Handley, J., Initial in vitro screening approach to investigate the potential health and environmental hazards of Envirox™-a nanoparticulate cerium oxide diesel fuel additive. *Particle Fibre Toxicol* **2007,** *4*, (12), 4-12.

19. Du, X.; Graedel, T. E., Global in-use stocks of the rare earth elements: a first estimate. *Environmental Science & Technology* **2011,** *45*, (9), 4096-4101.

20. Wang, S. Z.; Karpinski, E. A. *ENGINEERED NANOPARTICLES Health and Safety Considerations*; august 2016, 2016.

21. Canada, G. o. List of substances in the third phase of CMP (2016-2021): July 2019 update. https://www.canada.ca/en/environment-climate-change/services/evaluating-existing-substances/cmp-third-phase-update.html#toc1

22. Möller, P.; Morteani, G.; Dulski, P., Anomalous gadolinium, cerium, and yttrium contents in the Adige and Isarco river waters and in the water of their tributaries (Provinces Trento and Bolzano/Bozen, NE Italy). *Acta Hydrochimica et Hydrobiologica* **2003,** *31*, (3), 225-239.

23. MacMillan, G. A.; Chetelat, J.; Heath, J. P.; Mickpegak, R.; Amyot, M., Rare earth elements in freshwater, marine, and terrestrial ecosystems in the eastern Canadian Arctic. *Environmental Science: Processes & Impacts* **2017,** *19*, (10), 1336-1345.

24. Amyot, M.; Clayden, M. G.; MacMillan, G. A.; Perron, T.; Arscott-Gauvin, A., Fate and trophic transfer of rare earth elements in temperate lake food webs. *Environmental Science & Technology* **2017,** *51*, (11), 6009-6017.

25. Noack, C. W.; Dzombak, D. A.; Karamalidis, A. K., Rare earth element distributions and trends in natural waters with a focus on groundwater. *Environmental Science & Technology* **2014,** *48*, (8), 4317-4326.

26. Mayfield, D. B.; Fairbrother, A., Examination of rare earth element concentration patterns in freshwater fish tissues. *Chemosphere* **2015,** *120*, 68-74.

27. Kulaksız, S.; Bau, M., Anthropogenic dissolved and colloid/nanoparticle-bound samarium, lanthanum and gadolinium in the Rhine River and the impending destruction of the natural rare earth element distribution in rivers. *Earth and Planetary Science Letters* **2013,** *362*, 43-50.

28. Pourret, O.; Davranche, M.; Gruau, G.; Dia, A., New insights into cerium anomalies in organic-rich alkaline waters. *Chemical Geology* **2008,** *251*, (1-4), 120-127.

29. Grulke, E.; Reed, K.; Beck, M.; Huang, X.; Cormack, A.; Seal, S., Nanoceria: factors affecting its pro-and anti-oxidant properties. *Environmental Science: Nano* **2014,** *1*, (5), 429-444.

30. El-Akl, P.; Smith, S.; Wilkinson, K. J., Linking the chemical speciation of cerium to its bioavailability in water for a freshwater alga. *Environmental Toxicology and Chemistry* **2015,** *34*, (8), 1711-1719.

31. Dahle, J.; Livi, K.; Arai, Y., Effects of pH and phosphate on CeO_2 nanoparticle dissolution. *Chemosphere* **2014**.

32. Röhder, L. A.; Brandt, T.; Sigg, L.; Behra, R., Influence of agglomeration of cerium oxide nanoparticles and speciation of cerium (III) on short term effects to the green algae *Chlamydomonas reinhardtii*. *Aquatic Toxicology* **2014,** *152*, 121-130.

33. Dahle, J. T.; Livi, K.; Arai, Y., Effects of pH and phosphate on CeO_2 nanoparticle dissolution. *Chemosphere* **2014**.

34. Cao, X.; Chen, Y.; Wang, X.; Deng, X., Effects of redox potential and pH value on the release of rare earth elements from soil. *Chemosphere* **2001,** *44*, (4), 655-661.

35. Bau, M., Scavenging of dissolved yttrium and rare earths by precipitating iron oxyhydroxide: experimental evidence for Ce oxidation, Y-Ho fractionation, and lanthanide tetrad effect. *Geochimica et Cosmochimica Acta* **1999,** *63*, (1), 67-77.

36. Dia, A.; Gruau, G.; Olivié-Lauquet, G.; Riou, C.; Molénat, J.; Curmi, P., The distribution of rare earth elements in groundwaters: assessing the role of source-rock composition, redox changes and colloidal particles. *Geochimica et Cosmochimica Acta* **2000,** *64*, (24), 4131-4151.

37. Thill, A.; Zeyons, O.; Spalla, O.; Chauvat, F.; Rose, J.; Auffan, M.; Flank, A. M., Cytotoxicity of CeO2 nanoparticles for Escherichia coli. Physico-chemical insight of the cytotoxicity mechanism. *Environmental Science & Technology* **2006,** *40*, (19), 6151-6156.

38. Marie, T.; Mélanie, A.; Lenka, B.; Julien, I.; Isabelle, K.; Christine, P.; Elise, M.; Catherine, S.; Bernard, A.; Ester, A., Transfer, transformation, and impacts of ceria nanomaterials in aquatic mesocosms simulating a pond ecosystem. *Environmental Science & Technology* **2014,** *48*, (16), 9004-9013.

39. Tyler, G., Rare earth elements in soil and plant systems-A review. *Plant and soil* **2004,** *267*, (1-2), 191-206.

40. Cassee, F. R.; van Balen, E. C.; Singh, C.; Green, D.; Muijser, H.; Weinstein, J.; Dreher, K., Exposure, health and ecological effects review of engineered nanoscale cerium and cerium oxide associated with its use as a fuel additive. *Critical Reviews in Toxicology* **2011,** *41*, (3), 213-229.

41. Limbach, L. K.; Bereiter, R.; Müller, E.; Krebs, R.; Gälli, R.; Stark, W. J., Removal of oxide nanoparticles in a model wastewater treatment plant: influence of agglomeration and surfactants on clearing efficiency. *Environmental science & technology* **2008,** *42*, (15), 5828-5833.

42. Campbel, P., Interactions between trace metals and aquatic organisms: a critique of the free-ion activity model. *Metal Speciation and Bioavailability in Aquatic Systems* **1995**.

43. Di Toro, D. M.; Allen, H. E.; Bergman, H. L.; Meyer, J. S.; Paquin, P. R.; Santore, R. C., Biotic ligand model of the acute toxicity of metals. 1. Technical basis. *Environmental Toxicology and Chemistry* **2001,** *20*, (10), 2383-2396.

44. Slaveykova, V. I.; Wilkinson, K. J., Predicting the bioavailability of metals and metal complexes: Critical review of the biotic ligand model. *Environmental Chemistry* **2005,** *2*, (1), 9-24.

45. El-Akl, P.; Smith, S.; Wilkinson, K. J., Linking the chemical speciation of Ce to its bioavailability in water for a freshwater alga. *Environmental Toxicology and Chemistry* **2015**.

46. Gustafsson, J. P., Visual MINTEQ 3.0 user guide. *KTH, Department of Land and Water Recources, Stockholm, Sweden* **2011**.

47. Tipping, E., WHAMC—a chemical equilibrium model and computer code for waters, sediments, and soils incorporating a discrete site/electrostatic model of ion-binding by humic substances. *Computers & Geosciences* **1994,** *20*, (6), 973-1023.

48. Tessier, A.; Turner, D. R., *Metal speciation and bioavailability in aquatic systems*. J. Wiley: 1995.

49. Courbiere, B.; Auffan, M.; Rollais, R.; Tassistro, V.; Bonnefoy, A.; Botta, A.; Rose, J.; Orsière, T.; Perrin, J., Ultrastructural Interactions and Genotoxicity Assay of Cerium Dioxide Nanoparticles on Mouse Oocytes. *International Journal of Molecular Sciences* **2013,** *14*, (11), 21613-21628.

50. Crémazy, A.; Campbell, P. G.; Fortin, C., The biotic ligand model can successfully predict the uptake of a trivalent ion by a unicellular alga below pH 6.50 but not above: possible role of hydroxo-species. *Environmental Science & Technology* **2013,** *47*, (5), 2408-2415.

51. Nordberg, H.; Cantor, M.; Dusheyko, S.; Hua, S.; Poliakov, A.; Shabalov, I.; Smirnova, T.; Grigoriev, I. V.; Dubchak, I., The genome portal of the Department of Energy Joint Genome Institute: 2014 updates. *Nucleic Acids Research* **2014,** *42*, (Database issue), D26-D31.

52. Shrager, J.; Hauser, C.; Chang, C.-W.; Harris, E. H.; Davies, J.; McDermott, J.; Tamse, R.; Zhang, Z.; Grossman, A. R., *Chlamydomonas reinhardtii* genome project. A guide to the generation and use of the cDNA information. *Plant Physiology* **2003,** *131*, (2), 401-408.

53. Merchant, S. S.; Prochnik, S. E.; Vallon, O.; Harris, E. H.; Karpowicz, S. J.; Witman, G. B.; Terry, A.; Salamov, A.; Fritz-Laylin, L. K.; Maréchal-Drouard, L.; Marshall, W. F.; Qu, L.-H.; Nelson, D. R.; Sanderfoot, A. A.; Spalding, M. H.; Kapitonov, V. V.; Ren, Q.; Ferris, P.; Lindquist, E.; Shapiro, H.; Lucas, S. M.; Grimwood, J.; Schmutz, J.; Cardol, P.; Cerutti, H.; Chanfreau, G.; Chen, C.-L.; Cognat, V.; Croft, M. T.; Dent, R.; Dutcher, S.; Fernández, E.; Fukuzawa, H.; González-Ballester, D.; González-Halphen, D.; Hallmann, A.; Hanikenne, M.; Hippler, M.; Inwood, W.; Jabbari, K.; Kalanon, M.; Kuras, R.; Lefebvre, P. A.; Lemaire, S. D.; Lobanov, A. V.; Lohr, M.; Manuell, A.; Meier, I.; Mets, L.; Mittag, M.; Mittelmeier, T.; Moroney, J. V.; Moseley, J.; Napoli, C.; Nedelcu, A. M.; Niyogi, K.; Novoselov, S. V.; Paulsen, I. T.; Pazour, G.; Purton, S.; Ral, J.-P.; Riaño-Pachón, D. M.; Riekhof, W.; Rymarquis, L.; Schroda, M.; Stern, D.; Umen, J.; Willows, R.; Wilson, N.; Zimmer, S. L.; Allmer, J.; Balk, J.; Bisova, K.; Chen, C.-J.; Elias, M.; Gendler, K.; Hauser, C.; Lamb, M. R.; Ledford, H.; Long, J. C.; Minagawa, J.; Page, M. D.; Pan, J.; Pootakham, W.; Roje, S.; Rose, A.; Stahlberg, E.; Terauchi, A. M.; Yang, P.; Ball, S.; Bowler, C.; Dieckmann, C. L.; Gladyshev, V. N.; Green, P.;

Jorgensen, R.; Mayfield, S.; Mueller-Roeber, B.; Rajamani, S.; Sayre, R. T.; Brokstein, P.; Dubchak, I.; Goodstein, D.; Hornick, L.; Huang, Y. W.; Jhaveri, J.; Luo, Y.; Martínez, D.; Ngau, W. C. A.; Otillar, B.; Poliakov, A.; Porter, A.; Szajkowski, L.; Werner, G.; Zhou, K.; Grigoriev, I. V.; Rokhsar, D. S.; Grossman, A. R., The Chlamydomonas Genome Reveals the Evolution of Key Animal and Plant Functions. *Science* **2007,** *318*, (5848), 245-250.

54. Yang, G.; Tan, Q. G.; Zhu, L.; Wilkinson, K. J., The role of complexation and competition in the biouptake of europium by a unicellular alga. *Environmental Toxicology and Chemistry* **2014,** *33*, (11), 2609-2615.

55. Tan, Q.-G.; Yang, G.; Wilkinson, K. J., Biotic ligand model explains the effects of competition but not complexation for Sm biouptake by *Chlamydomonas reinhardtii*. *Chemosphere* **2017,** *168*, 426-434.

56. Zhao, C.-M.; Wilkinson, K. J., Biotic ligand model does not predict the bioavailability of rare earth elements in the presence of organic ligands. *Environmental Science & Technology* **2015,** *49*, (4), 2207-2214.

57. Yang, G.; Wilkinson, K. J., Biouptake of a rare earth metal (Nd) by *Chlamydomonas reinhardtii*–Bioavailability of small organic complexes and role of hardness ions. *Environmental Pollution* **2018,** *243*, 263-269.

58. Taylor, N. S.; Merrifield, R.; Williams, T. D.; Chipman, J. K.; Lead, J. R.; Viant, M. R., Molecular toxicity of cerium oxide nanoparticles to the freshwater alga *Chlamydomonas reinhardtii* is associated with supra-environmental exposure concentrations. *Nanotoxicology* **2016,** *10*, (1), 32-41.

59. Pulido-Reyes, G.; Briffa, S. M.; Hurtado-Gallego, J.; Yudina, T.; Leganés, F.; Puntes, V.; Valsami-Jones, E.; Rosal, R.; Fernández-Piñas, F., Internalization and toxicological mechanisms of uncoated and PVP-coated cerium oxide nanoparticles in the freshwater alga *Chlamydomonas reinhardtii*. *Environmental Science: Nano* **2019,** *6*, (6), 1959-1972.

60. née Röhder, L. A. K.; Brandt, T.; Sigg, L.; Behra, R., Uptake and effects of cerium (III) and cerium oxide nanoparticles to *Chlamydomonas reinhardtii*. *Aquatic Toxicology* **2018,** *197*, 41-46.

61. Goodenough, U. W.; Heuser, J. E., The Chlamydomonas cell wall and its constituent glycoproteins analyzed by the quick-freeze, deep-etch technique. *The Journal of Cell Biology* **1985,** *101*, (4), 1550-1568.

62. Sendra, M.; Yeste, P.; Moreno-Garrido, I.; Gatica, J.; Blasco, J., CeO2 NPs, toxic or protective to phytoplankton? Charge of nanoparticles and cell wall as factors which cause changes in cell complexity. *Science of The Total Environment* **2017,** *590*, 304-315.

63. Schwab, F.; Zhai, G.; Kern, M.; Turner, A.; Schnoor, J. L.; Wiesner, M. R., Barriers, pathways and processes for uptake, translocation and accumulation of nanomaterials in plants–Critical review. *Nanotoxicology* **2016,** *10*, (3), 257-278.

64. Bloodgood, R. A., The Chlamydomonas flagellar membrane and its dynamic properties. In *The Chlamydomonas Sourcebook*, Elsevier: 2009; pp 309-368.

65. Roiter, Y.; Ornatska, M.; Rammohan, A. R.; Balakrishnan, J.; Heine, D. R.; Minko, S., Interaction of nanoparticles with lipid membrane. *Nano Letters* **2008,** *8*, (3), 941-944.

66. Wong, M. H.; Misra, R. P.; Giraldo, J. P.; Kwak, S.-Y.; Son, Y.; Landry, M. P.; Swan, J. W.; Blankschtein, D.; Strano, M. S., Lipid exchange envelope penetration (LEEP) of nanoparticles for plant engineering: a universal localization mechanism. *Nano Letters* **2016,** *16*, (2), 1161-1172.

67. Zhao, L.; Peralta-Videa, J. R.; Varela-Ramirez, A.; Castillo-Michel, H.; Li, C.; Zhang, J.; Aguilera, R. J.; Keller, A. A.; Gardea-Torresdey, J. L., Effect of surface coating and organic matter on the uptake of CeO2 NPs by corn plants grown in soil: Insight into the uptake mechanism. *Journal of Hazardous Materials* **2012,** *225*, 131-138.

68. Wu, H.; Tito, N.; Giraldo, J. P., Anionic cerium oxide nanoparticles protect plant photosynthesis from abiotic stress by scavenging reactive oxygen species. *ACS Nano* **2017,** *11*, (11), 11283-11297.

69. Spielman-Sun, E.; Lombi, E.; Donner, E.; Howard, D.; Unrine, J. M.; Lowry, G. V., Impact of surface charge on cerium oxide nanoparticle uptake and translocation by wheat (*Triticum aestivum*). *Environmental Science & Technology* **2017,** *51*, (13), 7361-7368.

70. Auffan, M.; Rose, J.; Bottero, J.-Y.; Lowry, G. V.; Jolivet, J.-P.; Wiesner, M. R., Towards a definition of inorganic nanoparticles from an environmental, health and safety perspective. *Nature Nanotechnology* **2009,** *4*, (10), 634.

71. Rodea-Palomares, I.; Gonzalo, S.; Santiago-Morales, J.; Leganés, F.; García-Calvo, E.; Rosal, R.; Fernández-Pinas, F., An insight into the mechanisms of nanoceria toxicity in aquatic photosynthetic organisms. *Aquatic Toxicology* **2012,** *122*, 133-143.

72. Collin, B.; Auffan, M.; Johnson, A. C.; Kaur, I.; Keller, A. A.; Lazareva, A.; Lead, J. R.; Ma, X.; Merrifield, R. C.; Svendsen, C., Environmental release, fate and ecotoxicological effects of manufactured ceria nanomaterials. *Environmental Science: Nano* **2014,** *1*, (6), 533-548.

73. González, V.; Vignati, D. A.; Pons, M.-N.; Montarges-Pelletier, E.; Bojic, C.; Giamberini, L., Lanthanide ecotoxicity: First attempt to measure environmental risk for aquatic organisms. *Environmental Pollution* **2015,** *199*, 139-147.

74. Rogers, N. J.; Franklin, N. M.; Apte, S. C.; Batley, G. E.; Angel, B. M.; Lead, J. R.; Baalousha, M., Physico-chemical behaviour and algal toxicity of nanoparticulate CeO2 in freshwater. *Environmental Chemistry* **2010,** *7*, (1), 50-60.

75. Wiesner, M. R.; Lowry, G. V.; Jones, K. L.; Hochella, J., Michael F; Di Giulio, R. T.; Casman, E.; Bernhardt, E. S., Decreasing uncertainties in assessing environmental exposure, risk, and ecological implications of nanomaterials. In ACS Publications: 2009.

76. Thié, A.; Jong, L. D.; Issartel, J.; Moreau, X.; Saez, G.; Barthé, l. P.; Bestel, I.; Santaella, C.; Achouak, W., Effects of metallic and metal oxide nanoparticles in aquatic and terrestrial food chains. Biomarkers responses in invertebrates and bacteria. *International Journal of Nanotechnology* **2012,** *9*, (3), 181.

77. Pagano, G.; Guida, M.; Tommasi, F.; Oral, R., Health effects and toxicity mechanisms of rare earth elements—Knowledge gaps and research prospects. *Ecotoxicology and Environmental Safety* **2015,** *115*, 40-48.

78. Gonzalez, V.; Vignati, D. A. L.; Leyval, C.; Giamberini, L., Environmental fate and ecotoxicity of lanthanides: Are they a uniform group beyond chemistry? *Environment International* **2014,** *71*, 148-157.

79. Pulido-Reyes, G.; Rodea-Palomares, I.; Das, S.; Sakthivel, T. S.; Leganes, F.; Rosal, R.; Seal, S.; Fernández-Piñas, F., Untangling the biological effects of cerium oxide nanoparticles: the role of surface valence states. *Scientific Reports* **2015,** *5*, 15613.

80. Klaper, R.; Arndt, D.; Bozich, J.; Dominguez, G., Molecular interactions of nanomaterials and organisms: defining biomarkers for toxicity and high-throughput screening using traditional and next-generation sequencing approaches. *Analyst* **2014,** *139*, (5), 882-895.

81. Yokel, R. A.; Hussain, S.; Garantziotis, S.; Demokritou, P.; Castranova, V.; Cassee, F. R., The yin: an adverse health perspective of nanoceria: uptake, distribution, accumulation, and mechanisms of its toxicity. *Environmental Science: Nano* **2014,** *1*, (5), 406-428.

82. Xu, Y.; Wang, C.; Hou, J.; Wang, P.; You, G.; Miao, L., Effects of cerium oxide nanoparticles on bacterial growth and behaviors: Induction of biofilm formation and stress response. *Environmental Science and Pollution Research* **2019,** *26*, (9), 9293-9304.

83. Ma, Y.; Kuang, L.; He, X.; Bai, W.; Ding, Y.; Zhang, Z.; Zhao, Y.; Chai, Z., Effects of rare earth oxide nanoparticles on root elongation of plants. *Chemosphere* **2010,** *78*, (3), 273-279.

84. Palasz, A.; Czekaj, P., Toxicological and cytophysiological aspects of lanthanides action. **2000**.

85. Pietrobon, D.; Di Virgilio, F.; Pozzan, T., Structural and functional aspects of calcium homeostasis in eukaryotic cells. *European Journal of Biochemistry* **1990,** *193*, (3), 599-622.

86. Bowler, C.; Fluhr, R., The role of calcium and activated oxygens as signals for controlling cross-tolerance. *Trends in Plant Science* **2000,** *5*, (6), 241-246.

87. Verret, F.; Wheeler, G.; Taylor, A. R.; Farnham, G.; Brownlee, C., Calcium channels in photosynthetic eukaryotes: implications for evolution of calcium-based signalling. *New Phytologist* **2010,** *187*, (1), 23-43.

88. Kuchma, M. H.; Komanski, C. B.; Colon, J.; Teblum, A.; Masunov, A. E.; Alvarado, B.; Babu, S.; Seal, S.; Summy, J.; Baker, C. H., Phosphate ester hydrolysis of biologically relevant molecules by cerium oxide nanoparticles. *Nanomedicine: Nanotechnology, Biology and Medicine* **2010,** *6*, (6), 738-744.

89. Walker, J. C.; Willows, D. R., Mechanism and regulation of Mg-chelatase. *Biochemical Journal* **1997,** *327*, (2), 321-333.

90. Riedmaier, I.; Pfaffl, M. W., Transcriptional biomarkers–High throughput screening, quantitative verification, and bioinformatical validation methods. *Methods* **2013,** *59*, (1), 3-9.

91. Fisichella, M.; Berenguer, F.; Steinmetz, G.; Auffan, M.; Rose, J.; Prat, O., Toxicity evaluation of manufactured CeO2 nanoparticles before and after alteration: combined physicochemical and whole-genome expression analysis in Caco-2 cells. *BMC genomics* **2014,** *15*, (1), 700.

92. Simon, D. F.; Domingos, R. F.; Hauser, C.; Hutchins, C. M.; Zerges, W.; Wilkinson, K. J., Transcriptome sequencing (RNA-seq) analysis of the effects of metal nanoparticle exposure

on the transcriptome of *Chlamydomonas reinhardtii*. *Applied and Environmental Microbiology* **2013,** *79*, (16), 4774-4785.

93. Ruotolo, R.; Maestri, E.; Pagano, L.; Marmiroli, M.; White, J. C.; Marmiroli, N., Plant response to metal-containing engineered nanomaterials: an omics-based perspective. *Environmental Science & Technology* **2018,** *52*, (5), 2451-2467.

94. Lee, T.-L.; Raitano, J. M.; Rennert, O. M.; Chan, S.-W.; Chan, W.-Y., Accessing the genomic effects of naked nanoceria in murine neuronal cells. *Nanomedicine: Nanotechnology, Biology and Medicine* **2012,** *8*, (5), 599-608.

95. Sneller, F.; Kalf, D.; Weltje, L.; Van Wezel, A. *Maximum permissible concentrations and negligible concentrations for rare earth elements (REEs)*; 2000.

96. Keller, A. A.; Wang, H.; Zhou, D.; Lenihan, H. S.; Cherr, G.; Cardinale, B. J.; Miller, R.; Ji, Z., Stability and aggregation of metal oxide nanoparticles in natural aqueous matrices. *Environmental Science & Technology* **2010,** *44*, (6), 1962-1967.

97. Merdzan, V.; Domingos, R. F.; Monteiro, C. E.; Hadioui, M.; Wilkinson, K. J., The effects of different coatings on zinc oxide nanoparticles and their influence on dissolution and bioaccumulation by the green alga, *C. reinhardtii*. *Science of the Total Environment* **2014,** *488*, 316-324.

98. Domingos, R. F.; Baalousha, M. A.; Ju-Nam, Y.; Reid, M. M.; Tufenkji, N.; Lead, J. R.; Leppard, G. G.; Wilkinson, K. J., Characterizing manufactured nanoparticles in the environment: multimethod determination of particle sizes. *Environmental Science & Technology* **2009,** *43*, (19), 7277-7284.

99. Hadioui, M.; Knapp, G. v.; Azimzada, A.; Jreije, I.; Frechette-Viens, L.; Wilkinson, K. J., Lowering the size detection limits of Ag and TiO2 nanoparticles by Single Particle ICP-MS. *Analytical Chemistry* **2019,** *91*, (20), 13275-13284.

100. Azimzada, A.; Farner, J. M.; Hadioui, M.; Liu-Kang, C.; Jreije, I.; Tufenkji, N.; Wilkinson, K. J., Release of TiO2 nanoparticles from painted surfaces in cold climates: characterization using a high sensitivity single-particle ICP-MS. *Environmental Science: Nano* **2020**.

101. Laborda, F.; Bolea, E.; Jiménez-Lamana, J., Single particle inductively coupled plasma mass spectrometry: a powerful tool for nanoanalysis. In ACS Publications: 2013.

102. Baalousha, M.; Lead, J., Rationalizing nanomaterial sizes measured by atomic force microscopy, flow field-flow fractionation, and dynamic light scattering: sample preparation, polydispersity, and particle structure. *Environmental Science & Technology* **2012,** *46*, (11), 6134-6142.

103. Cheloni, G.; Slaveykova, V. I., Optimization of the C11-BODIPY581/591 dye for the determination of lipid oxidation in *Chlamydomonas reinhardtii* by flow cytometry. *Cytometry Part A* **2013,** *83*, (10), 952-961.

104. Cheloni, G.; Cosio, C.; Slaveykova, V. I., Antagonistic and synergistic effects of light irradiation on the effects of copper on *Chlamydomonas reinhardtii*. *Aquatic toxicology* **2014,** *155*, 275-282.

105. Park, B.; Donaldson, K.; Duffin, R.; Tran, L.; Kelly, F.; Mudway, I.; Morin, J.-P.; Guest, R.; Jenkinson, P.; Samaras, Z., Hazard and risk assessment of a nanoparticulate cerium oxide-based diesel fuel additive—a case study. *Inhalation Toxicology* **2008,** *20*, (6), 547-566.

106. Johnson, A. C.; Park, B., Predicting contamination by the fuel additive cerium oxide engineered nanoparticles within the United Kingdom and the associated risks. *Environmental Toxicology and Chemistry* **2012,** *31*, (11), 2582-2587.

107. Walkey, C.; Das, S.; Seal, S.; Erlichman, J.; Heckman, K.; Ghibelli, L.; Traversa, E.; McGinnis, J. F.; Self, W. T., Catalytic properties and biomedical applications of cerium oxide nanoparticles. *Environmental Science: Nano* **2015,** *2*, (1), 33-53.

108. White, J. C.; Gardea-Torresdey, J., Achieving food security through the very small. *Nature nanotechnology* **2018,** *13*, (8), 627.

109. Feng, Y.; Lu, H.; Liu, Y.; Xue, L.; Dionysiou, D. D.; Yang, L.; Xing, B., Nano-cerium oxide functionalized biochar for phosphate retention: preparation, optimization and rice paddy application. *Chemosphere* **2017,** *185*, 816-825.

110. Booth, A.; Størseth, T.; Altin, D.; Fornara, A.; Ahniyaz, A.; Jungnickel, H.; Laux, P.; Luch, A.; Sørensen, L., Freshwater dispersion stability of PAA-stabilised cerium oxide nanoparticles and toxicity towards *Pseudokirchneriella subcapitata*. *Science of the Total Environment* **2015,** *505*, 596-605.

111. Hoecke, K. V.; Quik, J. T.; Mankiewicz-Boczek, J.; Schamphelaere, K. A. D.; Elsaesser, A.; Meeren, P. V. d.; Barnes, C.; McKerr, G.; Howard, C. V.; Meent, D. V. D., Fate and effects of CeO2 nanoparticles in aquatic ecotoxicity tests. *Environmental Science & Technology* **2009,** *43*, (12), 4537-4546.

112. Auffan, M.; Masion, A.; Labille, J.; Diot, M.-A.; Liu, W.; Olivi, L.; Proux, O.; Ziarelli, F.; Chaurand, P.; Geantet, C., Long-term aging of a CeO2 based nanocomposite used for wood protection. *Environmental Pollution* **2014,** *188*, 1-7.

113. Barton, L. E.; Auffan, M.; Bertrand, M.; Barakat, M.; Santaella, C.; Masion, A.; Borschneck, D.; Olivi, L.; Roche, N.; Wiesner, M. R., Transformation of pristine and citrate-functionalized CeO2 nanoparticles in a laboratory-scale activated sludge reactor. *Environmental Science & Technology* **2014,** *48*, (13), 7289-7296.

114. Manier, N.; Bado-Nilles, A.; Delalain, P.; Aguerre-Chariol, O.; Pandard, P., Ecotoxicity of non-aged and aged CeO2 nanomaterials towards freshwater microalgae. *Environmental Pollution* **2013,** *180*, 63-70.

115. Andreescu, D.; Bulbul, G.; Özel, R. E.; Hayat, A.; Sardesai, N.; Andreescu, S., Applications and implications of nanoceria reactivity: measurement tools and environmental impact. *Environmental Science: Nano* **2014,** *1*, (5), 445-458.

116. Asati, A.; Santra, S.; Kaittanis, C.; Perez, J. M., Surface-charge-dependent cell localization and cytotoxicity of cerium oxide nanoparticles. *ACS nano* **2010,** *4*, (9), 5321-5331.

117. Fisichella, M.; Berenguer, F.; Steinmetz, G.; Auffan, M.; Rose, J.; Prat, O., Toxicity evaluation of manufactured CeO2 nanoparticles before and after alteration: combined physicochemical and whole-genome expression analysis in Caco-2 cells. *BMC Genomics* **2014,** *15*, (1), 700.

118. Keller, A. A.; Lazareva, A., Predicted releases of engineered nanomaterials: from global to regional to local. *Environmental Science & Technology Letters* **2013,** *1*, (1), 65-70.

119. Rodea-Palomares, I.; Boltes, K.; Fernández-Pinas, F.; Leganés, F.; García-Calvo, E.; Santiago, J.; Rosal, R., Physicochemical characterization and ecotoxicological assessment of CeO2 nanoparticles using two aquatic microorganisms. *Toxicological Sciences* **2010,** *119*, (1), 135-145.

120. Hussain, S. M.; Warheit, D. B.; Ng, S. P.; Comfort, K. K.; Grabinski, C. M.; Braydich-Stolle, L. K., At the crossroads of nanotoxicology in vitro: past achievements and current challenges. *Toxicological Sciences* **2015,** *147*, (1), 5-16.

121. Navarro, E.; Baun, A.; Behra, R.; Hartmann, N. B.; Filser, J.; Miao, A.-J.; Quigg, A.; Santschi, P. H.; Sigg, L., Environmental behavior and ecotoxicity of engineered nanoparticles to algae, plants, and fungi. *Ecotoxicology* **2008,** *17*, (5), 372-386.

122. Abràmoff, M. D.; Magalhães, P. J.; Ram, S. J., Image processing with ImageJ. *Biophotonics international* **2004,** *11*, (7), 36-42.

123. Collins, T. J., ImageJ for microscopy. *Biotechniques* **2007,** *43*, (S1), S25-S30.

124. Frechette-Viens, L.; Hadioui, M.; Wilkinson, K. J., Quantification of ZnO Nanoparticles and other Zn Containing Colloids in Natural Waters Using a High Sensitivity Single Particle ICP-MS. *Talanta (In press)* **2019**.

125. Shaw, P.; Donard, A., Nano-particle analysis using dwell times between 10 μs and 70 μs with an upper counting limit of greater than 3× 10 7 cps and a gold nanoparticle detection limit of less than 10 nm diameter. *Journal of Analytical Atomic Spectrometry* **2016,** *31*, (6), 1234-1242.

126. Newman, K.; Metcalfe, C.; Martin, J.; Hintelmann, H.; Shaw, P.; Donard, A., Improved single particle ICP-MS characterization of silver nanoparticles at environmentally relevant concentrations. *Journal of Analytical Atomic Spectrometry* **2016,** *31*, (10), 2069-2077.

127. Diaz, L.; Peyrot, C.; Wilkinson, K. J., Characterization of Polymeric Nanomaterials Using Analytical Ultracentrifugation. *Environmental Science & Technology* **2015,** *49*, (12), 7302-7309.

128. Harris, E., Culture and storage methods. *The Chlamydomonas Sourcebook. A Comprehensibe Guide to Biology and Laboratory Use* **1989**, 25-63.

129. Kola, H.; Wilkinson, K. J., Cadmium uptake by a green alga can be predicted by equilibrium modelling. *Environmental Science & Technology* **2005,** *39*, (9), 3040-3047.

130. Kola, H.; Laglera, L. M.; Parthasarathy, N.; Wilkinson, K. J., Cadmium adsorption by *Chlamydomonas reinhardtii* and its interaction with the cell wall proteins. *Environmental Chemistry* **2004,** *1*, (3), 172-179.

131. Andrews, S., FastQC: a quality control tool for high throughput sequence data. Babraham Bioinformatics. *Online [Mar 2016]* **2010**.

132. Krueger, F., Trim galore. *A wrapper tool around Cutadapt and FastQC to consistently apply quality and adapter trimming to FastQ files* **2015**.

133. Kim, D.; Pertea, G.; Trapnell, C.; Pimentel, H.; Kelley, R.; Salzberg, S. L., TopHat2: accurate alignment of transcriptomes in the presence of insertions, deletions and gene fusions. *Genome biology* **2013,** *14*, (4), R36.

134. Wang, L.; Wang, S.; Li, W., RSeQC: quality control of RNA-seq experiments. *Bioinformatics* **2012,** *28*, (16), 2184-2185.

135. Anders, S.; Pyl, P. T.; Huber, W., HTSeq—a Python framework to work with high-throughput sequencing data. *Bioinformatics* **2015,** *31*, (2), 166-169.

136. Love, M. I.; Huber, W.; Anders, S., Moderated estimation of fold change and dispersion for RNA-seq data with DESeq2. *Genome Biology* **2014,** *15*, (12), 550.

137. Usadel, B.; Poree, F.; Nagel, A.; Lohse, M.; Czedik-Eysenberg, A.; Stitt, M., A guide to using MapMan to visualize and compare Omics data in plants: a case study in the crop species, Maize. *Plant, Cell & Environment* **2009,** *32*, (9), 1211-1229.

138. Thimm, O.; Bläsing, O.; Gibon, Y.; Nagel, A.; Meyer, S.; Krüger, P.; Selbig, J.; Müller, L. A.; Rhee, S. Y.; Stitt, M., MAPMAN: a user-driven tool to display genomics data sets onto diagrams of metabolic pathways and other biological processes. *The Plant Journal* **2004,** *37*, (6), 914-939.

139. Goodstein, D. M.; Shu, S.; Howson, R.; Neupane, R.; Hayes, R. D.; Fazo, J.; Mitros, T.; Dirks, W.; Hellsten, U.; Putnam, N., Phytozome: a comparative platform for green plant genomics. *Nucleic Acids Research* **2011,** *40*, (D1), D1178-D1186.

140. Lopez, D.; Casero, D.; Cokus, S. J.; Merchant, S. S.; Pellegrini, M., Algal Functional Annotation Tool: a web-based analysis suite to functionally interpret large gene lists using integrated annotation and expression data. *BMC Bioinformatics* **2011,** *12*, (1), 282.

141. Tella, M.; Auffan, M.; Brousset, L.; Morel, E.; Proux, O.; Chanéac, C.; Angeletti, B.; Pailles, C.; Artells, E.; Santaella, C., Chronic dosing of a simulated pond ecosystem in indoor aquatic mesocosms: fate and transport of CeO 2 nanoparticles. *Environmental Science: Nano* **2015,** *2*, (6), 653-663.

142. Blaby, I. K.; Blaby-Haas, C. E.; Tourasse, N.; Hom, E. F.; Lopez, D.; Aksoy, M.; Grossman, A.; Umen, J.; Dutcher, S.; Porter, M., The Chlamydomonas genome project: a decade on. *Trends in plant science* **2014,** *19*, (10), 672-680.

143. Zones, J. M.; Blaby, I. K.; Merchant, S. S.; Umen, J. G., High-resolution profiling of a synchronized diurnal transcriptome from *Chlamydomonas reinhardtii* reveals continuous cell and metabolic differentiation. *The Plant Cell* **2015,** *27*, (10), 2743-2769.

144. Hilton, L. K.; Meili, F.; Buckoll, P. D.; Rodriguez-Pike, J. C.; Choutka, C. P.; Kirschner, J. A.; Warner, F.; Lethan, M.; Garces, F. A.; Qi, J., A forward genetic screen and whole genome sequencing identify deflagellation defective mutants in Chlamydomonas, including assignment of ADF1 as a TRP channel. *G3: Genes, Genomes, Genetics* **2016**, g3. 116.034264.

145. Keller, L. C.; Romijn, E. P.; Zamora, I.; Yates III, J. R.; Marshall, W. F., Proteomic analysis of isolated chlamydomonas centrioles reveals orthologs of ciliary-disease genes. *Current Biology* **2005,** *15*, (12), 1090-1098.

146. Quarmby, L. M., Deflagellation. In *The Chlamydomonas Sourcebook*, Elsevier: 2009; pp 43-69.

147. Molla-Herman, A.; Ghossoub, R.; Blisnick, T.; Meunier, A.; Serres, C.; Silbermann, F.; Emmerson, C.; Romeo, K.; Bourdoncle, P.; Schmitt, A., The ciliary pocket: an endocytic membrane domain at the base of primary and motile cilia. *J Cell Sci* **2010,** *123*, (10), 1785-1795.

148. Lyzenga, W. J.; Stone, S. L., Abiotic stress tolerance mediated by protein ubiquitination. *Journal of Experimental Botany* **2011,** *63*, (2), 599-616.

149. Vallentine, P.; Hung, C.-Y.; Xie, J.; Van Hoewyk, D., The ubiquitin–proteasome pathway protects Chlamydomonas reinhardtii against selenite toxicity, but is impaired as reactive oxygen species accumulate. *AoB Plants* **2014,** *6*.

150. Simon, D. F.; Domingos, R. F.; Hauser, C.; Hutchins, C. M.; Zerges, W.; Wilkinson, K. J., RNA-Seq analysis of the effects of metal nanoparticle exposure on the transcriptome of Chlamydomonas reinhardtii. *Applied and Environmental Microbiology* **2013**, AEM. 00998-13.

151. Lane, T. S.; Rempe, C. S.; Davitt, J.; Staton, M. E.; Peng, Y.; Soltis, D. E.; Melkonian, M.; Deyholos, M.; Leebens-Mack, J. H.; Chase, M., Diversity of ABC transporter genes across the plant kingdom and their potential utility in biotechnology. *BMC Biotechnology* **2016,** *16*, (1), 47.

152. Schulz, B.; Kolukisaoglu, H. Ü., Genomics of plant ABC transporters: the alphabet of photosynthetic life forms or just holes in membranes? *FEBS Letters* **2006,** *580*, (4), 1010-1016.

153. Simon, D. F.; Descombes, P.; Zerges, W.; Wilkinson, K. J., Global expression profiling of Chlamydomonas reinhardtii exposed to trace levels of free cadmium. *Environmental toxicology and chemistry* **2008,** *27*, (8), 1668-1675.

154. Beauvais-Flück, R.; Slaveykova, V. I.; Cosio, C., Cellular toxicity pathways of inorganic and methyl mercury in the green microalga Chlamydomonas reinhardtii. *Scientific reports* **2017,** *7*, (1), 8034.

155. Yokosho, K.; Yamaji, N.; Ma, J. F., Global transcriptome analysis of Al-induced genes in an Al-accumulating species, common buckwheat (*Fagopyrum esculentum Moench*). *Plant and Cell Physiology* **2014,** *55*, (12), 2077-2091.

156. Takanashi, K.; Shitan, N.; Yazaki, K., The multidrug and toxic compound extrusion (MATE) family in plants. *Plant Biotechnology* **2014,** *31*, (5), 417-430.

157. Yokosho, K.; Yamaji, N.; Ma, J. F., An Al-inducible MATE gene is involved in external detoxification of Al in rice. *The Plant Journal* **2011,** *68*, (6), 1061-1069.

158. Li, L.; Tutone, A. F.; Drummond, R. S.; Gardner, R. C.; Luan, S., A novel family of magnesium transport genes in Arabidopsis. *The Plant Cell* **2001,** *13*, (12), 2761-2775.

159. Moseley, J.; Grossman, A. R., Phosphate metabolism and responses to phosphorus deficiency. In *The Chlamydomonas sourcebook*, Elsevier: 2009; pp 189-215.

160. Blaby-Haas, C. E.; Merchant, S. S., The ins and outs of algal metal transport. *Biochimica et Biophysica Acta (BBA)-Molecular Cell Research* **2012,** *1823*, (9), 1531-1552.

161. Mittler, R., Oxidative stress, antioxidants and stress tolerance. *Trends in plant science* **2002,** *7*, (9), 405-410.

162. Tsunekawa, S.; Sivamohan, R.; Ito, S.; Kasuya, A.; Fukuda, T., Structural study on monosize CeO2-x nano-particles. *Nanostructured Materials* **1999,** *11*, (1), 141-147.

163. Tsunekawa, S.; Fukuda, T.; Kasuya, A., X-ray photoelectron spectroscopy of monodisperse CeO2− x nanoparticles. *Surface Science* **2000,** *457*, (3), L437-L440.

164. Kulacki, K. J.; Cardinale, B. J.; Keller, A. A.; Bier, R.; Dickson, H., How do stream organisms respond to, and influence, the concentration of titanium dioxide nanoparticles? A mesocosm study with algae and herbivores. *Environmental Toxicology and Chemistry* **2012,** *31*, (10), 2414-2422.

165. Auffan, M. Nanoparticules d'oxydes métalliques: relations entre la réactivité de surface et des réponses biologiques. Université Paul Cézanne-Aix-Marseille III, 2007.

166. Domingos, R. F.; Simon, D. F.; Hauser, C.; Wilkinson, K. J., Bioaccumulation and effects of CdTe/CdS quantum dots on *Chlamydomonas reinhardtii*–nanoparticles or the free ions? *Environmental Science & Technology* **2011,** *45*, (18), 7664-7669.

167. Leclerc, S.; Wilkinson, K. J., Bioaccumulation of Nanosilver by Chlamydomonas reinhardtii · Nanoparticle or the Free Ion? *Environmental Science & Technology* **2013,** *48*, (1), 358-364.

168. Liu, J.; Hurt, R. H., Ion release kinetics and particle persistence in aqueous nano-silver colloids. *Environmental Science & Technology* **2010,** *44*, (6), 2169-2175.

169. Hadioui, M.; Leclerc, S.; Wilkinson, K. J., Multimethod quantification of Ag+ release from nanosilver. *Talanta* **2013,** *105*, 15-19.

170. Hutchins, C.; Simon, D.; Zerges, W.; Wilkinson, K., Transcriptomic signatures in *Chlamydomonas reinhardtii* as Cd biomarkers in metal mixtures. *Aquatic toxicology* **2010,** *100*, (1), 120-127.

171. Morel, E.; Jreije, I.; Tetreault, V.; Hauser, C.; Zerges, W.; Wilkinson, K. J., Bioavailability and cellular processes of Ce nanoparticles with different surface coatings as revealed by RNA-Seq in *Chlamydomonas reinhardtii*. *Submitted in NanoImpact* **2019**.

172. Ruijter, J. M.; Pfaffl, M. W.; Zhao, S.; Spiess, A. N.; Boggy, G.; Blom, J.; Rutledge, R. G.; Sisti, D.; Lievens, A.; De Preter, K., Evaluation of qPCR curve analysis methods for reliable biomarker discovery: bias, resolution, precision, and implications. *Methods* **2013,** *59*, (1), 32-46.

173. Hassler, C. S.; Slaveykova, V. I.; Wilkinson, K. J., Discriminating between intra-and extracellular metals using chemical extractions. *Limnology and Oceanography: Methods* **2004,** *2*, (7), 237-247.

174. Bustin, S. A.; Benes, V.; Garson, J. A.; Hellemans, J.; Huggett, J.; Kubista, M.; Mueller, R.; Nolan, T.; Pfaffl, M. W.; Shipley, G. L., The MIQE guidelines: minimum information for publication of quantitative real-time PCR experiments. *Clinical Chemistry* **2009,** *55*, (4), 611-622.

175. Castruita, M.; Casero, D.; Karpowicz, S. J.; Kropat, J.; Vieler, A.; Hsieh, S. I.; Yan, W.; Cokus, S.; Loo, J. A.; Benning, C., Systems biology approach in Chlamydomonas reveals connections between copper nutrition and multiple metabolic steps. *The Plant Cell* **2011,** *23*, (4), 1273-1292.

176. Wakao, S.; Chin, B. L.; Ledford, H. K.; Dent, R. M.; Casero, D.; Pellegrini, M.; Merchant, S. S.; Niyogi, K. K., Phosphoprotein SAK1 is a regulator of acclimation to singlet oxygen in *Chlamydomonas reinhardtii*. *Elife* **2014,** *3*, e02286.

177. Fischer, B. B.; Dayer, R.; Schwarzenbach, Y.; Lemaire, S. D.; Behra, R.; Liedtke, A.; Eggen, R. I., Function and regulation of the glutathione peroxidase homologous gene GPXH/GPX5 in *Chlamydomonas reinhardtii*. *Plant Molecular Biology* **2009,** *71*, (6), 569-583.

178. Merchant, S. S.; Prochnik, S. E.; Vallon, O.; Harris, E. H.; Karpowicz, S. J.; Witman, G. B.; Terry, A.; Salamov, A.; Fritz-Laylin, L. K.; Maréchal-Drouard, L., The Chlamydomonas genome reveals the evolution of key animal and plant functions. *Science* **2007,** *318*, (5848), 245-250.

179. Schroda, M.; Vallon, O., Chaperones and proteases. In *The Chlamydomonas sourcebook*, Elsevier: 2009; pp 671-729.

180. Yang, L.; Fu, F.-L.; Deng, L.-Q.; Zhou, S.-F.; Yong, T.-M.; Li, W.-C., Cloning and characterization of functional keratinassociated protein 5-4 gene in maize. *African Journal of Biotechnology* **2012,** *11*, (29).

181. Dahle, J. T.; Livi, K.; Arai, Y., Effects of pH and phosphate on CeO2 nanoparticle dissolution. *Chemosphere* **2015,** *119*, 1365-1371.

182. Miekeley, N.; de Jesus, H. C.; da Silveira, C. P.; Linsalata, P.; Morse, R., Rare-earth elements in groundwaters from the Osamu Utsumi mine and Morro do Ferro analogue study sites, Poços de Caldas, Brazil. *Journal of Geochemical Exploration* **1992,** *45*, (1-3), 365-387.

183. Binnemans, K.; Jones, P. T.; Blanpain, B.; Van Gerven, T.; Yang, Y.; Walton, A.; Buchert, M., Recycling of rare earths: a critical review. *Journal of Cleaner Production* **2013,** *51*, 1-22.

184. Pang, X.; Li, D.; Peng, A., Application of rare-earth elements in the agriculture of China and its environmental behavior in soil. *Environmental Science and Pollution Research* **2002,** *9*, (2), 143.

185. Galhardi, J. A.; Leles, B. P.; de Mello, J. W. V.; Wilkinson, K. J., Bioavailability of trace metals and rare earth elements (REE) from the tropical soils of a coal mining area. *Science of The Total Environment* **2019**, 134484.

186. Li, B.; Byrne, R. H., Ionic strength dependence of rare earth–NTA stability constants at 25 C. *Aquatic Geochemistry* **1997,** *3*, (2), 99-115.

187. Borgmann, U.; Couillard, Y.; Doyle, P.; Dixon, D. G., Toxicity of sixty-three metals and metalloids to *Hyalella azteca* at two levels of water hardness. *Environmental Toxicology and Chemistry* **2005,** *24*, (3), 641-652.

188. Weltje, L.; Heidenreich, H.; Zhu, W.; Wolterbeek, H. T.; Korhammer, S.; de Goeij, J. J.; Markert, B., Lanthanide concentrations in freshwater plants and molluscs, related to those in surface water, pore water and sediment. A case study in The Netherlands. *Science of the Total Environment* **2002,** *286*, (1-3), 191-214.

189. Tsuruta, T., Accumulation of rare earth elements in various microorganisms. *Journal of Rare Earths* **2007,** *25*, (5), 526-532.

190. Borgmann, U.; Norwood, W. P.; Dixon, D. G., Modelling bioaccumulation and toxicity of metal mixtures. *Human and Ecological Risk Assessment* **2008,** *14*, (2), 266-289.

191. Bau, M.; Dulski, P., Anthropogenic origin of positive gadolinium anomalies in river waters. *Earth and Planetary Science Letters* **1996,** *143*, (1-4), 245-255.

192. Komjarova, I.; Blust, R., Multi-metal interactions between Cd, Cu, Ni, Pb and Zn in water flea *Daphnia magna*, a stable isotope experiment. *Aquat. Toxicol.* **2008,** *90*, (2), 138-144.

193. Komjarova, I.; Blust, R., Multimetal interactions between Cd, Cu, Ni, Pb, and Zn uptake from water in the zebrafish *Danio rerio*. *Environ Sci Technol* **2009,** *43*, (19), 7225-9.

194. Chen, Z.; Zhu, L.; Wilkinson, K. J., Validation of the Biotic Ligand Model in Metal Mixtures: Bioaccumulation of Lead and Copper. *Environ. Sci. Technol.* **2010,** *44*, (9), 3580-3586.

195. Hutchins, C. M.; Simon, D. F.; Zerges, W.; Wilkinson, K. J., Transcriptomic signatures in *Chlamydomonas reinhardtii* as Cd biomarkers in metal mixtures. *Aquatic Toxicology* **2010,** *100*, (1), 120-127.

196. Song, Y.; Asselman, J.; De Schamphelaere, K. A.; Salbu, B.; Tollefsen, K. E., Deciphering the combined effects of environmental stressors on gene transcription: a conceptual approach. *Environmental science & technology* **2018,** *52*, (9), 5479-5489.

197. Han, J.; Kaufman, R. J., The role of ER stress in lipid metabolism and lipotoxicity. *Journal of Lipid Research* **2016,** *57*, (8), 1329-1338.

198. Goecke, F.; Jerez, C. G.; Zachleder, V.; Figueroa, F. L.; Bišová, K.; Řezanka, T.; Vítová, M., Use of lanthanides to alleviate the effects of metal ion-deficiency in *Desmodesmus quadricauda* (Sphaeropleales, Chlorophyta). *Frontiers in Microbiology* **2015,** *6*, 2.

199. Michalak, M.; Parker, J. R.; Opas, M., Ca2+ signaling and calcium binding chaperones of the endoplasmic reticulum. *Cell Calcium* **2002,** *32*, (5-6), 269-278.

200. Schurch, N. J.; Schofield, P.; Gierliński, M.; Cole, C.; Sherstnev, A.; Singh, V.; Wrobel, N.; Gharbi, K.; Simpson, G. G.; Owen-Hughes, T., How many biological replicates are needed in an RNA-seq experiment and which differential expression tool should you use? *Rna* **2016,** *22*, (6), 839-851.

201. Chen, F.; Xiao, Z.; Yue, L.; Wang, J.; Feng, Y.; Zhu, X.; Wang, Z.; Xing, B., Algae response to engineered nanoparticles: current understanding, mechanisms and implications. *Environmental Science: Nano* **2019,** *6*, (4), 1026-1042.

202. Brockmeier, E. K.; Hodges, G.; Hutchinson, T. H.; Butler, E.; Hecker, M.; Tollefsen, K. E.; Garcia-Reyero, N.; Kille, P.; Becker, D.; Chipman, K., The role of omics in the application of adverse outcome pathways for chemical risk assessment. *Toxicological Sciences* **2017,** *158*, (2), 252-262.

203. Zhang, Z.; He, X.; Zhang, H.; Ma, Y.; Zhang, P.; Ding, Y.; Zhao, Y., Uptake and distribution of ceria nanoparticles in cucumber plants. *Metallomics* **2011,** *3*, (8), 816-822.

204. Marie, T.; Mélanie, A.; Lenka, B.; Julien, I.; Isabelle, K.; Christine, P.; Elise, M.; Catherine, S.; Bernard, A.; Ester, A.; Jérôme, R.; Alain, T.; Jean-Yves, B., Transfer, Transformation, and Impacts of Ceria Nanomaterials in Aquatic Mesocosms Simulating a Pond Ecosystem. *Environmental Science & TÉechnology* **2014,** *48*, (16), 9004-9013.

Annexes

Formes chimiques du Ce

Comme il n'existe pas de Ce NMs modèles, possédant l'ensemble des caractéristiques des nanoparticules utilisées par l'industrie, cinq types de ENPs ont été initialement sélectionnés pour représenter des nanoparticules de tailles et d'enrobages différents (**Tableau I**). Les suspensions stock de CeO_2 enrobées citrate (Ce NMs-Cit) sont commercialisées sous le nom de Nanobyk®-3810 et sont principalement utilisées comme protection UV pour des revêtements (Byk, Allemagne). Les suspensions stock de Ce NMs enrobées de poly(acrylique acide) (Ce NMs-PAA) et les Ce NMs non enrobées ont été achetées chez Vive Nano (Canada), Sigma Aldrich (Canada), SprySpringNanomaterials (USA) et NanoAmor (USA) respectivement.

Tableau I : Identification et caractéristiques indiquées par le producteur des ENPs de CeO_2 sélectionnées.

Identification	**Forme**	**Concentration stock ($g.L^{-1}$)**	**Diamètre (nm)**	**Enrobage (concentration)**
Ce NMs-Cit	Dispersion	187 ± 2	10 (D_H)[204]	Citrate (5 $g.L^{-1}$)[204]
Ce NMs-PAA	Dispersion	1,54 ± 0,02	1-10 (D_p)	Polyacrylique acide (75 % (m/m))
Ce NMs-non-enrobées	Poudre	-	10-30	non
Ce NMs-non-enrobées	Poudre	-	15-30	non
Ce NMs-non-enrobées	Poudre	-	< 25	non

D_H et D_p précise le type de diamètre mesuré ; diamètre hydrodynamique ou physique respectivement. Les informations indiquées par [204] sont issues de Tella et *al.*, 2014.

Attaques acides et dosage du Ce total

Une digestion acide préalable aux analyses de dosage par spectroscopie de masse couplée à une induction plasma (ICP-MS) est réalisée sur tous les échantillons y compris comprenant du Ce sous forme ionique afin de dissoudre les diverses matrices (ex. algues, filtres) et/ou de solubiliser les Ce NMs et/ou les nanoparticules naturellement formées à partir de la solution ioniques. Cette digestion est réalisée à 80°C pendant 4 h après rajout de HNO_3 et de H_2O_2 à 20% et de 3% (v/v) respectivement puisque le HNO_3 à 20% (v/v) seul ne permet pas d'atteindre un pourcentage de recouvrement du Ce satisfaisant pour les CeO_2 NMs non enrobées (**Figure 1**). Les concentrations initiales des suspensions mères des nanoparticules obtenues sous forme de poudres ont également été mesurées suivant ces deux protocoles mais aucune différence significative n'a pu être observée entre les deux types d'attaque (**Figure 2**).

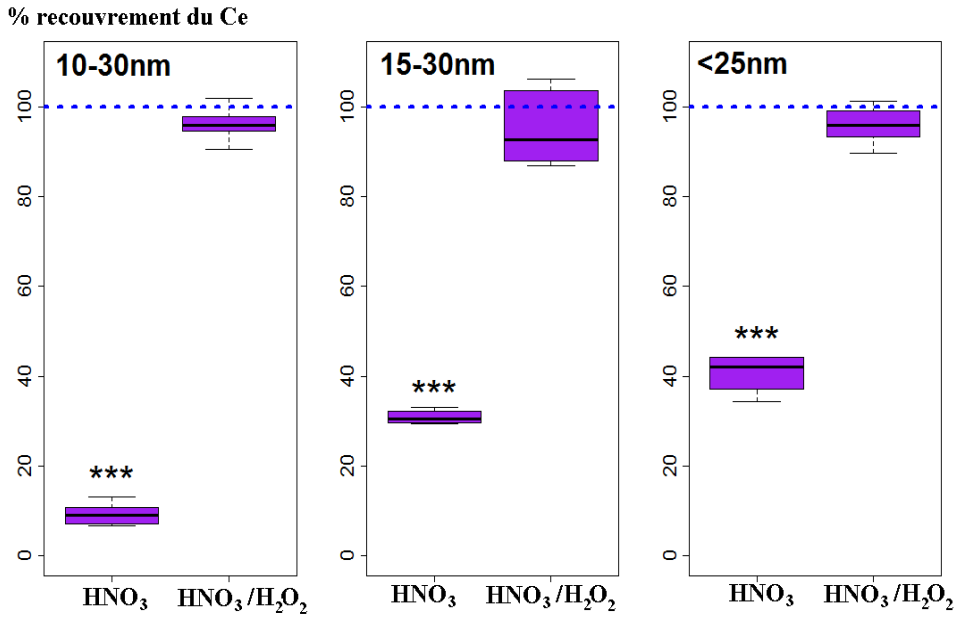

Figure 1. – Pourcentage de recouvrement du Ce mesuré pour les différentes suspensions de Ce NMs non enrobées digérées à 80°C pendant 4 h avec du HNO_3 seul à 20% (v/v) ou un mélange HNO_3/H_2O_2 à 20%/3% (v/v) (n=7 à 8,Test de student, *** $p \leq 0,01$).

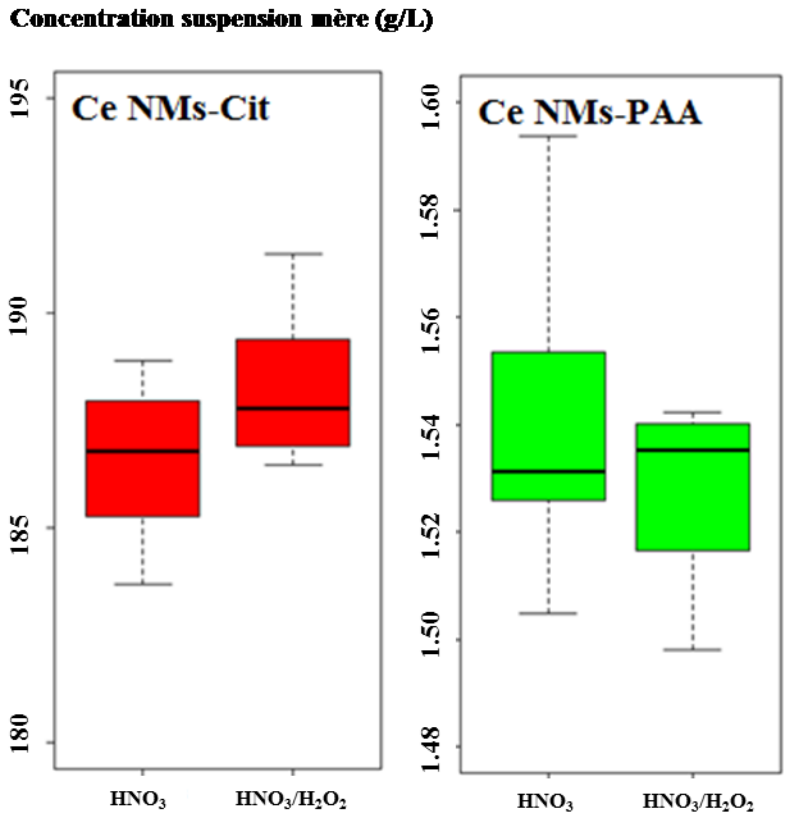

Figure 2. – Concentrations des suspensions mères obtenues pour les Ce NMs enrobées de citrate et de PAA mesurées à 80°C pendant 4 h avec du HNO_3 seul à 20% (v/v) ou un mélange HNO_3/H_2O_2 à 20%/3% (v/v) (n=8 à 16).

Stabilisation des solutions/suspensions d'exposition

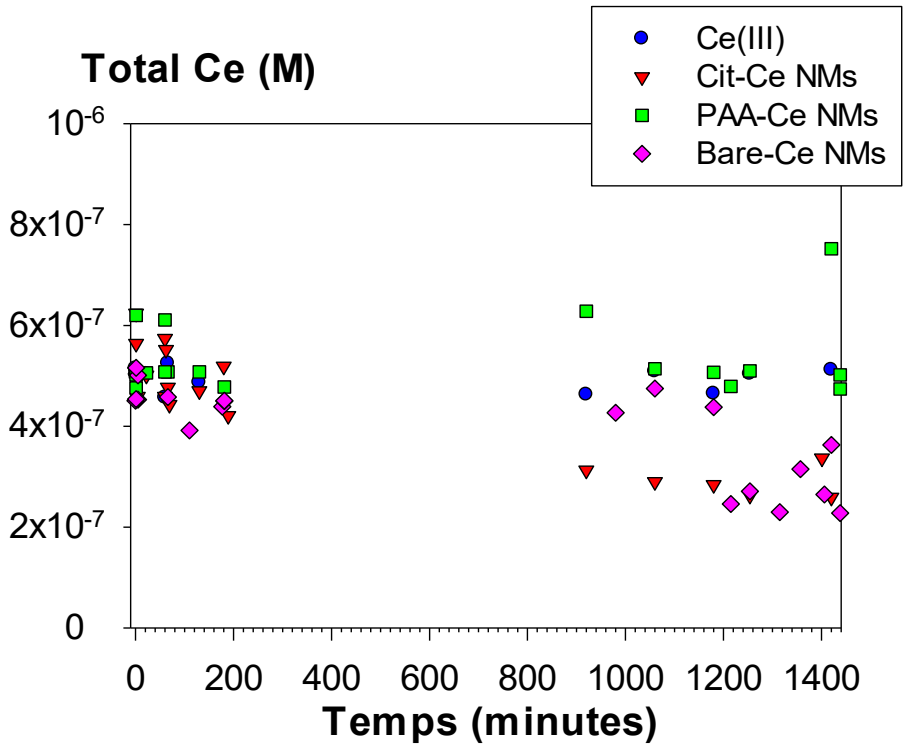

Figure 3. – Evolution de la concentration en cérium totale en fonction du temps de stabilisation (24h) avant l'introduction des algues pour les solutions/suspensions de Ce ionique, Ce NMs enrobées de citrate et de PAA et CeNMs non enrobées (nominale concentration = $5x10^{-7}$ M Ce) à pH 7.0 préparées dans des flasques en téflon.